Cosmic Magnetic Fields: Theory

Krzysztof Nalewajko

31 May 2022

Contents

1 Electrodynamics

Lorentz force. The *magnetic field* $\vec{B}$ can be defined together with the *electric field* $\vec{E}$ by the way in which they accelerate charged *test particles*, i.e., the *Lorentz force*:

$$\vec{F}_{\mathrm{L}} = \frac{d\vec{p}}{dt} = q(\vec{E} + \vec{\beta} \times \vec{B})\,, \tag{1.1}$$

where q is the electric charge of the particle, $\vec{\beta} = \vec{v}/c$ is the particle dimensionless velocity normalized to the speed of light c, and $\vec{p}$ is the particle momentum.

There is a fundamental difference in how the electric and magnetic fields accelerate charged particles. For a particle of mass m let us introduce Lorentz factor $\gamma = (1 - \beta^2)^{-1/2}$, so that its energy is $\mathcal{E} = \gamma mc^2$ and momentum is $\vec{p} = \gamma\vec{\beta}mc$. One can show that:

$$\vec{p} \cdot \vec{F}_{\mathrm{L}} = \frac{1}{2}\frac{\mathrm{d}p^2}{\mathrm{d}t} = \frac{1}{2}\frac{\mathrm{d}(\gamma^2 - 1)}{\mathrm{d}t}m^2c^2 = \gamma\frac{\mathrm{d}\gamma}{\mathrm{d}t}m^2c^2 = \gamma m\frac{\mathrm{d}\mathcal{E}}{\mathrm{d}t}\,, \tag{1.2}$$

$$\vec{p} \cdot \vec{F}_{\mathrm{L}} = \gamma\vec{\beta}mc \cdot q\left(\vec{E} + \vec{\beta} \times \vec{B}\right) = \gamma m\, q\vec{v} \cdot \vec{E}\,, \tag{1.3}$$

so that the particle energy change is:

$$\frac{\mathrm{d}\mathcal{E}}{\mathrm{d}t} = \frac{\mathrm{d}\gamma}{\mathrm{d}t}mc^2 = q\vec{v} \cdot \vec{E}\,. \tag{1.4}$$

Particle energy changes due to the electric field component parallel to the particle velocity vector.

Motion of charged particles in uniform magnetic field. The effect of magnetic field is to rotate the particle velocity vector without changing its energy. In the case of uniform magnetic field $\vec{B} = \mathrm{const}$, one would find:

$$\frac{d\vec{\beta}}{dt} = \frac{q}{\gamma mc}(\vec{\beta} \times \vec{B}) \tag{1.5}$$

Decomposing the velocity vector $\vec{\beta} = \vec{\beta}_\| + \vec{\beta}_\perp$ into components parallel and perpendicular to $\vec{B}$, one would find that $\beta_\|, \beta_\perp = \mathrm{const}$, and the $\vec{\beta}_\perp$ vector would rotate at the *gyrofrequency* (or Larmor frequency) $\Omega_{\mathrm{L}} = qB/(\gamma mc)$. Such particle would follow a helical trajectory along the $\vec{B}$ vector with the *gyroradius* (or Larmor radius) $R_{\mathrm{L}} = \gamma\beta_\perp mc^2/(qB) = p_\perp c/(qB)$ and the *pitch length* of $\Delta z = 2\pi\gamma\beta_\| mc^2/(qB)$.

- This scaling between the gyroradius R_{L}, the particle energy $\mathcal{E} \sim p_\perp c$. and the magnetic field strength B is the basis of the Hillas plot discussed in the Introduction.

More formally, consider the case of $\vec{B} = B\hat{x}$, which means that $\vec{v} \times \vec{B} = B(0, \beta_z, -\beta_y) = B(0, \dot{z}, -\dot{y})$. The corresponding equations of motion are $\ddot{x} = 0$, $\ddot{y} = \Omega\dot{z}$ and $\ddot{z} = -\Omega\dot{y} = -\Omega_{\mathrm{L}}^2 z$. Introducing $r^2 = y^2 + z^2$, one can show that $\dot{r} = (y/r)\dot{y} + (z/r)\dot{z} = 0$. The resulting motion is a combination of uniform motion in x and circular oscillation in y, z.

- An accelerated charge is a source of electromagnetic radiation and is subject to radiative energy losses. This will be discussed later on.

If the magnetic field is not uniform, the motion of charged particles can be modified in different ways. If the variations of the field are not too strong, the particle will try to follow the local field line. It may gyrate about a line called the *guiding center* that is not straight but curved, and not strictly aligned with the local magnetic field. Such departures of the guiding center are usually referred to as drifts. There are several types of drifts that will be mentioned only briefly:

- *gradient drift*, when the magnetic strength gradient $\vec{\nabla}B$ is perpendicular to $\vec{B}$;

- *curvature drift*, when the magnetic field lines are curved, e.g. if there exists an axis represented by unit vector $\hat{z}$ such that $\vec{\nabla}B \parallel \vec{B} \times \hat{z}$;

- *magnetic mirror*, when $\vec{\nabla}B \parallel \vec{B}$;

- $\vec{E} \times \vec{B}$ *drift*, in the presence of uniform electric field $\vec{E}$.

Maxwell's equations. Evolution of electric field $\vec{E}$ and magnetic field $\vec{B}$ is governed by the *Maxwell's equations*:

$$\vec{\nabla} \cdot \vec{E} = 4\pi\rho\,, \tag{1.6}$$

$$\vec{\nabla} \cdot \vec{B} = 0\,, \tag{1.7}$$

$$\vec{\nabla} \times \vec{E} = -\frac{1}{c}\frac{\partial \vec{B}}{\partial t}\,, \tag{1.8}$$

$$\vec{\nabla} \times \vec{B} = \frac{4\pi}{c}\vec{j} + \frac{1}{c}\frac{\partial \vec{E}}{\partial t}\,, \tag{1.9}$$

where $\rho = \sum_i q_i n_i$ is the charge density and $\vec{j} = \sum_i q_i n_i \vec{v}_i$ is the current density, summing over different species of charged particles. The first two equations are known as the *Gauss's laws*, the third one is the *Maxwell-Faraday equation*, and the last one is the *Ampère-Maxwell equation*. The final term of the Ampère-Maxwell equation is called the *displacement current*.

Conservation of electric charge. Combining the time derivative of the Gauss law for electric field (Eq. 1.6) with the divergence of the Ampère-Maxwell equation (Eq. 1.9) leads to the charge conservation:

$$\frac{\partial \rho}{\partial t} + \vec{\nabla} \cdot \vec{j} = 0\,. \tag{1.10}$$

Introducing the *electric four-current density* $j^\mu = (\rho c, \vec{j})$ ($\mu \in \{0, 1, 2, 3\}$), this can be written in a covariant form $\partial_\mu j^\mu = 0$.

Magnetic monopoles. The Maxwell's equations are not exactly symmetric with respect to the $\vec{E}, \vec{B}$ fields. Two of them contain source terms: the charge density ρ_e can be treated as the source of $\vec{E}$, and the current density $\vec{j}$ can be treated (although in a different dense) as the source of $\vec{B}$. One can consider hypothetical particles called *magnetic monopoles* of charge density $\rho_m = \sum_i q_{m,i} n_i$ and associated current density $\vec{j}_m = \sum_i q_{m,i} n_i \vec{v}_i$, extending the Maxwell's equations quite naturally to a more symmetric form:

$$\vec{\nabla} \cdot \vec{E} = 4\pi\rho_e\,, \tag{1.11}$$

$$\vec{\nabla} \cdot \vec{B} = 4\pi\rho_m\,, \tag{1.12}$$

$$\vec{\nabla} \times \vec{E} = -\frac{4\pi}{c}\vec{j}_m - \frac{1}{c}\frac{\partial \vec{B}}{\partial t}\,, \tag{1.13}$$

$$\vec{\nabla} \times \vec{B} = \frac{4\pi}{c}\vec{j} + \frac{1}{c}\frac{\partial \vec{E}}{\partial t}\,. \tag{1.14}$$

It has to be stressed that there is no evidence for the existence of magnetic monopoles, although various claims have been made historically and such a possibility is being tested in experiments.

It has been noted by Parker (2007) that if magnetic monopoles existed in significant numbers, the electrodynamics would be completely different from what we know and experience. In particular, magnetic monopoles would be the true sources of $\vec{B}$ and they would easily screen strong magnetic fields, in the same way in which the electric charges screen strong electric fields. The magnetic fields would not extend to large distances and would not be able to play such interesting roles in the Universe.

Magnetic flux. Given a surface S, the *magnetic flux* through that surface is $\Phi = \iint_S \vec{B} \cdot \hat{n} \, \mathrm{d}S$, where $\hat{n}$ is a unit vector normal to the surface element $\mathrm{d}S$.

A finite surface S_1 with net magnetic flux can be extended along the field lines into a *magnetic flux tube*. The side walls of such a tube by definition satisfy $\vec{B} \cdot \hat{n}$. Consider another surface crossing such a tube with the part within the tube denoted as S_2. The magnetic flux difference satisfies the divergence theorem:

$$\Phi_2 - \Phi_1 = \iint_{S_2} \vec{B} \cdot \hat{n} \, \mathrm{d}S - \iint_{S_1} \vec{B} \cdot \hat{n} \, \mathrm{d}S = \iiint_V \left(\vec{\nabla} \cdot \vec{B}\right) \mathrm{d}V \tag{1.15}$$

The Gauss's law for magnetism $\vec{\nabla} \cdot \vec{B} = 0$ implies that $\Phi_2 = \Phi_1$. The magnetic flux will be the same for any other surface crossing the same flux tube, hence magnetic flux is its defining property.

- A magnetic field line can be considered as an infinitely thin magnetic flux tube.

Electric energy density. In order to demonstrate that electric field is a form of energy, consider two large flat parallel plates of thickness δz with opposite electric charges of uniform surface densities $\pm(\Sigma_{\mathrm{e}} = \rho_{\mathrm{e}} \, \delta z)$ — a capacitor. Using the Gauss's law for electricity $\vec{\nabla} \cdot \vec{E} = 4\pi \rho_{\mathrm{e}}$, the electric field between the plates is $E_z \simeq 4\pi \rho_{\mathrm{e}} \, \delta z = 4\pi \Sigma_{\mathrm{e}}$. Each plate is attracted to the other by the Lorentz force of surface density

$$\frac{\Delta F_{\mathrm{L},z}}{\Delta A} = \frac{E_z}{2} \Sigma_{\mathrm{e}} = \frac{E^2}{8\pi} \tag{1.16}$$

(the $1/2$ factor accounts for the linear decay of E_z across each plate). In order to increase the separation between the plates by Δz against the Lorentz force, one must perform a work $\Delta W = \Delta F_{\mathrm{L},z} \, \Delta z = \Delta E_{\mathrm{E}}$ increasing the electric energy $\mathcal{E}_E$ for constant E_z. The electric energy density is thus:

$$u_{\mathrm{E}} = \frac{\Delta \mathcal{E}_{\mathrm{E}}}{\Delta A \, \Delta z} = \frac{\Delta F_{\mathrm{L},z}}{\Delta A} = \frac{E^2}{8\pi} \, . \tag{1.17}$$

Magnetic energy density. An analogous argument can be made for the energy of magnetic fields. The large flat plates instead of electric charge may carry electric current at opposite directions, distributed uniformly over each plate, e.g., with the current surface density of $\pm(\mathcal{I}_x = j_x \, \delta z)$. Using the Ampère-Maxwell equation $\vec{\nabla} \times \vec{B} = (4\pi/c)\vec{j}$, the magnetic field between the plates is $B_y \simeq (4\pi/c)\mathcal{I}_x$. Each plate is attracted to the other by the Lorentz force of surface density

$$\frac{\Delta F_{\mathrm{L},z}}{\Delta A} = \frac{B_y}{2} \frac{\mathcal{I}_x}{c} = \frac{B^2}{8\pi} \, . \tag{1.18}$$

The magnetic energy density is thus[1]

$$u_{\mathrm{B}} = \frac{B^2}{8\pi} \, . \tag{1.19}$$

Magnetic field is a form of energy, and since it may extend over large volumes it can store large amounts of energy. The possibility of releasing (dissipating) this energy is of fundamental astrophysical importance. One of the key mechanism that can enable that is magnetic reconnection.

- Roger Blandford coined the term *magnetoluminescence* as a generic mechanism of efficient and rapid conversion of magnetic energy into radiation. Such mechanism is necessary in order to explain the high radiative efficiency of extreme cosmic sources that are locally dominated by magnetic energy (relativistic magnetization $\sigma = B^2/(4\pi \rho c^2) > 1$), such as Pulsar Wind Nebulae (PWN), blazars, Gamma Ray Bursts (GRB) and magnetars (Blandford et al., 2017). Magnetoluminescence likely involves magnetic reconnection, but only as the first step. Reconnection is a local process that enables the release of volumetric magnetic fields, e.g., in the process of magnetic relaxation. The magnetic energy would be transformed into particles by means of heating and non-thermal particle acceleration. Finally, if the energetic particles undergo rapid radiative cooling (e.g., in the synchrotron process), their energy can be efficiently converted into radiation. The overall efficiency of magnetoluminescence depends on the efficiencies of all these intermediate processes.

Electromagnetic energy change. Knowing what is the energy density of electric and magnetic fields, let us calculate how it evolves in time according to the Maxwell's equations:

$$\frac{\partial u_{\mathrm{E}}}{\partial t} = \frac{c}{4\pi} \vec{E} \cdot \left(\vec{\nabla} \times \vec{B} \right) - \vec{E} \cdot \vec{j}, \tag{1.20}$$

$$\frac{\partial u_{\mathrm{B}}}{\partial t} = -\frac{c}{4\pi} \vec{B} \cdot \left(\vec{\nabla} \times \vec{E} \right) . \tag{1.21}$$

---

[1]This implies that $1\,\mathrm{G}^2 \equiv 8\pi \, \mathrm{erg/cm}^3$.

The last term in the electric energy change $-\vec{E} \cdot \vec{j}$ represents *Ohmic dissipation*. For the most basic Ohm's law $\vec{j} = \sigma \vec{E}$ with scalar resistivity σ, it equals $-\sigma E^2$. The remaining terms can be combined by considering the change of total electromagnetic energy:

$$\frac{\partial u_{\mathrm{EM}}}{\partial t} \equiv \frac{\partial (u_{\mathrm{E}} + u_{\mathrm{B}})}{\partial t} = -\frac{c}{4\pi} \vec{\nabla} \cdot \left(\vec{E} \times \vec{B} \right) - \vec{E} \cdot \vec{j}. \tag{1.22}$$

Introducing the *Poynting flux* $\vec{S} = (c/4\pi)(\vec{E} \times \vec{B})$, we can write the *energy equation for electromagnetic fields* as:

$$\frac{\partial u_{\mathrm{EM}}}{\partial t} = -\vec{\nabla} \cdot \vec{S} - \vec{E} \cdot \vec{j}. \tag{1.23}$$

Notice that in the absence of Ohmic dissipation, the electromagnetic energy density may decrease due to the divergence of the Poynting flux. This means the Poynting flux carries electromagnetic energy between places (this is particularly true for the electromagnetic radiation), hence *the Poynting flux is an electromagnetic equivalent of the momentum density*.

Poynting flux change. Let us derive an equivalent of the momentum equation for electromagnetic fields by calculating the change of Poynting flux:

$$\partial_t S^i = \frac{c}{4\pi} \epsilon_{ijk} (B^k \partial_t E^j + E^j \partial_t B^k) \tag{1.24}$$

$$\frac{\partial_t S^i}{c^2} = -\partial_i \frac{E^2 + B^2}{8\pi} + \partial_j \frac{E^i E^j + B^i B^j}{4\pi} - \rho_{\mathrm{e}} E^i - \frac{1}{c} \left(\vec{j} \times \vec{B} \right)^i \tag{1.25}$$

In the last equation, the first two terms on the RHS can be identified as a divergence of symmetric tensor $\partial_j T_{\mathrm{EM}}^{ij}$ known as the (minus) Maxwell stress tensor:

$$T_{\mathrm{EM}}^{ij} = \frac{E^2 + B^2}{8\pi} \delta^{ij} - \frac{E^i E^j + B^i B^j}{4\pi}. \tag{1.26}$$

The remaining two terms constitute the Lorentz force density $\vec{f}_{\mathrm{L}} = \rho_{\mathrm{e}} \vec{E} + (\vec{j} \times \vec{B})/c$. The stress tensor consists of two main components: the first one (diagonal) is the *pressure* of electric field $P_{\mathrm{E}} = E^2/8\pi = u_{\mathrm{E}}$ and magnetic field $P_{\mathrm{B}} = B^2/8\pi = u_{\mathrm{B}}$; the second one is the electromagnetic *tension* $-E^i E^j/4\pi - B^i B^j/4\pi$, which for the diagonal terms has an opposite sign to the pressure.

- Example: consider uniform $\vec{B} = (B_x, 0, 0)$ and $\vec{E} = 0$. In such case, $T_{\mathrm{EM}}^{ij} = (B_x^2/8\pi) \mathrm{diag}(-1, 1, 1)$, which corresponds to a positive pressure across the field line and *negative pressure* along the field line. The fundamental difference between pressure and tension: *pressure pushes, tension pulls*.

- In fluid dynamics one can relate pressure P to the internal energy density $u_{\mathrm{int}} = P/(\kappa - 1)$, where $\kappa = 1 + P/u_{\mathrm{int}}$ is the adiabatic index. For the magnetic field we can infer an adiabatic index $\kappa_{\mathrm{B}} = 1 + P_{\mathrm{B}}/u_{\mathrm{B}} = 2$. It is also possible to define a *magnetic enthalpy density* $w_{\mathrm{B}} = u_{\mathrm{B}} + P_{\mathrm{B}} = 2u_{\mathrm{B}} = B^2/4\pi$. The ratio of magnetic and fluid enthalpy densities is known as the *magnetization* $\sigma = w_{\mathrm{B}}/w = B^2/4\pi w$.

We can thus write the *momentum equation for electromagnetic fields* as:

$$\frac{1}{c^2} \frac{\partial \vec{S}}{\partial t} = -\vec{\nabla} \cdot \boldsymbol{T}_{\mathrm{EM}} - \vec{f}_{\mathrm{L}}. \tag{1.27}$$

Energy-momentum tensor. The spatial Maxwell stress tensor can be extended to the spacetime energy-momentum tensor by identifying:

$$T_{\mathrm{EM}}^{00} = u_{\mathrm{EM}} = \frac{E^2 + B^2}{8\pi}, \tag{1.28}$$

$$T_{\mathrm{EM}}^{0i} = \frac{S^i}{c} = \frac{1}{4\pi} \left(\vec{E} \times \vec{B} \right)^i, \tag{1.29}$$

$$T_{\mathrm{EM}}^{ij} = \frac{E^2 + B^2}{8\pi} \delta^{ij} - \frac{E^i E^j + B^i B^j}{4\pi}. \tag{1.30}$$

With this, the energy and momentum equations can be generalized as the energy-momentu conservation law[2]:

$$\partial_\mu T_{\text{EM}}^{\mu\nu} = -f_{\text{L}}^\mu \, , \tag{1.31}$$

where $f_{\text{L}}^\mu = \{(\vec{E} \cdot \vec{j})/c, f_{\text{L}}^i\}$.

- *Inverse cascade* is a property of magnetized turbulence that magnetic energy may transfer from small scales to large scales. This is a tendency opposite to the *forward cascade* characteristic for unmagnetized turbulence in which energy trasfers from large scales to small scales. Inverse cascade is possible due to the magnetic tension which tries to shorten magnetic field lines as much as allowed by their topology. Complex topologies can be simplified locally by means of magnetic reconnection. A related problem of *magnetic relaxation* (Taylor, 1974), in which magnetic fields of short coherence scale relax to a configuration characterized by long coherence scale, has been studied numerically (e.g., Zrake & East, 2016).

Force-free electrodynamics. In certain situations, the Lorentz force density may vanish $\vec{f}_{\text{L}} = 0$. In particular, this can be expected in regions dominated energetically by magnetic fields (pulsar magnetospheres, base regions of relativistic jets), where the pressure and inertia of matter can be neglected. A basic consequence of vanishing Lorentz force is that $\vec{f}_{\text{L}} \cdot \vec{B} = \rho_{\text{e}}(\vec{E} \cdot \vec{B}) = 0$. Unless $\rho_{\text{e}} = 0$ (e.g., in the vacuum), this can be satisfied for $\vec{E} \cdot \vec{B} = 0$. It is then possible to derive an explicit formula for current density $\vec{j}$ as function of instantaneous $\vec{E}, \vec{B}$ fields (without any time derivatives). First, consider the change of $\vec{E} \cdot \vec{B}$, using the Maxwell-Faraday equation to eliminate $\partial \vec{B}/\partial t$:

$$0 = \frac{\partial}{c\,\partial t}\left(\vec{E} \cdot \vec{B}\right) = \vec{B} \cdot \frac{\partial \vec{E}}{c\,\partial t} + \vec{E} \cdot \frac{\partial \vec{B}}{c\,\partial t} = \vec{B} \cdot \frac{\partial \vec{E}}{c\,\partial t} - \vec{E} \cdot \left(\vec{\nabla} \times \vec{E}\right) . \tag{1.32}$$

Next, use the Ampère-Maxwell equation to eliminate the $\partial \vec{E}/\partial t$ term:

$$\vec{B} \cdot \left(\vec{\nabla} \times \vec{B}\right) = \frac{4\pi}{c} \vec{B} \cdot \vec{j} + \vec{B} \cdot \frac{\partial \vec{E}}{c\,\partial t} \, , \tag{1.33}$$

$$\vec{j} \cdot \vec{B} = \frac{c}{4\pi}\left[\vec{B} \cdot \left(\vec{\nabla} \times \vec{B}\right) - \vec{E} \cdot \left(\vec{\nabla} \times \vec{E}\right)\right] . \tag{1.34}$$

Finally, we take the cross produce $\vec{f}_{\text{L}} \times \vec{B}$:

$$0 = \frac{\vec{\nabla} \cdot \vec{E}}{4\pi}\vec{E} \times \vec{B} + \frac{1}{c}\left[\left(\vec{j} \cdot \vec{B}\right)\vec{B} - B^2 \vec{j}\right] \tag{1.35}$$

$$B^2 \vec{j} = c\frac{\vec{\nabla} \cdot \vec{E}}{4\pi}\vec{E} \times \vec{B} + \left(\vec{j} \cdot \vec{B}\right)\vec{B} \tag{1.36}$$

$$\vec{j}(\vec{E}, \vec{B}) = \frac{c}{4\pi B^2}\left\{\left(\vec{\nabla} \cdot \vec{E}\right)\left(\vec{E} \times \vec{B}\right) + \vec{B}\left[\vec{B} \cdot \left(\vec{\nabla} \times \vec{B}\right) - \vec{E} \cdot \left(\vec{\nabla} \times \vec{E}\right)\right]\right\} \tag{1.37}$$

Using this relation, it is possible to construct numerical codes that evolve $\vec{E}, \vec{B}$ fields in highly magnetized environments, including covariant formulations in general relativity (e.g., McKinney, 2006).

Electromagnetic potentials. The electric and magnetic fields can be expressed in terms of the *electric scalar potential* ϕ and *magnetic vector potential* $\vec{A}$:

$$\vec{E} = -\frac{1}{c}\frac{\partial \vec{A}}{\partial t} - \vec{\nabla}\phi \, , \tag{1.38}$$

$$\vec{B} = \vec{\nabla} \times \vec{A} \, . \tag{1.39}$$

The electromagnetic potentials by design satisfy the Gauss law for magnetic fields (Eq. 1.7) and the Maxwell-Faraday equation (Eq. 1.8).

Given the $\vec{E}, \vec{B}$ fields, the potential values are not unique and they can be fixed using an arbitrary *gauge function* $\psi(t, \vec{r})$, such that $\vec{A} \to \vec{A} + \vec{\nabla}\psi$ and $\phi \to \phi - (1/c)\partial_t \psi$. The most common gauge conditions are:

---

[2]$\partial_\mu \equiv \partial/\partial x^\mu$ for $\mu \in \{0, 1, 2, 3\}$ with $x^0 = ct$

- *Coulomb gauge*: $\vec{\nabla} \cdot \vec{A} = 0$, most suitable for slowly varying fields;

- *Lorenz gauge*: $\partial_\mu A^\mu = (1/c)\partial_t \phi + \vec{\nabla} \cdot \vec{A} = 0$, introducing the *electromagnetic four-potential* $A^\mu = (\phi, \vec{A})$, most suitable for rapidly varying fields (radiation).

Magnetic moment and dipole   Sources of magnetic field (e.g., magnets) can be characterized by the *magnetic moment* $\vec{m}$. When placed in external magnetic field $\vec{B}_0$, a torque is induced $\vec{\tau} = \vec{m} \times \vec{B}_0$. Magnetic moment generates a *magnetic dipole* described by vector potential

$$\vec{A} = \frac{\vec{m} \times \vec{R}}{R^3}\,. \tag{1.40}$$

In cylindrical coordinates (r, ϕ, z) in which $\vec{m} = (0, 0, m)$ we have

$$\vec{A} = \frac{mr}{R^3}\,\hat{\phi} = \frac{m}{R^2}\sin\theta\,\hat{\phi}\,. \tag{1.41}$$

where $\theta = \angle(\vec{m}, \vec{R})$. The corresponding dipole magnetic field is:

$$\begin{aligned}
\vec{B} &=& \vec{\nabla} \times \vec{A} = -\frac{\partial A_\phi}{\partial z}\hat{r} + \left(\frac{A_\phi}{r} + \frac{\partial A_\phi}{\partial r}\right)\hat{z}\,, \tag{1.42} \\
\vec{B} &=& \frac{m}{R^3}\left[3\sin\theta\cos\theta\,\hat{r} + (3\cos^2\theta - 1)\hat{z}\right] = \frac{1}{R^3}\left[3\left(\vec{m}\cdot\hat{R}\right)\hat{R} - \vec{m}\right]\,. \tag{1.43}
\end{aligned}$$

   Magnetic dipole is the lowest-order component of the multipole expansion and the simplest example of a *poloidal field* (a field that in spherical coordinates (R, θ, ϕ) has only B_R, B_θ components). The dipole magnetic field strength decays like R^{-3}, and it dominates over higher-order components at large distances (in the so-called far-field regime).

- Magnetic dipole with magnetic moment m_0 is the field produced by a thin circular loop of electric current $I_0 = m_0/\pi R_0^2$ in the limit of infinitely small loop radius $R_0 \to 0$ (e.g., Jackson, 1998).

2   Magnetohydrodynamics (MHD)

Lorentz transformation.   Electromagnetic fields undergo Lorentz transformation. The transformation of components parallel and perpendicular to the boost vector $\vec{v} = \vec{\beta}c$ is:

$$\begin{aligned}
\vec{E}'_\parallel &=& \vec{E}_\parallel\,, \tag{2.1} \\
\vec{B}'_\parallel &=& \vec{B}_\parallel\,, \tag{2.2} \\
\vec{E}'_\perp &=& \Gamma\left(\vec{E}_\perp + \vec{\beta} \times \vec{B}\right)\,, \tag{2.3} \\
\vec{B}'_\perp &=& \Gamma\left(\vec{B}_\perp - \vec{\beta} \times \vec{E}\right)\,, \tag{2.4}
\end{aligned}$$

where $\Gamma = (1 - \beta^2)^{-1/2}$ is the Lorentz factor. These equations can be generalized to:

$$\begin{aligned}
\vec{E}' &=& \Gamma\vec{E} - \frac{\Gamma - 1}{\beta^2}\left(\vec{E}\cdot\vec{\beta}\right)\vec{\beta} + \Gamma\vec{\beta} \times \vec{B}\,, \tag{2.5} \\
\vec{B}' &=& \Gamma\vec{B} - \frac{\Gamma - 1}{\beta^2}\left(\vec{B}\cdot\vec{\beta}\right)\vec{\beta} - \Gamma\vec{\beta} \times \vec{E}\,. \tag{2.6}
\end{aligned}$$

One can also demonstrate the invariance of $E^2 - B^2$:

$$\begin{aligned}
(E')^2 - E^2 = (B')^2 - B^2 &=& \Gamma^2\left[(\vec{\beta} \times \vec{B})^2 + (\vec{\beta} \times \vec{E})^2 - 2\vec{\beta}\cdot(\vec{E} \times \vec{B})\right]\,, \tag{2.7} \\
(E')^2 - (B')^2 &=& E^2 - B^2\,. \tag{2.8}
\end{aligned}$$

- It can also be shown that Maxwell's equations are Lorentz invariant.

In the non-relativistic limit $\beta \ll 1$, hence $\Gamma \simeq 1 + \beta^2/2$, one can show that the transformation reduces to:

$$
\begin{aligned}
\vec{E}' &\simeq \vec{E} + \vec{\beta} \times \vec{B}\,, & (2.9) \\
\vec{B}' &\simeq \vec{B} - \vec{\beta} \times \vec{E}\,. & (2.10)
\end{aligned}
$$

One can note that the Lorentz transformations of $\vec{E}, \vec{B}$ fields are quite symmetric.

Ohm's law. The co-moving electric field $\vec{E}'$ and be related to the co-moving current density $\vec{j}'$ by an Ohm's law. A basic Ohm's law has the form $\vec{j}' = \sigma \vec{E}'$ with the scalar *electric conductivity* σ. If the conductivity is sufficiently high ($\sigma \gg c^2/vL$), we have $E' \ll E$, hence $\vec{E} \simeq \vec{B} \times \vec{\beta}$, hence $E \sim B\beta \ll B$, hence $\vec{B}' \simeq \vec{B}$. Hence, the symmetry of the Lorentz transformations is broken. One can further show that $\vec{j}' \simeq \vec{j}$, which means that in general reference frame $\vec{j} \simeq \sigma \left(\vec{E} + \vec{\beta} \times \vec{B} \right)$.

Magnetic diffusivity. Electric conductivity σ can be associated with the resistive (Faraday) time scale $\tau_\sigma = 1/(4\pi\sigma)$. We also introduce the electric field variability time scale $\tau_E = E/|\partial E/\partial t|$ in order to scale the displacement current term in the Ampère-Maxwell equation:

$$
\begin{aligned}
\vec{\nabla} \times \vec{B} &\simeq \frac{\vec{E} + \vec{\beta} \times \vec{B}}{c\tau_\sigma} + \frac{\vec{E}}{c\tau_E}\,, & (2.11) \\
\left(1 + \frac{\tau_\sigma}{\tau_E}\right) \vec{E} &\simeq \vec{B} \times \vec{\beta} + \frac{\eta}{c}\left(\vec{\nabla} \times \vec{B}\right)\,. & (2.12)
\end{aligned}
$$

where we introduced the *magnetic diffusivity* $\eta = \tau_\sigma c^2 = c^2/(4\pi\sigma)$.

The displacement current term can be neglected for $\tau_E \gg \tau_\sigma$. From the Spitzer resistivity, the standard estimate for magnetic diffusivity is $\eta \simeq 10^4\, T_6^{-3/2}\ \mathrm{cm^2\,s^{-1}}$ with $T_6 = T/(10^6\,\mathrm{K})$ (e.g., Brandenburg & Subramanian, 2005). This implies microscopically small resistive length scales $c\tau_\sigma \simeq 3\,T_6^{-3/2}\ \mathrm{nm}$, hence *it is really safe to neglect the displacement current for all astrophysical objects*. When we do that, we have:

$$
\begin{aligned}
\vec{j} &\simeq \frac{c}{4\pi}\left(\vec{\nabla} \times \vec{B}\right)\,, & (2.13) \\
\vec{E} &\simeq \vec{B} \times \vec{\beta} + \frac{\eta}{c}\left(\vec{\nabla} \times \vec{B}\right)\,. & (2.14)
\end{aligned}
$$

The Maxwell-Faraday equation becomes the *induction equation*:

$$
\frac{\partial \vec{B}}{\partial t} = \vec{\nabla} \times \left(\vec{v} \times \vec{B} - \eta \vec{\nabla} \times \vec{B}\right)\,, \tag{2.15}
$$

the basic equation of *resistive magnetohydrodynamics* (MHD).

Magnetic diffusion. For a static equilibrium ($\vec{v} = 0$) with uniform η, the induction equation reduces to:

$$
\frac{\partial \vec{B}}{\partial t} = \eta \nabla^2 \vec{B}\,. \tag{2.16}
$$

This is a diffusion equation (Fick's second law) with diffusion coefficient η.

Example: for a Gaussian magnetic field $B_x(t, y) = B_0(t) \exp\left[-y^2/2\sigma_y^2(t)\right]$, the solution is $\sigma_y(t) = \sqrt{2\eta t}$ and $B_0(t) \propto 1/\sqrt{t}$.

Diffusive time scale. For a system of finite length scale L, magnetic diffusivity can be associated with the *diffusive time scale* $\tau_\eta = L^2/\eta$.[3] This is the time scale on which magnetic field strength decays in the absence of regeneration mechanism. It can be estimated for key astrophysical objects as follows:

- Earth's outer core: $L \sim 3.5 \times 10^8$ cm, $T \sim 3 \times 10^3$ K, $\eta \sim 10^4$ cm^2/s, resulting in $\tau_\eta \sim 5 \times 10^4$ yr, very short on geological scale.

- Sun's interior: $L \sim 1.5 \times 10^{10}$ cm, $T \sim 10^7$ K, $\eta \sim 2 \times 10^3$ cm^2/s, resulting in $\tau_\eta \sim 2 \times 10^{10}$ yr, longer than the Sun's age.

- Galaxy: $L \sim 6 \times 10^{20}$ cm, $T \sim 10^3$ K, $\eta \sim 3 \times 10^8$ cm^2/s, resulting in $\tau_\eta \sim 4 \times 10^{25}$ yr, much longer than the Universe's age.

Magnetic Reynolds and Prandtl numbers. Given a characteristic velocity scale v, the diffusive time scale τ_η can be compared with the *dynamical time scale* $\tau_v = L/v$. The ratio of these time scales is known as the *magnetic Reynolds number*:

$$R_{\rm m} \equiv \frac{\text{induction}}{\text{diffusion}} = \frac{\tau_\eta}{\tau_v} = \frac{vL}{\eta}\,. \tag{2.17}$$

Magnetic diffusivity η is analogous to the *kinematic viscosity* ν in fluid dynamics. Both these parameters have the same units cm^2/s. In the same sense, magnetic Reynolds number is analogous to the *Reynolds number*:

$$R \equiv \frac{\text{advection}}{\text{viscosity}} = \frac{\tau_\nu}{\tau_v} = \frac{vL}{\nu}\,, \tag{2.18}$$

where $\tau_\nu = L^2/\nu$ is the *viscous time scale*. Furthermore, magnetic diffusivity can be compared directly to kinematic viscosity through the *magnetic Prandtl number*:

$$P_{\rm m} = \frac{R_{\rm m}}{R} \equiv \frac{\text{viscosity}}{\text{diffusion}} = \frac{\tau_\eta}{\tau_\nu} = \frac{\nu}{\eta}\,. \tag{2.19}$$

Typical values of $R_{\rm m}$ and $P_{\rm m}$ for various astrophysics objects are reported in Table 1 of Brandenburg & Subramanian (2005). Most of these objects are inferred to have $R_{\rm m} \gg 1$ (except the protostellar disks with $R_{\rm m} \sim 10$), which means that induction dominates the diffusion. At the same time, stellar-scale objects have $P_{\rm m} \ll 1$ (diffusion dominates the viscosity), while galaxy-scale objects have $P_{\rm m} \gg 1$ (viscosity dominates the diffusion).

Ideal MHD. Since most astrophysical systems satisfy $R_{\rm m} \gg 1$ (which is equivalent to $L \gg \eta/v$ or $\sigma \gg c^2/vL$), at least globally, magnetic diffusion can often be neglected. This leads us to the limit of *ideal MHD* with simplified expressions for the electric field and the induction equation:

$$\vec{E} \quad \simeq \quad \vec{B} \times \vec{\beta}\,, \tag{2.20}$$

$$\frac{\partial \vec{B}}{\partial t} \quad \simeq \quad \vec{\nabla} \times \left(\vec{v} \times \vec{B}\right)\,. \tag{2.21}$$

Additional microscopic conditions for ideal MHD can be formulated using two dimensionless parameters: $y = \langle R_{\rm L}\rangle/L$, the ratio of typical gyroradius $\langle R_{\rm L}\rangle$ to the system size L; and $x = \sqrt{m_i/m_e}(\langle v\rangle\,\tau_{\rm coll}/L)$, with $\langle v\rangle$ the mean thermal particle speed, and $\tau_{\rm coll}$ the collisional time scale. These conditions are:

1. small gyroradius: $y \ll 1$;

2. large collisionality: $x \ll 1$;

3. small resistivity: $y^2 \ll x$.

For more details, see Sec. II.G-H of Freidberg (1982).

---

[3]For dipole magnetic field, it can be defined more accurately as $\tau_\eta = L^2/(\pi^2\eta)$.

Magnetic flux freezing. In a plasma satisfying the ideal MHD limit, consider a surface S at time t threaded by the magnetic flux $\Phi(t) = \iint_S \vec{B}(t) \cdot d\vec{S}$. The surface evolves by following the velocity field $\vec{U}$ and by the time $t' = t + \delta t$ it becomes surface S' that has magnetic flux $\Phi'(t') = \iint_{S'} \vec{B}(t') \cdot d\vec{S}'$ and that has swept volume element δV. Note that the tube connecting the surfaces S and S' is not a magnetic flux tube, it is defined by the velocity field and there may be net magnetic flux through its sides. Indeed, the magnetic flux through the sides at time t' can be related to the magnetic fluxes through S and S' using the divergence theorem:

$$\Phi'(t') - \Phi(t') + \Phi_{\text{side}}(t') = \iiint_{dV} \left(\vec{\nabla} \cdot \vec{B}(t') \right) dV = 0 \,, \tag{2.22}$$

$$\Phi_{\text{side}}(t') = \oint_C \vec{B}(t') \cdot \left(d\vec{l} \times \vec{U} \, dt \right) . \tag{2.23}$$

Using the cyclic identity for the scalar triple product $\left(d\vec{l} \times \vec{U} \right) \cdot \vec{B} = \left(\vec{U} \times \vec{B} \right) \cdot d\vec{l}$, we find:

$$\frac{d\Phi}{dt} = \frac{\partial \Phi}{\partial t} - \oint_C \left(\vec{U} \times \vec{B} \right) \cdot d\vec{l}. \tag{2.24}$$

Finally we apply to Stokes' theorem to convert the contour integral into surface integral:

$$\frac{d\Phi}{dt} = \iint_S \frac{\partial \vec{B}}{\partial t} \cdot d\vec{S} - \iint_S \vec{\nabla} \times \left(\vec{U} \times \vec{B} \right) \cdot d\vec{S} = \iint_S \left[\frac{\partial \vec{B}}{\partial t} - \vec{\nabla} \times \left(\vec{U} \times \vec{B} \right) \right] \cdot d\vec{S}. \tag{2.25}$$

In the final term we identify the induction equation for ideal MHD, hence $d\Phi = 0$, which means that *magnetic flux is frozen into the flow*. This result is also known as the *Alfvén theorem*.

This derivation followed Section 3.3 and Figure 3.1 of Brandenburg & Subramanian (2005).

Lorentz force density in non-relativistic MHD. Recall that the general form of the Lorentz force density is $\vec{f}_L = \rho_e \vec{E} + \frac{1}{c} \left(\vec{j} \times \vec{B} \right)$. In ideal MHD, both the electric charge and current densities can be expressed as functions of magnetic and velocity fields:

$$\rho_e = \frac{1}{4\pi} \vec{\nabla} \cdot \vec{E} = \frac{1}{4\pi c} \vec{\nabla} \cdot \left(\vec{B} \times \vec{v} \right) \,, \tag{2.26}$$

$$\vec{j} = \frac{c}{4\pi} \left(\vec{\nabla} \times \vec{B} \right) . \tag{2.27}$$

In the non-relativistic limit $\beta \ll 1$, the $\rho_e \vec{E}$ term is $\mathcal{O}(\beta^2 B^2)$ and it can be neglected. The Lorentz force density is then

$$\vec{f}_L \simeq \frac{1}{4\pi} \left[\left(\vec{\nabla} \times \vec{B} \right) \times \vec{B} \right] = \frac{1}{4\pi} \left(\vec{B} \cdot \vec{\nabla} \right) \vec{B} - \frac{1}{8\pi} \vec{\nabla} \left(B^2 \right) . \tag{2.28}$$

The first term on the RHS is the magnetic tension, the mathematic form of which is a material derivative. A basic example of a field that has a tension is toroidal field in cylindrical coordinates $\vec{B} = B_\phi(r, z)\hat{\phi}$, in which case the tension force is directed radially inwards:

$$\left(\vec{B} \cdot \vec{\nabla} \right) \vec{B} = -\frac{B_\phi^2}{r} \hat{r} \,. \tag{2.29}$$

The second term on the RHS of Eq. (2.28) is the gradient of magnetic pressure $-\vec{\nabla}(B^2/8\pi) \equiv -\vec{\nabla} P_B$. A basic example is a unidirectional field with strength gradient perpendicular to the field line $\vec{B} = B_x(y)\hat{x}$, for which

$$\vec{\nabla} \left(B^2 \right) = \frac{\partial(B_x^2)}{\partial y} \hat{y} \,. \tag{2.30}$$

Uniform magnetic field is force-free. Non-zero Lorentz force requires some structure in the magnetic fields, although it is possible to have structured magnetic fields that are force-free.

Energy-momentum tensor in ideal MHD. Substituting $\vec{E} = \vec{B} \times \vec{\beta}$ to the energy-momentum tensor, one obtains:

$$T_{\mathrm{EM}}^{00} = u_{\mathrm{EM}} = \frac{E^2 + B^2}{8\pi} = \frac{(1+\beta^2)B^2 - (\vec{\beta} \cdot \vec{B})^2}{8\pi}\,, \tag{2.31}$$

$$T_{\mathrm{EM}}^{0i} = \frac{S^i}{c} = \frac{1}{4\pi}\left(\vec{E} \times \vec{B}\right)^i = \frac{B^2\beta^i - (\vec{\beta} \cdot \vec{B})B^i}{4\pi}\,, \tag{2.32}$$

$$\begin{aligned} T_{\mathrm{EM}}^{ij} &= \frac{E^2 + B^2}{8\pi}\delta^{ij} - \frac{E^i E^j + B^i B^j}{4\pi} \\ &= \frac{B^2}{4\pi}\beta^i\beta^j + \frac{(1-\beta^2)B^2 + (\vec{\beta} \cdot \vec{B})^2}{8\pi}\delta^{ij} - (1-\beta^2)\frac{B^i B^j}{4\pi} - \frac{\vec{\beta} \cdot \vec{B}}{4\pi}\left(\beta^i B^j + \beta^j B^i\right)\,. \end{aligned} \tag{2.33}$$

3 Fluid dynamics

This is a concise summary of essential fluid dynamics without magnetic fields, that will be used in the subsequent sections. We attempt to introduce a consistent notation, paying particular attention to distinguishing the extensive parameters (e.g., particle number δN) from the intensive parameters (e.g., particle number density n). This section is partially based on Thorne & Blandford (2017).

Conservation of particle number and mass, continuity equation. Consider a Lagrangian volume element δV containing δN particles. The particle number density is $n = \delta N/\delta V$. Unless particles can be created or destroyed, *the particle number is conserved*, $\mathrm{d}(\delta N) = 0$.

For particles of mass m the mass element $\delta M = m\,\delta N$ is conserved, $\mathrm{d}(\delta M) = 0$. Mass density is $\rho = \delta M/\delta V = mn$.

A volume element evolves according to the local velocity field $\vec{v}(\vec{r})$. During a time interval $\mathrm{d}t$ it will be displaced by $\mathrm{d}\vec{r} = \vec{v}\,\mathrm{d}t$ and expand by $\mathrm{d}(\delta V) = \delta V \left(\vec{\nabla} \cdot \vec{v}\right)\mathrm{d}t$.

We now use the material derivative to express the variation of particle density:

$$\frac{\partial n}{\partial t} + \left(\vec{v} \cdot \vec{\nabla}\right)n = \frac{\mathrm{d}n}{\mathrm{d}t} = \frac{\mathrm{d}(\delta N/\delta V)}{\mathrm{d}t} = -n\left(\vec{\nabla} \cdot \vec{v}\right)\,. \tag{3.1}$$

From this one can derive the *continuity equation*

$$\frac{\partial n}{\partial t} + \vec{\nabla} \cdot (n\vec{v}) = 0\,, \tag{3.2}$$

which has an identical form for the mass density ρ.

Conservation of momentum, Euler equation. Consider a force $\delta\vec{F}$ acting on a fluid element of volume δV, mass δM, velocity $\vec{v}$ and momentum $\delta\vec{p} = \vec{v}\,\delta M = \rho\vec{v}\,\delta V$. The Newton's second law states that:

$$\delta\vec{F} = \frac{\mathrm{d}(\delta\vec{p})}{\mathrm{d}t} = \frac{\mathrm{d}\vec{v}}{\mathrm{d}t}\,\delta M\,. \tag{3.3}$$

From that, one can derive the *Euler's equation*:

$$\frac{\partial\vec{v}}{\partial t} + (\vec{v} \cdot \vec{\nabla})\vec{v} = \frac{\mathrm{d}\vec{v}}{\mathrm{d}t} = \frac{\delta\vec{F}}{\delta M} = \frac{\vec{f}}{\rho}\,, \tag{3.4}$$

introducing the *force density* $\vec{f} = \delta\vec{F}/\delta V$. Combined with the continuity equation, this can also be written in a tensor form $\partial_t(\rho v^i) + \partial_j(\rho v^i v^j) = f^i$.

Kinetic energy density. This is defined as $u_{\text{kin}} = \delta\mathcal{E}_{\text{kin}}/\delta V = \rho v^2/2$. The dot product of the Euler's equation with velocity

$$\vec{v} \cdot \left[\frac{\partial \vec{v}}{\partial t} + (\vec{v} \cdot \vec{\nabla})\vec{v}\right] = \vec{v} \cdot \frac{\vec{f}}{\rho} \tag{3.5}$$

combined with the continuity equation results in the evolution equation for kinetic energy density:

$$\frac{\partial u_{\text{kin}}}{\partial t} + \vec{\nabla} \cdot (u_{\text{kin}}\vec{v}) = \frac{\mathrm{d}u_{\text{kin}}}{\mathrm{d}t} + u_{\text{kin}}\left(\vec{\nabla} \cdot \vec{v}\right) = \vec{f} \cdot \vec{v}, \tag{3.6}$$

where the last term represents work done on the fluid element in unit time.

Internal energy density. This is defined as $u_{\text{int}} = \delta\mathcal{E}_{\text{int}}/\delta V$. The first law of thermodynamics states that $\mathrm{d}(\delta\mathcal{E}_{\text{int}}) = T\,\mathrm{d}(\delta S) - P\,\mathrm{d}(\delta V)$, where T is the temperature, δS is the entropy element, and P is the pressure. In an adiabatic process, entropy is conserved, $\mathrm{d}(\delta S) = 0$, hence $\mathrm{d}(\delta\mathcal{E}_{\text{int}}) = -P\,\mathrm{d}(\delta V)$. In term of the internal energy energy, this corresponds to:

$$\frac{\mathrm{d}u_{\text{int}}}{\mathrm{d}t} = -(u_{\text{int}} + P)\left(\vec{\nabla} \cdot \vec{v}\right). \tag{3.7}$$

One can introduce the enthalpy density $w = u_{\text{int}} + P = \kappa u_{\text{int}}$, where κ is the adiabatic index (specific heats ratio). For ideal non-relativistic monoatomic gas: $\kappa = 5/3$, $u_{\text{int}} = (3/2)P$ and $w = (5/2)P$. Since $u_{\text{int}} \propto P$, one can write an equation for pressure evolution:

$$\frac{\partial P}{\partial t} + \left(\vec{v} \cdot \vec{\nabla}\right)P = \frac{\mathrm{d}P}{\mathrm{d}t} = -\kappa P\left(\vec{\nabla} \cdot \vec{v}\right). \tag{3.8}$$

Conservation of energy. We have seen that (1) kinetic energy density u_{kin} changes due to work (density) $\vec{f} \cdot \vec{v}$ done by force density $\vec{f}$, on the other hand (2) internal energy density u_{int} is proportional to pressure P. Pressure gradient is a force density $\vec{f}_{\text{P}} = -\vec{\nabla}P$ In the absence of other forces, the work done by pressure gradient on a fluid element changes its kinetic energy:

$$\mathrm{d}(\delta\mathcal{E}_{\text{kin}}) = \mathrm{d}(\delta W_{\text{P}}) = \delta V\left(\vec{f}_{\text{P}} \cdot \vec{v}\right)\mathrm{d}t = -\delta V\,\mathrm{d}P. \tag{3.9}$$

Compare this with the internal energy change and combine them to obtain the total energy change:

$$\mathrm{d}(\delta\mathcal{E}_{\text{int}}) = -P\,\mathrm{d}(\delta V), \tag{3.10}$$

$$\mathrm{d}(\delta\mathcal{E}_{\text{tot}}) = \mathrm{d}(\delta\mathcal{E}_{\text{kin}} + \delta\mathcal{E}_{\text{int}}) = -\mathrm{d}(P\,\delta V). \tag{3.11}$$

Conservation of total energy of a fluid element can be thus stated as:

$$\mathrm{d}(\delta\mathcal{E}_{\text{tot}} + P\,\delta V) = 0. \tag{3.12}$$

Dividing this equation by the mass element δM leads to the *Bernoulli's equation*:

$$\frac{\mathrm{d}(\delta\mathcal{E}_{\text{tot}} + P\,\delta V)}{\delta M} = \mathrm{d}\left(\frac{v^2}{2} + \frac{w}{\rho}\right) = 0. \tag{3.13}$$

One can also obtain an equivalent tensor form:

$$\frac{\partial u_{\text{tot}}}{\partial t} + \vec{\nabla} \cdot [(u_{\text{tot}} + P)\,\vec{v}] = 0. \tag{3.14}$$

It is important to note that evolution of kinetic energy derives entirely from the conservation of mass and momentum. Given those two conservation laws, the conservation of total energy is equivalent to the evolution of pressure dictated by the adopted equation of state.

Conservation of entropy, adiabatic equation of state. The velocity divergence can be used to relate the variations of density and pressure:

$$\vec{\nabla} \cdot \vec{v} = -\frac{1}{\rho}\frac{d\rho}{dt} = -\frac{1}{\kappa P}\frac{dP}{dt}. \tag{3.15}$$

This is equivalent the invariance of $d[\ln(P/\rho^\kappa)] = 0$ (the *adiabatic invariant*), which implies an *adiabatic equation of state* $P \propto \rho^\kappa$ (valid for any given Lagrangian fluid element).

The adiabatic invariant is related to the specific entropy (entropy per unit mass) $s = \delta S/\delta M = c_V \ln(P/\rho^\kappa)$, where $c_V = (3/2)(k_B/m)$ is the specific heat capacity at constant volume. Specific entropy of a given fluid element is thus an invariant, $ds = 0$. Moreover, the conservation of mass implies the conservation of entropy $d(\delta S) = 0$.

Linearization of the conservation equations. Fluid dynamics can thus be described using 3 equations expressing the conservation of mass (continuity equation), conservation of momentum (Euler's equation), and conservation of energy (pressure equation derived from the adiabatic equation of state). Various physical phenomena can be investigated by considering a zero-order (background) stationary ($\partial_t = 0$) equilibrium and first-order (linear) perturbations. Every fluid parameter can be decomposed into background and perturbation components, e.g., mass density can be decomposed as $\rho = \rho_0 + \rho_1$, so that $|\rho_1| \ll |\rho_0|$, etc.

The linearized continuity, Euler's and pressure equations are:

$$\frac{\partial \rho_1}{\partial t} \quad + \quad \vec{\nabla} \cdot (\rho_1 \vec{v}_0) + \vec{\nabla} \cdot (\rho_0 \vec{v}_1) = 0, \tag{3.16}$$

$$\frac{\partial \vec{v}_1}{\partial t} \quad + \quad \left(\vec{v}_1 \cdot \vec{\nabla}\right)\vec{v}_0 + \left(\vec{v}_0 \cdot \vec{\nabla}\right)\vec{v}_1 = \frac{\vec{f}_1}{\rho_0} - \frac{\vec{f}_0}{\rho_0^2}\rho_1, \tag{3.17}$$

$$\frac{\partial P_1}{\partial t} \quad + \quad \left(\vec{v}_1 \cdot \vec{\nabla}\right)P_0 + \left(\vec{v}_0 \cdot \vec{\nabla}\right)P_1 + \kappa P_1 \left(\vec{\nabla} \cdot \vec{v}_0\right) + \kappa P_0 \left(\vec{\nabla} \cdot \vec{v}_1\right) = 0, \tag{3.18}$$

respectively.

Uniform static background, sound waves. Consider the case of a static ($\vec{v}_0 = 0$) and uniform (constant ρ_0, P_0) background. This implies that $\vec{f}_0 = -\vec{\nabla}P_0 = 0$, hence an equilibrium.

The linearized continuity, Euler's and pressure equations become:

$$\frac{\partial \rho_1}{\partial t} \quad = \quad -\rho_0 \left(\vec{\nabla} \cdot \vec{v}_1\right), \tag{3.19}$$

$$\frac{\partial \vec{v}_1}{\partial t} \quad = \quad -\frac{\vec{\nabla}P_1}{\rho_0}, \tag{3.20}$$

$$\frac{\partial P_1}{\partial t} \quad = \quad -\kappa P_0 \left(\vec{\nabla} \cdot \vec{v}_1\right), \tag{3.21}$$

respectively. Note that these equations imply a feedback loop between pressure perturbation P_1 and velocity perturbation $\vec{v}_1$, while the density perturbation ρ_1 is driven by $\vec{v}_1$ without a feedback. Hence, we only need to consider the Euler's and pressure equations.

Adopt an oscillatory velocity perturbation $\vec{v}_1 \propto \exp\left(i\omega t + i\vec{k} \cdot \vec{r}\right)$, where the frequency ω and the wave vector $\vec{k}$ are independent of time and space.

The pressure equation becomes:

$$i\omega P_1 = -\kappa P_0 \left(i\vec{k} \cdot \vec{v}_1\right). \tag{3.22}$$

Since P_0 is uniform, this implies that pressure perturbation has the same oscillatory form $P_1 \propto \exp\left(i\omega t + i\vec{k} \cdot \vec{r}\right)$.

The Euler equation becomes:

$$i\omega \vec{v}_1 = -\frac{i\vec{k}P_1}{\rho_0} = \frac{i\vec{k}}{\rho_0}\frac{\kappa P_0}{\omega}\left(\vec{k} \cdot \vec{v}_1\right). \tag{3.23}$$

Taking a dot product with $-i\omega\vec{k}$:

$$\omega^2 \left(\vec{k} \cdot \vec{v}_1 \right) = k^2 \frac{\kappa P_0}{\rho_0} \left(\vec{k} \cdot \vec{v}_1 \right) . \tag{3.24}$$

This results in a *dispersion relation*

$$\frac{\omega^2}{k^2} = \frac{\kappa P_0}{\rho_0} \equiv c_{\mathrm{s},0}^2 \tag{3.25}$$

the describes a stable ($\omega^2 > 0$) wave – the *sound wave*, for which $c_{\mathrm{s},0}$ is both the phase and group speed (uniform and isotropic) – the *speed of sound*.

Maxwell-Jüttner distribution, relativistic ideal gas.   We have so far discussed the properties of non-relativistic ideal gas, for which the adiabatic index is $\kappa = 5/3$, and the speed of sound is $c_{\mathrm{s}} = \sqrt{\kappa P/\rho}$. The particles of such gas satisfy the *Maxwell-Boltzmann velocity distribution*:

$$f(\vec{v})\, \mathrm{d}^3 v \quad = \quad \left(\frac{m}{2\pi k_{\mathrm{B}} T} \right)^{3/2} \exp\left(-\frac{mv^2}{2k_{\mathrm{B}} T} \right)\, \mathrm{d}^3 v\,, \tag{3.26}$$

where k_{B} is the Boltzmann's constant. This distribution is valid as long $k_{\mathrm{B}} T \ll mc^2$, or introducing dimensionless relativistic temperature $\Theta = k_{\mathrm{B}} T/mc^2 \ll 1$.

The Maxwell-Boltzmann distribution can be generalized to the *Maxwell-Jüttner energy distribution*, which is valid for arbitrary temperatures:

$$f(\gamma)\, \mathrm{d}\gamma = \frac{\gamma^2 \beta\, \mathrm{d}\gamma}{\Theta\, K_2(1/\Theta)} \exp\left(-\frac{\gamma}{\Theta} \right)\,, \tag{3.27}$$

where $\gamma = (1 - \beta^2)^{-1/2}$ is the particle Lorentz factor (dimensionless energy), and $K_2(x)$ is the modified Bessel function of the second kind. Using this distribution one can calculate: the mean particle particle energy $\langle \gamma \rangle = 3\Theta + h(\Theta)$, where $h(\Theta) = K_1(1/\Theta)/K_2(1/\Theta)$; pressure $P = nk_{\mathrm{B}} T = \Theta\rho c^2$; relativistic enthalpy density $w = \rho c^2 + [\kappa/(\kappa - 1)]P = [4\Theta + h(\Theta)]\rho c^2$; adiabatic index $\kappa = 1 + \Theta/(\langle \gamma \rangle - 1)$; the speed of sound $c_{\mathrm{s}} = c\sqrt{\kappa P/w}$.

In the limit of non-relativistic temperatures ($\Theta \ll 1$), with $h(\Theta) \simeq 1 - \frac{3}{2}\Theta$, one obtains the standard results, e.g., $\kappa = 5/3$, $w \simeq \rho c^2 + (5/2)P$ and $c_{\mathrm{s}} = c\sqrt{(5/3)\Theta}$.

In the limit of ultra-relativistic temperatures ($\Theta \gg 1$), with $h(\Theta) \simeq 1/(2\Theta)$, one obtains $\kappa \simeq 4/3$, $w \simeq 4P$ and $c_{\mathrm{s}} \simeq c/\sqrt{3}$.

Relativistic fluid equations.   For a fluid propagating in a *laboratory reference frame* with relativistic bulk velocity $\vec{v} = \vec{\beta} c$ we define the bulk Lorentz factor $\Gamma = (1 - \beta^2)^{-1/2}$ and four-velocity $u^\mu = \Gamma(c, \vec{v}) = u(1, \vec{\beta})$.

The continuity equation can be written in the following form:

$$\partial_\mu \left(\rho u^\mu \right) = 0\,, \tag{3.28}$$

where $\partial_\mu \equiv \partial/\partial x^\mu$ with $x^\mu = (ct, \vec{x})$. This can be expanded to:

$$\frac{\partial(\Gamma\rho)}{\partial t} + \vec{\nabla} \cdot (\Gamma\rho\,\vec{v}) = 0\,. \tag{3.29}$$

In the above, ρ is the mass density measured in the fluid *co-moving reference frame*, and $\Gamma\rho$ is the mass density measured in the laboratory frame.

The conservation equations for the energy and momentum can be written as:

$$\partial_\mu T_{\mathrm{fl}}^{\mu\nu} = 0\,, \tag{3.30}$$

where $T_{\mathrm{fl}}^{\mu\nu}$ is the energy-momentum tensor of the fluid. For an ideal gas with isotropic pressure P:

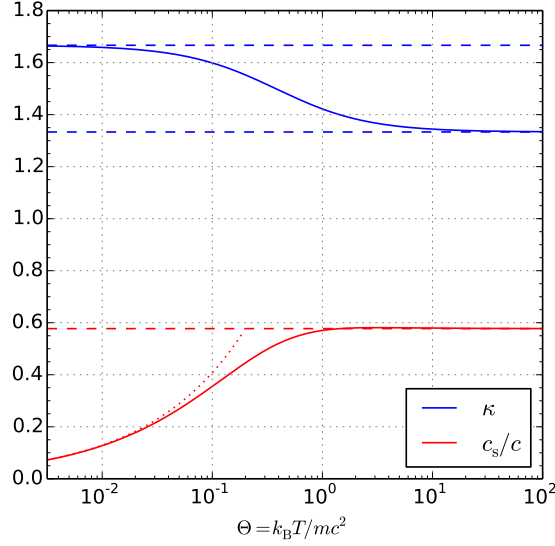$$T_{\mathrm{fl}}^{\mu\nu} = w\frac{u^\mu u^\nu}{c^2} + Pg^{\mu\nu}\,, \tag{3.31}$$

14

Figure 1: Speed of sound c_s and adiabatic index κ as functions of the dimensionless temperature $\Theta = k_B T/mc^2$ calculated from the Maxwell-Jüttner distribution. The dashed red line indicates $1/\sqrt{3}$, the dotted red line indicates $\sqrt{(5/3)\Theta}$, the dashed blue lines indicate $4/3$ and $5/3$.

where $w = \rho c^2 + u_{\text{int}} + P$ is the relativistic enthalpy density, and $g^{\mu\nu}$ is the (Minkowski) metric tensor of signature $(-+++)$. Components of the energy-momentum tensor are:

$$
\begin{align}
T_{\text{fl}}^{00} &= \Gamma^2 w - P\,, \tag{3.32}\\
T_{\text{fl}}^{0i} &= \Gamma^2 w \beta^i\,, \tag{3.33}\\
T_{\text{fl}}^{ij} &= \Gamma^2 w \beta^i \beta^j + P\delta^{ij}\,. \tag{3.34}
\end{align}
$$

The energy and momentum equations can be expanded as:

$$
\begin{align}
0 &= \partial_t\left(\Gamma^2 w - P\right) + \vec{\nabla}\cdot\left(\Gamma^2 w\vec{v}\right)\,, \tag{3.35}\\
0 &= \partial_t\left(\Gamma^2 w v^i\right) + \partial_j\left(\Gamma^2 w v^i v^j\right) + \partial_i P c^2\,. \tag{3.36}
\end{align}
$$

In the limit of non-relativistic velocity $\beta = v/c \ll 1$ and non-relativistic temperature $\Theta = k_B T/mc^2 \ll 1$, substituting $w = \rho c^2 + u_{\text{int}} + P$, introducing the kinetic energy density $u_{\text{kin}} = \rho v^2/2$, using the continuity equation and the identity $\mathrm{d}\Gamma = \Gamma^3 \beta\, \mathrm{d}\beta \simeq \mathrm{d}\beta^2/2$, the energy equation becomes:

$$
\begin{align}
0 &= \rho c^2 \partial_t \Gamma + \partial_t u_{\text{int}} + \rho c^2 (\vec{v}\cdot\vec{\nabla})\Gamma + \vec{\nabla}\cdot\left[(u_{\text{int}} + P)\vec{v}\right]\,, \tag{3.37}\\
0 &= \partial_t(u_{\text{kin}} + u_{\text{int}}) + \vec{\nabla}\cdot\left[(u_{\text{kin}} + u_{\text{int}} + P)\,\vec{v}\right]\,, \tag{3.38}
\end{align}
$$

consistent with Eq. (3.14). The momentum equation becomes (keeping only the terms including c^2 factors):

$$
\begin{align}
0 &\simeq \rho c^2 \partial_t v^i + \partial_t[(u_{\text{int}} + P)v^i] + \rho c^2 (\vec{v}\cdot\vec{\nabla})v^i + \partial_j[(u_{\text{int}} + P)v^i v^j] + \partial_i P c^2\,, \tag{3.39}\\
0 &\simeq \rho\left(\partial_t + \vec{v}\cdot\vec{\nabla}\right)\vec{v} + \vec{\nabla}P\,, \tag{3.40}
\end{align}
$$

identical with the Euler equation.

4   MHD waves

Consider a static background $\vec{v}_0 = 0$ with uniform magnetic field $\vec{B}_0$. Since $\vec{j}_0 = 0$, there is no background Lorentz force density $\vec{f}_{L,0} = 0$, and with uniform background pressure P_0 we have $\vec{f}_0 = 0$.

15

The linearized Euler equation is

$$\frac{\partial \vec{v}_1}{\partial t} + \left(\vec{v}_1 \cdot \vec{\nabla}\right)\vec{v}_0 + \left(\vec{v}_0 \cdot \vec{\nabla}\right)\vec{v}_1 \;\; = \;\; \frac{\vec{f}_1}{\rho_0} - \frac{\vec{f}_0}{\rho_0^2}\rho_1 \,, \tag{4.1}$$

$$\rho_0 \frac{\partial \vec{v}_1}{\partial t} \;\; = \;\; \vec{f}_1 = -\vec{\nabla}P_1 + \vec{f}_{\mathrm{L},1} \,. \tag{4.2}$$

Linearization of the Lorentz force density. Since $\vec{j}_0 = 0$, the linearized Lorentz force density is

$$\vec{f}_{\mathrm{L},1} = \frac{\vec{j}_1 \times \vec{B}_0}{c} \,. \tag{4.3}$$

Substituting the linearized Ampére equation $\vec{j}_1 = (c/4\pi)(\vec{\nabla} \times \vec{B}_1)$, we have

$$\vec{f}_{\mathrm{L},1} = \frac{1}{4\pi}\left(\vec{\nabla} \times \vec{B}_1\right) \times \vec{B}_0 \,. \tag{4.4}$$

The perturbed magnetic field can be related to the velocity perturbation using the linearized induction equation in ideal MHD:

$$\frac{\partial \vec{B}_1}{\partial t} = \vec{\nabla} \times \left(\vec{v}_1 \times \vec{B}_0\right) \,. \tag{4.5}$$

Like in the hydrodynamic case, we adopt an oscillatory velocity perturbation $\vec{v}_1 \propto \exp\left(i\omega t + i\vec{k}\cdot\vec{r}\right)$:

$$i\omega \vec{B}_1 \;\; = \;\; i\vec{k} \times \left(\vec{v}_1 \times \vec{B}_0\right) \,, \tag{4.6}$$

$$\vec{f}_{\mathrm{L},1} \;\; = \;\; \frac{i}{4\pi}\left(\vec{k} \times \vec{B}_1\right) \times \vec{B}_0 = \frac{i}{4\pi\omega}\left\{\vec{k} \times \left[\vec{k} \times \left(\vec{v}_1 \times \vec{B}_0\right)\right]\right\} \times \vec{B}_0 \,. \tag{4.7}$$

Note the quadrupole cross product! This appears to be the main reason for the much richer structure of the solutions that we are going to obtain. This quadrupole cross product can be reduced usign the chain rule starting from the square bracket:

$$\vec{k} \times \left(\vec{v}_1 \times \vec{B}_0\right) \;\; = \;\; \left(\vec{k} \cdot \vec{B}_0\right)\vec{v}_1 - \left(\vec{k} \cdot \vec{v}_1\right)\vec{B}_0 \,, \tag{4.8}$$

$$\vec{f}_{\mathrm{L},1} \;\; = \;\; \frac{i}{4\pi\omega}\left\{\left(\vec{k} \cdot \vec{B}_0\right)\left[\left(\vec{k} \times \vec{v}_1\right) \times \vec{B}_0\right] - \left(\vec{k} \cdot \vec{v}_1\right)\left[\left(\vec{k} \times \vec{B}_0\right) \times \vec{B}_0\right]\right\} \,. \tag{4.9}$$

And now we reduce the two double cross products:

$$\left(\vec{k} \times \vec{v}_1\right) \times \vec{B}_0 \;\; = \;\; \left(\vec{B}_0 \cdot \vec{k}\right)\vec{v}_1 - \left(\vec{B}_0 \cdot \vec{v}_1\right)\vec{k} \,, \tag{4.10}$$

$$\left(\vec{k} \times \vec{B}_0\right) \times \vec{B}_0 \;\; = \;\; \left(\vec{B}_0 \cdot \vec{k}\right)\vec{B}_0 - \left(B_0^2\right)\vec{k} \,, \tag{4.11}$$

$$\vec{f}_{\mathrm{L},1} \;\; = \;\; \frac{i}{4\pi\omega}\left\{\left(\vec{k} \cdot \vec{B}_0\right)^2 \vec{v}_1 - \left(\vec{k} \cdot \vec{B}_0\right)\left(\vec{k} \cdot \vec{v}_1\right)\vec{B}_0\right\}$$

$$+ \;\; \frac{i}{4\pi\omega}\left[B_0^2\left(\vec{k} \cdot \vec{v}_1\right) - \left(\vec{k} \cdot \vec{B}_0\right)\left(\vec{B}_0 \cdot \vec{v}_1\right)\right]\vec{k} \,. \tag{4.12}$$

The perturbed Lorentz force density has thus three components along $\vec{v}_1$, $\vec{B}_0$ and $\vec{k}$. To proceed further, we will project $f_{\mathrm{L},1}$ along three independent vectors $\vec{B}_0$, $\vec{k}$ and $\vec{k} \times \vec{B}_0$:

$$\vec{f}_{\mathrm{L},1} \cdot \vec{B}_0 \;\; = \;\; 0 \,, \tag{4.13}$$

$$\vec{f}_{\mathrm{L},1} \cdot \vec{k} \;\; = \;\; \frac{ik^2}{4\pi\omega}\left[B_0^2\left(\vec{k} \cdot \vec{v}_1\right) - \left(\vec{k} \cdot \vec{B}_0\right)\left(\vec{B}_0 \cdot \vec{v}_1\right)\right] \,, \tag{4.14}$$

$$\vec{f}_{\mathrm{L},1} \cdot \left(\vec{k} \times \vec{B}_0\right) \;\; = \;\; \frac{i}{4\pi\omega}\left(\vec{k} \cdot \vec{B}_0\right)^2\left[\vec{v}_1 \cdot \left(\vec{k} \times \vec{B}_0\right)\right] \,. \tag{4.15}$$

The perturbed Lorentz force density is thus perpendicular to the background magnetic field $\vec{B}_0$.

Linearized Euler equation along $\vec{k} \times \vec{B}_0$. Project the linearized Euler equation along the $\vec{k} \times \vec{B}_0$ vector:

$$i\omega\rho_0\vec{v}_1 \cdot \left(\vec{k} \times \vec{B}_0\right) = -iP_1\vec{k} \cdot \left(\vec{k} \times \vec{B}_0\right) + \vec{f}_{\mathrm{L},1} \cdot \left(\vec{k} \times \vec{B}_0\right) . \tag{4.16}$$

The pressure term disappears since $\vec{k} \cdot (\vec{k} \times \vec{B}_0) = 0$. In this case the linearized Euler equation states that velocity perturbation $\vec{v}_1$ is driven by the perturbed Lorentz force density $\vec{f}_{\mathrm{L},1}$, which is a function of current density perturbation $\vec{j}_1$, which by the linearized Ampére equation is a function of magnetic field perturbation $\vec{B}_1$, which by the linearized induction equation is driven by $\vec{v}_1$. This makes a single feedback loop

$$\vec{v}_1 \rightarrow (i\omega)\vec{B}_1 \rightarrow \vec{j}_1 \rightarrow \vec{f}_{\mathrm{L},1} \rightarrow (i\omega)\vec{v}_1 , \tag{4.17}$$

in which the time derivative $\partial_t \equiv i\omega$ is applied twice.

Substituting $\vec{f}_{\mathrm{L},1} \cdot (\vec{k} \times \vec{B}_0)$:

$$i\omega\rho_0\vec{v}_1 \cdot \left(\vec{k} \times \vec{B}_0\right) = \frac{i}{4\pi\omega} \left(\vec{k} \cdot \vec{B}_0\right)^2 \left[\vec{v}_1 \cdot \left(\vec{k} \times \vec{B}_0\right)\right] . \tag{4.18}$$

This can be rearranged to the form:

$$\left[\omega^2 - \frac{1}{4\pi\rho_0}\left(\vec{k} \cdot \vec{B}_0\right)^2\right] \left[\vec{v}_1 \cdot \left(\vec{k} \times \vec{B}_0\right)\right] = 0 . \tag{4.19}$$

We thus obtain the *Alfvén dispersion relation* describing stable waves ($\omega^2 > 0$). Introducing the wave vector inclination angle $\vec{k} \cdot \vec{B}_0 \equiv kB_0\cos\theta$ and the background *magnetization* $\sigma_0 = B_0^2/(4\pi\rho_0 c^2)$, we obtain the phase speed:

$$v_{\mathrm{A}}^2 \equiv \frac{\omega^2}{k^2} = \sigma_0 c^2 \cos^2\theta \equiv c_{\mathrm{A},0}^2 \cos^2\theta , \tag{4.20}$$

where $c_{\mathrm{A},0} = c\sqrt{\sigma_0} = B_0/\sqrt{4\pi\rho_0}$ is the *Alfvén speed*[4]. Because the phase speed depends on θ, the propagation of these waves is anisotropic, maximized along the background magnetic field $\vec{B}_0$.

Relativistic Alfvén speed. For relativistic plasmas we would use a momentum equation derived from the general energy-momentum tensor:

$$\left[\frac{\omega^2}{c^2}(1+\sigma_0)w_0 - \frac{1}{4\pi}\left(\vec{k} \cdot \vec{B}_0\right)^2\right] \left[\vec{v}_1 \cdot \left(\vec{k} \times \vec{B}_0\right)\right] = 0 , \tag{4.21}$$

where $w_0 = \rho_0 c^2 + [\kappa/(\kappa - 1)]P_0$ is the relativistic enthalpy density such that $\sigma_0 = B_0^2/(4\pi w_0)$ is the relativistic magnetization. The main difference from the non-relativistic Euler equation is the additional $(1 + \sigma_0)$ term. This term limits the phase speed be less than the speed of light:

$$v_{\mathrm{A}}^2 \equiv \frac{\omega^2}{k^2} = \frac{\sigma_0}{1+\sigma_0}c^2 \cos^2\theta \equiv c_{\mathrm{A},0}^2 \cos^2\theta , \tag{4.22}$$

where $c_{\mathrm{A},0} \equiv c\sqrt{\sigma_0/(1+\sigma_0)}$ is the *relativistic Alfvén speed*.

For ultra-relativistic magnetizations $\sigma_0 \gg 1$, hence the magnetic enthalpy density $B_0^2/4\pi \gg w_0 > \rho_0 c^2$, we have $c_{\mathrm{A},0} \simeq c$, with the corresponding *Alfvén Lorentz factor* $\Gamma_{\mathrm{A},0} = \sqrt{1+\sigma_0}$. In the limit of non-relativistic magnetization $\sigma_0 << 1$ and pressure $P_0 \ll \rho_0 c^2$, we recover $\sigma_0 \simeq B_0^2/(4\pi\rho_0 c^2)$ and $c_{\mathrm{A},9} \simeq c\sqrt{\sigma_0} \simeq B_0/\sqrt{4\pi\rho_0}$.

---

[4]We exclude the $\cos\theta$ factor from the definition of Alfvén speed $c_{\mathrm{A},0}$. In this view, solutions to the Alfvén dispersion relation can be called the Alfvén waves (or intermediate waves) for any value of θ, but their anisotropic propagation speeds are $v_{\mathrm{A}} = c_{\mathrm{A},0}\cos\theta$.

Linearized Euler equation along $\vec{B}_0$ and $\vec{k}$.   Since $\vec{f}_{\mathrm{L},1} \cdot \vec{B}_0 = 0$, the linearized Euler equation projected along $\vec{B}_0$ is rather simple:

$$i\omega\rho_0 \left(\vec{v}_1 \cdot \vec{B}_0\right) = -i\left(\vec{k} \cdot \vec{B}_0\right) P_1 \,. \tag{4.23}$$

Substituting $P_1 = -(\kappa P_0/\omega)(\vec{k} \cdot \vec{v}_1)$ from the linearized pressure equation:

$$\omega^2 \left(\vec{B}_0 \cdot \vec{v}_1\right) = \frac{\kappa P_0}{\rho_0}\left(\vec{k} \cdot \vec{B}_0\right)\left(\vec{k} \cdot \vec{v}_1\right) = c_{\mathrm{s},0}^2 \left(\vec{k} \cdot \vec{B}_0\right)\left(\vec{k} \cdot \vec{v}_1\right) \,. \tag{4.24}$$

This needs to be combined with the linearized Euler equation projected along $\vec{k}$:

$$i\omega\rho_0 \left(\vec{v}_1 \cdot \vec{k}\right) = -ik^2 P_1 + \frac{ik^2}{4\pi\omega}\left[B_0^2 \left(\vec{k} \cdot \vec{v}_1\right) - \left(\vec{k} \cdot \vec{B}_0\right)\left(\vec{B}_0 \cdot \vec{v}_1\right)\right] \,. \tag{4.25}$$

Substituting $P_1 = -(\kappa P_0/\omega)(\vec{k} \cdot \vec{v}_1)$:

$$\omega^2 \left(\vec{k} \cdot \vec{v}_1\right) = k^2 \frac{\kappa P_0}{\rho_0}\left(\vec{k} \cdot \vec{v}_1\right) + \frac{k^2 B_0^2}{4\pi\rho_0}\left(\vec{k} \cdot \vec{v}_1\right) - \frac{k^2}{4\pi\rho_0}\left(\vec{k} \cdot \vec{B}_0\right)\left(\vec{B}_0 \cdot \vec{v}_1\right) \,. \tag{4.26}$$

Combining with Eq. (4.24):

$$\omega^2 \left(\vec{k} \cdot \vec{v}_1\right) = k^2 \left[c_{\mathrm{s},0}^2 + \frac{B_0^2}{4\pi\rho_0} - \frac{c_{\mathrm{s},0}^2}{4\pi\rho_0\omega^2}\left(\vec{k} \cdot \vec{B}_0\right)^2\right]\left(\vec{k} \cdot \vec{v}_1\right) \,. \tag{4.27}$$

Unless $\vec{v}_1 \perp \vec{k}$, this result is the *magnetosonic dispersion relation*:

$$\frac{\omega^4}{k^4} - \left(c_{\mathrm{s},0}^2 + c_{\mathrm{A},0}^2\right)\frac{\omega^2}{k^2} + c_{\mathrm{s},0}^2 c_{\mathrm{A},0}^2 \cos^2\theta = 0 \,, \tag{4.28}$$

where we substituted $B_0^2/(4\pi\rho_0) = c_{\mathrm{A},0}^2$.

The magnetosonic dispersion relation can be represented using a graph consisting of 4 scalar nodes $P_1, \vec{k} \cdot \vec{v}_1, \vec{B}_0 \cdot \vec{v}_1, \vec{k} \cdot \vec{f}_{\mathrm{L},1}$ (omitting $\vec{B}_1$ and $\vec{j}_1$) and 6 relations (multiplications by ω or $i\omega$):

$$\vec{k} \cdot \vec{v}_1 \quad \rightarrow \quad (\omega)P_1 \,, \tag{4.29}$$
$$\vec{k} \cdot \vec{v}_1 \quad \rightarrow \quad (i\omega)(\vec{k} \cdot \vec{f}_{\mathrm{L},1}) \,, \tag{4.30}$$
$$P_1 \quad \rightarrow \quad (\omega)(\vec{k} \cdot \vec{v}_1) \,, \tag{4.31}$$
$$P_1 \quad \rightarrow \quad (\omega)(\vec{B}_0 \cdot \vec{v}_1) \,, \tag{4.32}$$
$$\vec{B}_0 \cdot \vec{v}_1 \quad \rightarrow \quad (i\omega)(\vec{k} \cdot \vec{f}_{\mathrm{L},1}) \,, \tag{4.33}$$
$$\vec{k} \cdot \vec{f}_{\mathrm{L},1} \quad \rightarrow \quad (i\omega)(\vec{k} \cdot \vec{v}_1) \,. \tag{4.34}$$

These relations make 3 distinct feedback loops starting and ending at $\vec{k} \cdot \vec{v}_1$:

$$\vec{k} \cdot \vec{v}_1 \quad \rightarrow \quad (\omega)P_1 \rightarrow (\omega)(\vec{k} \cdot \vec{v}_1) \,, \tag{4.35}$$
$$\vec{k} \cdot \vec{v}_1 \quad \rightarrow \quad (i\omega)(\vec{k} \cdot \vec{f}_{\mathrm{L},1}) \rightarrow (i\omega)(\vec{k} \cdot \vec{v}_1) \,, \tag{4.36}$$
$$\vec{k} \cdot \vec{v}_1 \quad \rightarrow \quad (\omega)P_1 \rightarrow (\omega)(\vec{B}_0 \cdot \vec{v}_1) \rightarrow (i\omega)(\vec{k} \cdot \vec{f}_{\mathrm{L},1}) \rightarrow (i\omega)(\vec{k} \cdot \vec{v}_1) \,, \tag{4.37}$$

with the longest loop producing the ω^4 term, and the parity of $i\omega$ factors guaranteeing that the dispersion relation is real.

The magnetosonic dispersion relation has two solutions:

$$v_\pm^2 \equiv \frac{\omega^2}{k^2} = \frac{1}{2}\left[c_{\mathrm{s},0}^2 + c_{\mathrm{A},0}^2 \pm \sqrt{\left(c_{\mathrm{s},0}^2 + c_{\mathrm{A},0}^2\right)^2 - 4c_{\mathrm{s},0}^2 c_{\mathrm{A},0}^2 \cos^2\theta}\right] \tag{4.38}$$

that are always real and positive. These solutions represent the *slow ($v_{\mathrm{SM}} \equiv v_-$) and fast ($v_{\mathrm{FM}} \equiv v_+$) magnetosonic waves.*

For relativistic magnetizations, the magnetisonic dispersion relation can be generalized to:

$$\frac{\omega^4}{k^4} - \left(\frac{1 + \sigma_0 \cos^2 \theta}{1 + \sigma_0} c_{s,0}^2 + c_{A,0}^2 \right) \frac{\omega^2}{k^2} + c_{s,0}^2 c_{A,0}^2 \cos^2 \theta = 0 \,, \tag{4.39}$$

and the solutions are:

$$v_{\pm}^2 = \frac{1}{2} \left[\frac{1 + \sigma_0 \cos^2 \theta}{1 + \sigma_0} c_{s,0}^2 + c_{A,0}^2 \pm \sqrt{ \left(\frac{1 + \sigma_0 \cos^2 \theta}{1 + \sigma_0} c_{s,0}^2 + c_{A,0}^2 \right)^2 - 4 c_{s,0}^2 c_{A,0}^2 \cos^2 \theta } \,. \right] \tag{4.40}$$

Waves along $\vec{B}_0$. Consider the case of $\theta = 0$, hence $\vec{k} \parallel \vec{B}_0$. Since $\vec{k} \times \vec{B}_0$, we can only use the magnetosonic dispersion relation, which simplifies to:

$$v_{\pm}^2 = \frac{1}{2} \left[c_{s,0}^2 + c_{A,0}^2 \pm \sqrt{ \left(c_{s,0}^2 - c_{A,0}^2 \right)^2 } \right] \in \left\{ c_{s,0}^2, c_{A,0}^2 \right\} \,. \tag{4.41}$$

This implies that these solutions have the character of sound and Alfvén waves.

For a more detailed picture, we decompose the velocity perturbation $\vec{v}_1 = \vec{v}_{1,\parallel} + \vec{v}_{1,\perp}$ into components parallel and perpendicular to $\vec{k}$. The pressure perturbation is then:

$$P_1 = -\frac{\kappa P_0}{\omega} k v_{1,\parallel} \,. \tag{4.42}$$

The perturbed magnetic field becomes:

$$\vec{B}_1 \;=\; \frac{1}{\omega} \left[\left(\vec{k} \cdot \vec{B}_0 \right) \vec{v}_1 - \left(\vec{k} \cdot \vec{v}_1 \right) \vec{B}_0 \right] = \frac{k B_0}{\omega} \vec{v}_{1,\perp} \,. \tag{4.43}$$

A similar simple form is obtained for the perturbed Lorentz force density:

$$\vec{f}_{L,1} \;=\; \frac{i}{4\pi\omega} \left\{ \left(\vec{k} \cdot \vec{B}_0 \right)^2 \vec{v}_1 - \left(\vec{k} \cdot \vec{B}_0 \right) \left(\vec{k} \cdot \vec{v}_1 \right) \vec{B}_0 + \left[B_0^2 \left(\vec{k} \cdot \vec{v}_1 \right) - \left(\vec{k} \cdot \vec{B}_0 \right) \left(\vec{B}_0 \cdot \vec{v}_1 \right) \right] \vec{k} \right\}$$

$$\;=\; \frac{i k^2 B_0^2}{4\pi\omega} \vec{v}_{1,\perp} \,. \tag{4.44}$$

Substituting the above to the linearized Euler equation:

$$i\omega \rho_0 \vec{v}_1 \;=\; -i\vec{k} P_1 + \vec{f}_{L,1} \,, \tag{4.45}$$

$$\omega \rho_0 \vec{v}_1 \;=\; k^2 \frac{\kappa P_0}{\omega} \vec{v}_{1,\parallel} + \frac{k^2 B_0^2}{4\pi\omega} \vec{v}_{1,\perp} \,, \tag{4.46}$$

$$\left(\omega^2 - k^2 c_{s,0}^2 \right) \vec{v}_{1,\parallel} + \left(\omega^2 - k^2 c_{A,0}^2 \right) \vec{v}_{1,\perp} \;=\; 0 \,. \tag{4.47}$$

The last equation shows that for each type of wave a different component of the velocity perturbation disappears.

For the *sound wave* we have $\omega^2 = k^2 c_{s,0}^2$, hence $\vec{v}_{1,\perp} = 0$: velocity perturbations are longitudinal ($\vec{v}_1 \parallel \vec{k}$) and compressible ($P_1 \neq 0$), there is no perturbed magnetic field ($\vec{B}_1 = 0$) and no Lorentz force ($\vec{f}_{L,1} = 0$).

For the *Alfvén wave* we have $\omega^2 = k^2 c_{A,0}^2$, hence $\vec{v}_{1,\parallel} = 0$: velocity perturbations are transverse ($\vec{v}_1 \perp \vec{k}$) and incompressible ($P_1 = 0$), the perturbed magnetic field and Lorentz force density are also transverse ($\vec{B}_1 \parallel \vec{f}_{L,1} \perp \vec{k}$), but not polarized.

Waves across $\vec{B}_0$. Now consider the case of $\theta = \pi/2$, hence $\vec{k} \perp \vec{B}_0$. Although $\vec{k} \times \vec{B}_0 \neq 0$, the Alfvén dispersion relation returns $\omega^2 \propto (\vec{k} \cdot \vec{B}_0)^2 = 0$. We again use the magnetosonic dispersion relation, which reduces to:

$$v_{\pm}^2 = \frac{1}{2} \left[c_{s,0}^2 + c_{A,0}^2 \pm \sqrt{ \left(c_{s,0}^2 + c_{A,0}^2 \right)^2 } \right] \in \left\{ 0, c_{s,0}^2 + c_{A,0}^2 \right\} \,. \tag{4.48}$$

Let us define the *fast magnetosonic speed*[5] $c^2_{\mathrm{FM},0} \equiv c^2_{\mathrm{s},0} + c^2_{\mathrm{A},0}$. This suggests that only a fast magnetosonic wave can propagate strictly perpendicular to the magnetic field.

Once again, we decompose the velocity perturbation $\vec{v}_1 = \vec{v}_{1,\parallel} + \vec{v}_{1,\perp}$ into components parallel and perpendicular to $\vec{k}$:

$$P_1 = -\frac{\kappa P_0}{\omega} k v_{1,\parallel}, \tag{4.49}$$

$$\vec{B}_1 = -\frac{k}{\omega} v_{1,\parallel} \vec{B}_0, \tag{4.50}$$

$$\vec{f}_{\mathrm{L},1} = \frac{ik^2 B_0^2}{4\pi\omega} \vec{v}_{1,\parallel}. \tag{4.51}$$

Substituting the above to the linearized Euler equation:

$$\omega \rho_0 \vec{v}_1 = k^2 \frac{\kappa P_0}{\omega} \vec{v}_{1,\parallel} + \frac{k^2 B_0^2}{4\pi\omega} \vec{v}_{1,\parallel}, \tag{4.52}$$

$$\left(\omega^2 - k^2 c^2_{\mathrm{FM},0} \right) \vec{v}_{1,\parallel} + \omega^2 \vec{v}_{1,\perp} = 0. \tag{4.53}$$

For the fast magnetosonic wave we substitute $\omega^2 = k^2 c^2_{\mathrm{FM},0}$, and hence $\vec{v}_{1,\perp} = 0$. Velocity perturbations are longitudinal ($\vec{v}_1 \parallel \vec{k}$) and compressible ($P_1 \neq 0$), like the sound waves. The perturbed magnetic field is $\vec{B}_1 \parallel \vec{B}_0$ (hence strictly polarized), while the perturbed Lorentz force density is $\vec{f}_{\mathrm{L},1} \parallel \vec{k}$.

MHD wave speeds. Figure 2 presents the propagation speeds for relativistic magnetizations, calculated from Eqs. (4.22, 4.40).
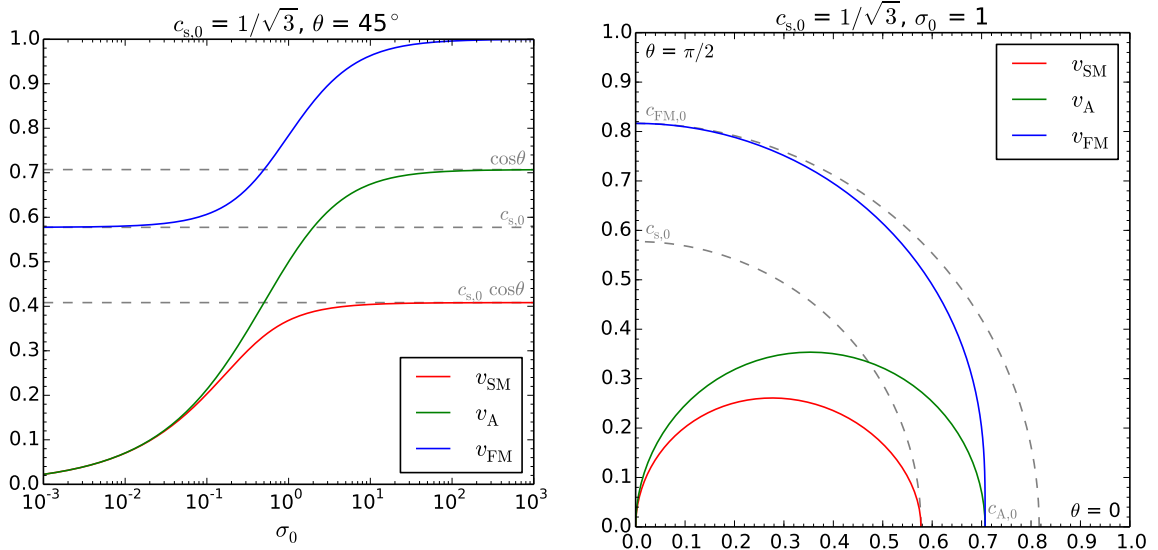
Figure 2: MHD wave propagation speeds $v_{\mathrm{SM}}, v_{\mathrm{A}}, v_{\mathrm{FM}}$ (in units of the speed of light $c = 1$) as functions of σ_0 (left panel) and θ (right panel). The limiting values $c_{\mathrm{s},0}, c_{\mathrm{A},0}, c_{\mathrm{FM},0}$ are indicated.

---

[5]The anisotropic propagation speeds of fast magnetosonic waves v^2_{FM} for intermediate values of θ are less than $c_{\mathrm{FM},0}$.

5 Rayleigh-Taylor instability (RTI)

5.1 RTI in HD

We now consider the effect of gravitational acceleration on a static equilibrium ($\vec{v}_0 = 0$). We will begin from the hydrodynamic case ($\vec{B}_0 = 0$) in order to discuss certain caveats.

The gravitational acceleration is specified in a standard terrestial convention $\vec{g} = -g\hat{z}$, where $\hat{z}$ is the unit vector pointing vertically up, and $g = \mathrm{const} > 0$. The vertical direction is now distinguished from the horizontal (x, y) plane. The *gravitational force density* is $\vec{f}_{\mathrm{g}} = \rho\vec{g}$. Under the gravitational acceleration, the static equilibrium is known as the *hydrostatic equilibrium*, where gravitational force density is balanced by the pressure gradient $\rho_0\vec{g} = \vec{\nabla}P_0$, hence

$$P_0'(z) \equiv \frac{dP_0}{dz} = -g\rho_0 < 0\,. \tag{5.1}$$

The prime $'$ will in general denote ∂_z.

Vertical profile of the background density is assumed to satisfy $\rho_0' = \rho_0/\lambda_\rho$ with $\lambda_\rho = \mathrm{const}$ the *density height scale*. We have thus introduced a length scale to our problem, which can be associated with the *'free-fall' time scale* $t_\rho \equiv \sqrt{|\lambda_\rho/g|}$ *and velocity* $v_\rho \equiv \sqrt{|g\lambda_\rho|}$ (where we neglect $\sqrt{2}$ factors).

Linearization. The linearized Euler equation is:

$$\rho_0\frac{\partial \vec{v}_1}{\partial t} = -\vec{\nabla}P_1 + \vec{g}\rho_1\,. \tag{5.2}$$

We now adopt an oscillatory form for the velocity perturbation $\vec{v}_1 \propto \exp(i\omega t + i\vec{k}\cdot\vec{r})$. We should note, however, that the dependence of other perturbed parameters ρ_1, P_1 can be more complex. The Euler equation becomes:

$$i\omega\rho_0 v_{1,x} = -ik_x P_1\,, \tag{5.3}$$
$$i\omega\rho_0 v_{1,y} = -ik_y P_1\,, \tag{5.4}$$
$$i\omega\rho_0 v_{1,z} = -P_1' - g\rho_1\,. \tag{5.5}$$

The horizontal components can be used to eliminate the horizontal velocity perturbations:

$$v_{1,x} = -\frac{k_x P_1}{\omega\rho_0}\,, \tag{5.6}$$

$$v_{1,y} = -\frac{k_y P_1}{\omega\rho_0}\,. \tag{5.7}$$

Next, we linearize the continuity equation:

$$\frac{\partial \rho_1}{\partial t} + \left(\vec{v}_1 \cdot \vec{\nabla}\right)\rho_0 + \rho_0\left(\vec{\nabla}\cdot\vec{v}_1\right) = 0\,, \tag{5.8}$$
$$i\omega\rho_1 + v_{1,z}\rho_0' + \rho_0\left(ik_x v_{1,x} + ik_y v_{1,y} + ik_z v_{1,z}\right) = 0\,. \tag{5.9}$$

The divergence of horizontal velocity is substituted as

$$ik_x v_{1,x} + ik_y v_{1,y} = -\frac{ik_{xy}^2}{\omega\rho_0}P_1\,, \tag{5.10}$$

$$i\omega\rho_1 + \frac{\rho_0}{\lambda_\rho}v_{1,z} - \frac{ik_{xy}^2}{\omega}P_1 + ik_z\rho_0 v_{1,z} = 0\,, \tag{5.11}$$

where $k_{xy}^2 = k_x^2 + k_y^2$. The density perturbation can be eliminated as

$$\rho_1 = \left(\frac{i}{\lambda_\rho} - k_z\right)\frac{\rho_0}{\omega}v_{1,z} + \frac{k_{xy}^2}{\omega^2}P_1\,. \tag{5.12}$$

Next, we linearize the pressure equation:

$$\frac{\partial P_1}{\partial t} + \left(\vec{v}_1 \cdot \vec{\nabla}\right) P_0 + \kappa P_0 \left(\vec{\nabla} \cdot \vec{v}_1\right) = 0, \tag{5.13}$$

$$i\omega P_1 + v_{1,z} P_0' + \kappa P_0 \left(ik_x v_{1,x} + ik_y v_{1,y} + ik_z v_{1,z}\right) = 0. \tag{5.14}$$

Substituting the horizontal velocities and the hydrostatic equilibrium $P_0' = -g\rho_0$:

$$i\omega P_1 - g\rho_0 v_{1,z} - \frac{ik_{xy}^2}{\omega} \frac{\kappa P_0}{\rho_0} P_1 + ik_z \kappa P_0 v_{1,z} = 0. \tag{5.15}$$

We identify the local speed of sound $v_{s,0}^2(z) = \kappa P_0(z)/\rho_0(z)$:

$$i\omega P_1 - g\rho_0 v_{1,z} - \frac{ik_{xy}^2}{\omega} v_{s,0}^2 P_1 + ik_z v_{s,0}^2 \rho_0 v_{1,z} = 0. \tag{5.16}$$

From this, we can eliminate the pressure perturbation:

$$\left(\omega^2 - k_{xy}^2 v_{s,0}^2\right) P_1 = -\left(ig + k_z v_{s,0}^2\right) \omega \rho_0 v_{1,z}, \tag{5.17}$$

$$P_1 = -\frac{ig + k_z v_{s,0}^2}{\omega^2 - k_{xy}^2 v_{s,0}^2} \omega \rho_0 v_{1,z}. \tag{5.18}$$

We have thus expressed ρ_1, P_1 in terms of $v_{1,z}$, and these can be substituted to the vertical component of the linearized Euler equation $i\omega \rho_0 v_{1,z} = -P_1' - g\rho_1$. However, calculating the derivative P_1' is a bit complicated in the general case. In order to simplify that term, one can consider either of the following three approximations: (1) short-wavelength, (2) incompressible, and (3) isothermal. We are going to discuss them in order.

Short-wavelength limit. In the short-wavelength limit, we assume that $k_{xy} \gg 1/\lambda_\rho$, that $|k_z| \lesssim k_{xy}$ (which means that it can be comparably large, but also much less, even zero), $\omega \sim 1/t_\rho$, and $v_{s,0} \sim v_\rho$. In particular, we can simplify the denominator in the formula for P_1 ($\omega^2 \ll k_{xy}^2 v_{s,0}^2$), but we need to keep the full nominator because of expected cancellations:

$$P_1 \simeq \frac{ig + k_z v_{s,0}^2}{k_{xy}^2 v_{s,0}^2} \omega \rho_0 v_{1,z}. \tag{5.19}$$

Substituting P_1 to the density perturbation (here a cancellation takes place):

$$\rho_1 \simeq i\left(\frac{1}{\lambda_\rho} + \frac{g}{v_{s,0}^2}\right) \frac{\rho_0}{\omega} v_{1,z}. \tag{5.20}$$

The pressure derivative becomes particularly simple:

$$P_1' \simeq ik_z P_1 \simeq \frac{k_z^2}{k_{xy}^2} i\omega \rho_0 v_{1,z}. \tag{5.21}$$

Substituting the above to the Euler equation:

$$i\omega \rho_0 v_{1,z} \simeq -i\omega \frac{k_z^2}{k_{xy}^2} \rho_0 v_{1,z} - ig\left(\frac{1}{\lambda_\rho} + \frac{g}{v_{s,0}^2}\right) \frac{\rho_0}{\omega} v_{1,z}. \tag{5.22}$$

From this, we obtain the dispersion relation:

$$\omega^2 \left(1 + \frac{k_z^2}{k_{xy}^2}\right) \simeq -\frac{g}{\lambda_\rho} - \frac{g^2}{v_{s,0}^2}. \tag{5.23}$$

Instability ($\omega^2 < 0$) requires that $v_{s,0}^2/(g\lambda_\rho) > -1$. Hence, any positive λ_ρ (density increasing vertically up, against $\vec{g}$) is unstable, but also a moderately negative λ_ρ can be unstable for $g(-\lambda_\rho) \equiv v_\rho^2 > v_{s,0}^2$ (a supersonic free-fall). One can also verify that the assumed relations between parameter magnitudes are indeed satisfied. In particular, the value of k_z is not very important, as long as it is not significantly larger than k_{xy}.

Incompressible limit. Here we consider the limit of strongly subsonic free-fall velocity $v_\rho \ll v_{s,0}$. Using the general expression for pressure perturbation (Eq. 5.18), one can calculate the divergence of velocity perturbation:

$$\vec{\nabla} \cdot \vec{v}_1 = -\frac{ik_{xy}^2}{\omega \rho_0} P_1 + ik_z v_{1,z} = \left(\frac{k_{xy}^2 v_\rho^2 - ik_z |\lambda_\rho| \omega^2}{k_{xy}^2 v_{s,0}^2 - \omega^2} \right) \frac{v_{1,z}}{|\lambda_\rho|} , \tag{5.24}$$

which tends to zero for $v_{s,0} \to \infty$. Hence, this limit means *incompressibility*.

The pressure perturbation simplifies to:

$$P_1 = -\frac{ig + k_z v_{s,0}^2}{\omega^2 - k_{xy}^2 v_{s,0}^2} \omega \rho_0 v_{1,z} \simeq \frac{k_z \omega}{k_{xy}^2} \rho_0 v_{1,z} . \tag{5.25}$$

With $v_{s,0}$ eliminated, the derivative of P_1 is then rather simple:

$$P_1' \simeq \frac{k_z \omega}{k_{xy}^2} (\rho_0 v_{1,z})' = \frac{k_z \omega}{k_{xy}^2} \left(\frac{1}{\lambda_\rho} + ik_z \right) \rho_0 v_{1,z} . \tag{5.26}$$

The density perturbation (Eq. 5.12) also takes a simple form:

$$\rho_1 = \left(\frac{i}{\lambda_\rho} - k_z \right) \frac{\rho_0}{\omega} v_{1,z} + \frac{k_{xy}^2}{\omega^2} P_1 \simeq \frac{i\rho_0}{\omega \lambda_\rho} v_{1,z} . \tag{5.27}$$

Substituting P_1' and ρ_1 to the vertical Euler equation:

$$i\omega \rho_0 v_{1,z} = -P_1' - g\rho_1 \quad \simeq \quad -\frac{k_z \omega}{k_{xy}^2 \lambda_\rho} \rho_0 v_{1,z} - \frac{ik_z^2 \omega}{k_{xy}^2} \rho_0 v_{1,z} - \frac{ig}{\omega \lambda_\rho} \rho_0 v_{1,z} , \tag{5.28}$$

$$\omega^2 \left(1 - \frac{ik_z}{k_{xy}^2 \lambda_\rho} + \frac{k_z^2}{k_{xy}^2} \right) v_{1,z} \quad \simeq \quad -\frac{g}{\lambda_\rho} v_{1,z} . \tag{5.29}$$

The imaginary term can be eliminated by modifying the z dependence of $v_{1,z}$. First, let us make a step backwards by substituting $ik_z \to \partial_z$:

$$\omega^2 \left(v_{1,z} - \frac{v_{1,z}'}{k_{xy}^2 \lambda_\rho} - \frac{v_{1,z}''}{k_{xy}^2} \right) \simeq -\frac{g}{\lambda_\rho} v_{1,z} . \tag{5.30}$$

Now substitute $v_{1,z} = f_0(z)\xi_1$ with $\xi_1 \propto \exp(ik_z z)$, effectively redefining k_z. The first and second derivatives are $v_{1,z}' = (f_0' + ik_z f_0)\xi_1$ and $v_{1,z}'' = (f_0'' + 2ik_z f_0' - k_z^2 f_0)\xi_1$. The result is:

$$\omega^2 \left(f_0 - \frac{f_0' + ik_z f_0}{k_{xy}^2 \lambda_\rho} - \frac{f_0'' + 2ik_z f_0' - k_z^2 f_0}{k_{xy}^2} \right) \xi_1 \simeq -\frac{g}{\lambda_\rho} f_0 \xi_1 . \tag{5.31}$$

The imaginary terms cancel out for $f_0'/f_0 = -1/(2\lambda_\rho)$, which means that $f_0 \propto 1/\sqrt{\rho_0}$ and $f_0''/f_0 = 1/(4\lambda_\rho^2)$. With this, we obtain a dispersion relation:

$$\omega^2 \left(1 + \frac{1}{4k_{xy}^2 \lambda_\rho^2} + \frac{k_z^2}{k_{xy}^2} \right) \simeq -\frac{g}{\lambda_\rho} . \tag{5.32}$$

While the LHS is a bit more complex than in the short-wavelength limit, the instability condition ($\omega^2 < 0$) is simply that $\lambda_\rho > 0$ (density increasing against $\vec{g}$).

Isothermal limit. The assumption that background temperature T_0 is constant implies that the speed of sound $v_{s,0}$ is constant. The derivative of $v_{s,0}$ can be expressed as $(v_{s,0}^2)' = -\kappa g - v_{s,0}^2/\lambda_\rho$, hence isothermality implies a particular scale height $\lambda_\rho = -v_{s,0}^2/(\kappa g) < 0$ (density increasing along $\vec{g}$, which suggests stability), and a particular free-fall velocity $v_\rho^2 = v_{s,0}^2/\kappa$ (the gas is thus compressible).

In the isothermal limit, calculation of the pressure perturbation is significantly simplified:

$$P'_1 \;\;=\;\; i\frac{\kappa g^2 - ik_z(\kappa+1)gv_{s,0}^2 - k_z^2 v_{s,0}^4}{v_{s,0}^2(\omega^2 - k_{xy}^2 v_{s,0}^2)}\omega\rho_0 v_{1,z}\,. \tag{5.33}$$

The vertical Euler equation becomes:

$$\omega^2 v_{1,z} \;\;=\;\; -(\kappa-1)\frac{k_{xy}^2 g^2}{\omega^2 - k_{xy}^2 v_{s,0}^2}v_{1,z} + \frac{\omega^2\kappa g}{\omega^2 - k_{xy}^2 v_{s,0}^2}v'_{1,z} - \frac{\omega^2 v_{s,0}^2}{\omega^2 - k_{xy}^2 v_{s,0}^2}v''_{1,z}\,. \tag{5.34}$$

The imaginary term can be again eliminated using the $v_{1,z} = f_0(z)\xi_1$ substitution, which allows to obtain a dispersion relation with all terms real:

$$(-\omega^2)\left[1 + \frac{1}{k_{xy}^2 v_{s,0}^2 - \omega^2}\left(k_z^2 v_{s,0}^2 + \frac{\kappa^2 g^2}{4v_{s,0}^2}\right)\right] + (\kappa-1)\frac{k_{xy}^2 g^2}{k_{xy}^2 v_{s,0}^2 - \omega^2} = 0\,. \tag{5.35}$$

One can see that for an unstable solution with $\omega^2 < 0$ the first term would be positive, and the second term could only be negative for $\kappa < 1$, a non-standard equation of state. Hence, for $\kappa > 1$ there is no unstable solution, which is consistent with the fact that $\lambda_\rho < 0$.

Physical principle. What is the simplest explanation for the Rayleigh-Taylor instability? Let us consider again the short wavelength limit $k_x \gg 1/|\lambda_\rho|$ in the special case of $k_y = k_z = 0$. The complete set of basic linearized equations is:

$$i\omega\frac{\rho_1}{\rho_0} \;\;=\;\; -ik_x v_{1,x} - \frac{v_{1,z}}{\lambda_\rho}\,, \tag{5.36}$$

$$i\omega\frac{P_1}{\rho_0} \;\;=\;\; -v_{s,0}^2\, ik_x v_{1,x} + g v_{1,z}\,, \tag{5.37}$$

$$i\omega v_{1,x} \;\;=\;\; -ik_x\frac{P_1}{\rho_0}\,, \tag{5.38}$$

$$i\omega v_{1,z} \;\;=\;\; -\frac{P'_1}{\rho_0} - g\frac{\rho_1}{\rho_0}\,. \tag{5.39}$$

Noting that $P_1/\rho_1 \sim \omega^2/k_x^2 \sim 1/(k_x^2\tau_\rho^2) \ll v_{s,0}^2$, we can neglect the pressure gradient term in the vertical Euler equation. The pressure equation can also be eliminated, since $\left|k_x v_{s,0}^2 v_{1,x}\right| = \left|(k_x^2/\omega)v_{s,0}^2(P_1/\rho_0)\right| \gg |\omega(P_1/\rho_0)|$. We are then left with just 3 equations for three unknowns:

$$i\omega\frac{\rho_1}{\rho_0} \;\;=\;\; -ik_x v_{1,x} - \frac{v_{1,z}}{\lambda_\rho}\,, \tag{5.40}$$

$$v_{s,0}^2\, ik_x v_{1,x} \;\;\simeq\;\; g v_{1,z}\,, \tag{5.41}$$

$$i\omega v_{1,z} \;\;\simeq\;\; -g\frac{\rho_1}{\rho_0}\,. \tag{5.42}$$

In analogy to the discussion in Section 4, one can identify in these equations two closed feedback loops:

- *Incompressible loop*: $v_{1,z} \to (i\omega)\rho_1 \to (i\omega)v_{1,z}$. Consider the case of $\lambda_\rho > 0$. Starting from vertical velocity pointing upwards ($v_{1,z} > 0$), gas of lower ρ_0 is advected from below, resulting in negative density perturbation $\rho_1 < 0$. This implies a reduced gravitational force, hence a gravitational perturbation pointing upwards $-g\rho_1 > 0$, which acts to further increase $v_{1,z}$.

- *Compressible loop*: $v_{1,z}(\to P_1) \to (i)v_{1,x} \to (\omega)\rho_1 \to (i\omega)v_{1,z}$. Consider the case of constant background density $(1/\lambda_\rho \to 0)$, in which there is no incompressible loop. Starting again from $v_{1,z} > 0$, a small but positive pressure perturbation $P_1 > 0$ is induced, which generates a horizontal sound wave with $iv_{1,x} > 0$, which compresses the gas with the effect of triggering a negative density perturbation $\rho_1 < 0$, with consequences like above. The compressible loop can only work in a warm gas with $v_{s,0} > 0$.

24

5.2 RTI in MHD

We now consider the same problem of a static background ($\vec{v}_0 = 0$) under uniform gravitational acceleration $\vec{g} = -g\hat{z}$, but we add a horizontal background magnetic field $\vec{B}_0 = B_0(z)\hat{x}$. We thus allow for the magnetic field strength to have a vertical gradient $B_0' \equiv \mathrm{d}B_0/\mathrm{d}z$, but no vertical curl, hence $B_{0,y} = B_{0,z} = 0$. We have thus distinguished one horizontal direction $\hat{x}$ as the direction of background magnetic field. The other horizontal direction $\hat{y}$ is the direction of background current density $\vec{j}_0 = (c/4\pi)B_0'\hat{y}$. And the background Lorentz force density is directed vertically $\vec{f}_{\mathrm{L},0} = (\vec{j}_0 \times \vec{B}_0)/c = -(B_0 B_0'/4\pi)\hat{z} = -[(B_0^2)'/8\pi]\hat{z} = -P_{\mathrm{B},0}'\hat{z}$, it amounts to the gradient of magnetic pressure $P_{\mathrm{B},0} = B_0^2/8\pi$.

Magnetohydrostatic equilibrium. The vertical force balance needs to be modified from the hydrodynamic case: $-\vec{\nabla}P_0 + \rho_0\vec{g} + \vec{f}_{\mathrm{L},0} = 0$ leads to $(P_0 + P_{\mathrm{B},0})' = -g\rho_0$. One can assume independent profiles of $\rho_0(z)$ and $B_0(z)$, and use them to integrate the gas pressure profile $P_0(z)$. Here we adopt exponential profiles with constant height scales λ_ρ, λ_B such that $\rho_0' = \rho_0/\lambda_\rho$ and $B_0' = B_0/\lambda_B$.

Linearization. The perturbed magnetic field is calculated from the linearized induction equation. This calculation is similar to that presented in Section 4, but with additional terms including the background magnetic strength gradient B_0':

$$\frac{\partial \vec{B}_1}{\partial t} = \left(\vec{B}_0 \cdot \vec{\nabla}\right)\vec{v}_1 - \left(\vec{v}_1 \cdot \vec{\nabla}\right)\vec{B}_0 - \vec{B}_0\left(\vec{\nabla}\cdot\vec{v}_1\right), \tag{5.43}$$

$$i\omega\vec{B}_1 = ik_x B_0 \vec{v}_1 - \vec{B}_0' v_{1,z} - \vec{B}_0\left(i\vec{k}\cdot\vec{v}_1\right), \tag{5.44}$$

$$i\omega B_{1,x} = -ik_y B_0 v_{1,y} - (B_0' + ik_z B_0)v_{1,z}, \tag{5.45}$$

$$i\omega B_{1,y} = ik_x B_0 v_{1,y}, \tag{5.46}$$

$$i\omega B_{1,z} = ik_x B_0 v_{1,z}. \tag{5.47}$$

The perturbed current density is:

$$j_{1,x} = \frac{c}{4\pi}(ik_y B_{1,z} - B_{1,y}') = \frac{ck_x B_0}{4\pi\omega}\left(-\frac{v_{1,y}}{\lambda_B} - v_{1,y}' + ik_y v_{1,z}\right), \tag{5.48}$$

$$j_{1,y} = \frac{c}{4\pi}(B_{1,x}' - ik_x B_{1,z}) = \frac{cB_0}{4\pi\omega}\left[-\frac{k_y}{\lambda_B}v_{1,y} - k_y v_{1,y}' + \left(\frac{i}{\lambda_B^2} - \frac{2k_z}{\lambda_B} - ik_{xz}^2\right)v_{1,z}\right], \tag{5.49}$$

$$j_{1,z} = \frac{ic}{4\pi}(k_x B_{1,y} - k_y B_{1,x}) = \frac{cB_0}{4\pi\omega}\left[ik_{xy}^2 v_{1,y} + k_y\left(\frac{1}{\lambda_B} + ik_z\right)v_{1,z}\right], \tag{5.50}$$

where $k_{xy}^2 \equiv k_x^2 + k_y^2$ and $k_{xz}^2 \equiv k_x^2 + k_z^2$.

The perturbed Lorentz force density is:

$$f_{\mathrm{L},1,x} = \frac{j_{0,y}B_{1,z}}{c} = \frac{k_x}{\lambda_B}\frac{B_0^2}{4\pi\omega}v_{1,z}, \tag{5.51}$$

$$f_{\mathrm{L},1,y} = \frac{j_{1,z}B_{0,x}}{c} = ik_{xy}^2\frac{B_0^2}{4\pi\omega}v_{1,y} + k_y\left(\frac{1}{\lambda_B} + ik_z\right)\frac{B_0^2}{4\pi\omega}v_{1,z}, \tag{5.52}$$

$$f_{\mathrm{L},1,z} = -\frac{j_{0,y}B_{1,x}}{c} - \frac{j_{1,y}B_{0,x}}{c} = k_y\frac{B_0^2}{4\pi\omega}\left(\frac{2}{\lambda_B}v_{1,y} + v_{1,y}'\right)$$
$$+ \left(-\frac{2i}{\lambda_B^2} + \frac{3k_z}{\lambda_B} + ik_{xz}^2\right)\frac{B_0^2}{4\pi\omega}v_{1,z}. \tag{5.53}$$

The linearized Euler equation is then:

$$\omega^2 v_{1,x} = -k_x \omega \frac{P_1}{\rho_0} - i k_x \frac{v_{\mathrm{A},0}^2}{\lambda_B} v_{1,z} , \tag{5.54}$$

$$\omega^2 v_{1,y} = -k_y \omega \frac{P_1}{\rho_0} + k_{xy}^2 v_{\mathrm{A},0}^2 v_{1,y} + k_y \left(k_z - \frac{i}{\lambda_B} \right) v_{\mathrm{A},0}^2 v_{1,z} , \tag{5.55}$$

$$\omega^2 v_{1,z} = i\omega \frac{P_1'}{\rho_0} + i\omega g \frac{\rho_1}{\rho_0} - i k_y v_{\mathrm{A},0}^2 \left(\frac{2}{\lambda_B} v_{1,y} + v_{1,y}' \right) + \left(k_{xz}^2 - \frac{3 i k_z}{\lambda_B} - \frac{2}{\lambda_B^2} \right) v_{\mathrm{A},0}^2 v_{1,z} , \tag{5.56}$$

where we introduced the background Alfvén velocity $v_{\mathrm{A},0}^2 = B_0^2/(4\pi\rho_0)$.

This is completed by the linearized continuity and pressure equations:

$$\omega \frac{\rho_1}{\rho_0} = -\left(\vec{k} \cdot \vec{v}_1 \right) + \frac{i v_{1,z}}{\lambda_\rho} , \tag{5.57}$$

$$\omega \frac{P_1}{\rho_0} = -v_{\mathrm{s},0}^2 \left(\vec{k} \cdot \vec{v}_1 \right) - \left(g + \frac{v_{\mathrm{A},0}^2}{\lambda_B} \right) i v_{1,z} , \tag{5.58}$$

where we substituted P_0' from the magnetohydrostatic equilibrium.

Interchange mode. Consider the case of $k_x = 0$ and $k_y \neq 0$, hence a transverse mode with $\vec{k} \perp \vec{B}_0$. In this case, the x component of the Euler equation becomes trivial and implies that $v_{1,x} = 0$. We are left with 4 linearized equations:

$$\omega \frac{\rho_1}{\rho_0} = -\left(\vec{k} \cdot \vec{v}_1 \right) + \frac{i v_{1,z}}{\lambda_\rho} , \tag{5.59}$$

$$\omega \frac{P_1}{\rho_0} = -v_{\mathrm{s},0}^2 \left(\vec{k} \cdot \vec{v}_1 \right) - \left(g + \frac{v_{\mathrm{A},0}^2}{\lambda_B} \right) i v_{1,z} , \tag{5.60}$$

$$\omega^2 v_{1,y} = -k_y \omega \frac{P_1}{\rho_0} + k_y^2 v_{\mathrm{A},0}^2 v_{1,y} + k_y \left(k_z - \frac{i}{\lambda_B} \right) v_{\mathrm{A},0}^2 v_{1,z} , \tag{5.61}$$

$$\omega^2 v_{1,z} = i\omega \frac{P_1'}{\rho_0} + i\omega g \frac{\rho_1}{\rho_0} - \frac{2 i k_y}{\lambda_B} v_{\mathrm{A},0}^2 v_{1,y} - i k_y v_{\mathrm{A},0}^2 v_{1,y}' + \left(k_z^2 - \frac{3 i k_z}{\lambda_B} - \frac{2}{\lambda_B^2} \right) v_{\mathrm{A},0}^2 v_{1,z} . \tag{5.62}$$

These equations can be reduced in the short-wavelength limit $k_y^2 v_{\mathrm{FM},0}^2 \gg \omega^2$, where $v_{\mathrm{FM},0} = \sqrt{v_{\mathrm{s},0}^2 + v_{\mathrm{A},0}^2}$ is the background fast magnetosonic speed. Lengthy calculations result in the following dispersion relation:

$$\left(1 + \frac{k_z^2}{k_y^2} \frac{v_{\mathrm{s},0}^2}{v_{\mathrm{FM},0}^2} \right) \omega^2 \simeq -\frac{g}{\lambda_\rho} - \frac{g^2}{v_{\mathrm{FM},0}^2} . \tag{5.63}$$

In the hydrodynamical limit ($B_0 = 0$ and $v_{\mathrm{FM},0} = v_{\mathrm{s},0}$), this is consistent with Eq. (5.23). The effect of magnetic field is merely to generalize the sound waves to the fast magnetosonic waves.

In the description of the physical principle of the Rayleigh-Taylor instability, in the short-wavelength limit $k_y \gg 1/|\lambda_\rho|$ and the special case of $k_z = 0$ and $B_0' = 0$ (since λ_B does not contribute to the dispersion relation), the complete set of basic linearized equations is:

$$i\omega \frac{B_{1,x}}{B_0} = -i k_y v_{1,y} , \tag{5.64}$$

$$i\omega \frac{\rho_1}{\rho_0} = -i k_y v_{1,y} - \frac{v_{1,z}}{\lambda_\rho} , \tag{5.65}$$

$$i\omega \frac{P_1}{\rho_0} = -i k_y v_{\mathrm{s},0}^2 v_{1,y} + g v_{1,z} , \tag{5.66}$$

$$i\omega v_{1,y} = -i k_y \frac{P_1}{\rho_0} - i k_y v_{\mathrm{A},0}^2 \frac{B_{1,x}}{B_0} , \tag{5.67}$$

$$i\omega v_{1,z} = -\frac{P_1'}{\rho_0} - g \frac{\rho_1}{\rho_0} . \tag{5.68}$$

26

Note that $B_0' = 0$ and $k_z = 0$ implies that $B_{1,x}' = 0$ and $j_{0,y} = 0$, hence also $j_{1,y} = 0$, and hence $f_{L,1,z} = 0$. This is why $B_{1,x}$ contributes only to the horizontal Euler equation.

It can be shown that P_1 and $B_{1,x}$ are small, allowing to combine the induction, pressure and horizontal Euler equations into $ik_y v_{FM,0}^2 v_{1,y} \simeq g v_{1,z}$, and to eliminate P_1' from the vertical Euler equation. Therefore, the compressible loop can be generalized to the *fast-magnetosonic loop* $v_{1,z}(\rightarrow P_1, B_{1,x}) \rightarrow (i)v_{1,y} \rightarrow (\omega)\rho_1 \rightarrow (i\omega)v_{1,z}$.

This unstable mode has been first demonstrated by Kruskal & Schwarzschild (1954), and was lated called the *interchange mode*, because in the version of the problem where a layer of unmagnetized plasma is placed over a layer of strong magnetic field, the plasma will slip between the magnetic field lines, with the final outcome of a plasma layer under the magnetic field (the interchange between plasma and magnetic field).

Parker mode. Consider the case of $k_y = 0$ and $k_x \neq 0$, hence a longitudinal mode with $\vec{k} \cdot \vec{B}_0 \neq 0$ (not exactly parallel if $k_z \neq 0$). In this case, it is the y component of the Euler equation that is trivial, hence $v_{1,y} = 0$. We are left with the following equations (x-Euler, continuity, pressure, z-Euler):

$$\frac{v_{1,x}}{v_{1,z}} = -\frac{k_x k_z v_{s,0}^2 + ik_x g}{k_x^2 v_{s,0}^2 - \omega^2} \,, \tag{5.69}$$

$$\frac{i\omega \rho_1}{\rho_0 v_{1,z}} = -\frac{1}{\lambda_\rho} - \frac{k_x^2 g - ik_z \omega^2}{k_x^2 v_{s,0}^2 - \omega^2} \,, \tag{5.70}$$

$$\frac{i\omega P_1}{\rho_0 v_{1,z}} = g + \frac{v_{A,0}^2}{\lambda_B} - v_{s,0}^2 \frac{k_x^2 g - ik_z \omega^2}{k_x^2 v_{s,0}^2 - \omega^2} \,, \tag{5.71}$$

$$-\omega^2 = -\frac{i\omega P_1'}{\rho_0 v_{1,z}} - g\frac{i\omega \rho_1}{\rho_0 v_{1,z}} + \left(\frac{2}{\lambda_B^2} + \frac{3ik_z}{\lambda_B} - k_{xz}^2\right) v_{A,0}^2 \,. \tag{5.72}$$

Applying the short-wavelength limit $k_x \gg 1/|\lambda_\rho|$ leads to the following dispersion relation:

$$\left(1 + \frac{k_z^2}{k_x^2}\right)\omega^2 \simeq -\frac{g^2}{v_{s,0}^2} - \frac{g}{\lambda_\rho} + k_{xz}^2 v_{A,0}^2 \,. \tag{5.73}$$

The last term on the RHS is dominant and stabilizing. Its origin can be traced to the $-j_{1,y}B_{0,x}$ term of the $f_{L,1,z}$ Lorentz force density, where $j_{1,y}$ includes the tension term $-ik_x(c/4\pi)B_{1,z}$, with the perturbed magnetic field $B_{1,z} = (k_x/\omega)B_{0,x}v_{1,z}$. Therefore, magnetic tension stabilizes sufficiently short longitudinal perturbations.

The pressure perturbation gradient has to be calculated in its general form:

$$\frac{i\omega P_1'}{\rho_0 v_{1,z}} = \left(\frac{1}{\lambda_\rho} + ik_z\right)g + \left(\frac{2}{\lambda_B} + ik_z\right)\frac{v_{A,0}^2}{\lambda_B} + \frac{k_x^2 g - ik_z \omega^2}{k_x^2 v_{s,0}^2 - \omega^2}\left[-\left(\frac{1}{\lambda_\rho} + ik_z\right)v_{s,0}^2 + \frac{\omega^2(v_{s,0}^2)'}{k_x^2 v_{s,0}^2 - \omega^2}\right] \,. \tag{5.74}$$

We can see that unless $(v_{s,0}^2)' = 0$, it will be even more complex. It is thus a good case to apply the isothermal limit, as has been done originally by Parker (1966). An additional assumption is that $(v_{A,0}^2)' = 0$, which means that $\lambda_B = 2\lambda_\rho$.

The vertical Euler equation becomes:

$$\omega^2 v_{1,z} = -\frac{k_x^2 g}{k_x^2 v_{s,0}^2 - \omega^2}\left(g + \frac{v_{s,0}^2}{\lambda_\rho}\right)v_{1,z} - \frac{1}{\lambda_\rho}\left(v_{A,0}^2 - \frac{\omega^2 v_{s,0}^2}{k_x^2 v_{s,0}^2 - \omega^2}\right)v_{1,z}' + \frac{\omega^2 v_{s,0}^2}{k_x^2 v_{s,0}^2 - \omega^2}v_{1,z}''$$
$$+ v_{A,0}^2(k_x^2 v_{1,z} - v_{1,z}'') \,. \tag{5.75}$$

Once again, it is possible to eliminate the $v_{1,z}'$ term by substituting $v_{1,z} = \exp(ik_z z - z/2\lambda_\rho)\xi_1$:

$$\omega^2 = -\frac{k_x^2 g}{k_x^2 v_{s,0}^2 - \omega^2}\left(g + \frac{v_{s,0}^2}{\lambda_\rho}\right) + \left(\frac{1}{4\lambda_\rho^2} + k_{xz}^2\right)v_{A,0}^2 - \left(\frac{1}{4\lambda_\rho^2} + k_z^2\right)\frac{\omega^2 v_{s,0}^2}{k_x^2 v_{s,0}^2 - \omega^2} \,. \tag{5.76}$$
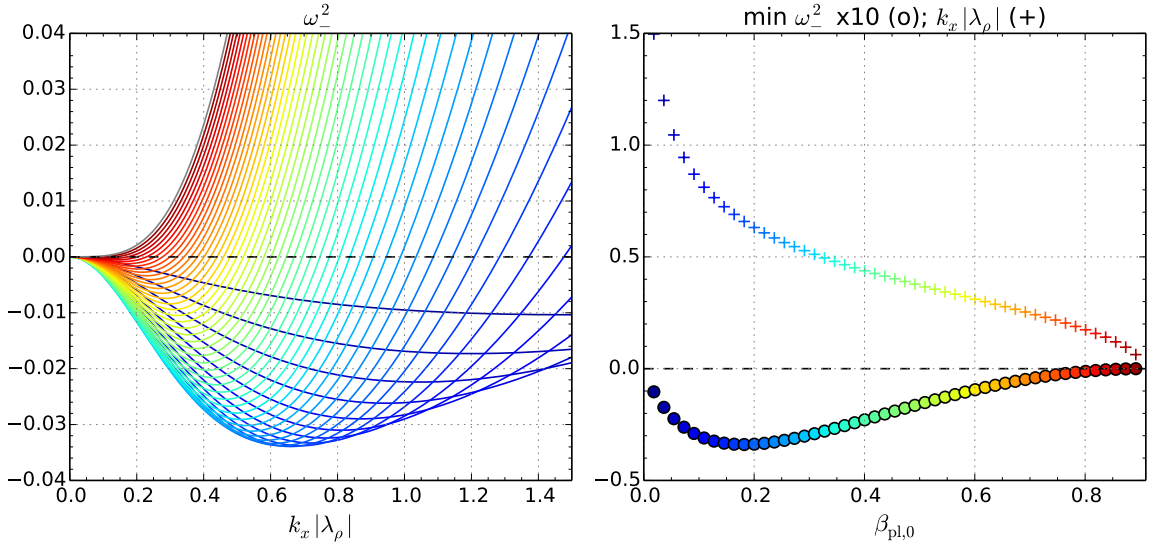
Figure 3: Solutions to the Parker dispersion relation (Eq. 5.77) for $\kappa = 5/3$ and $k_z = 0$ in units of $g = v_{s,0}^2 = 1$ (in which $\lambda_\rho = -(3/5)(1 + 1/\beta_{\mathrm{pl},0})$). The left panel shows ω^2 as function of $k_x|\lambda_\rho|$ for different values of $\beta_{\mathrm{pl},0}$ indicated by the line colors corresponding to colors of the symbols shown in the right panel. The right panel shows the lowest (most negative) values of ω^2 (circles) and the corresponding values of $k_x|\lambda_\rho|$ (crosses) as functions of $\beta_{\mathrm{pl},0}$.

Finally, we substitute the plasma beta parameter $\beta_{\mathrm{pl},0} = P_0/(B_{0,x}^2/8\pi)$ and $\lambda_\rho = -[v_{s,0}^2 + (\kappa/2)v_{A,0}^2]/\kappa g = -(1 + 1/\beta_{\mathrm{pl},0})v_{s,0}^2/\kappa g$ (a consequence of $(v_{s,0}^2)' = 0$), and obtain the *Parker dispersion relation* as a quadratic equation for ω^2 with all terms real:

$$\omega^4 - (1 + 4k_{xz}^2\lambda_\rho^2)\left(1 + \frac{2}{\kappa\beta_{\mathrm{pl},0}}\right)\frac{v_{s,0}^2}{4\lambda_\rho^2}\omega^2 + k_x^2 g^2 \left[\frac{2\kappa\beta_{\mathrm{pl},0}}{(1 + \beta_{\mathrm{pl},0})^2}k_{xz}^2\lambda_\rho^2 + \frac{\kappa\beta_{\mathrm{pl},0}}{2(1 + \beta_{\mathrm{pl},0})^2} + \frac{\kappa\beta_{\mathrm{pl},0}}{1 + \beta_{\mathrm{pl},0}} - 1\right] = 0.$$
(5.77)

Note that for any unstable solution ($\omega^2 < 0$), the first two terms would be positive, hence the last term would need to be negative. In the limit of $k_{xz} = 0$, that requirement leads to the condition:

$$2(\kappa - 1)\beta_{\mathrm{pl},0}^2 + (3\kappa - 4)\beta_{\mathrm{pl},0} - 2 < 0.$$
(5.78)

In the particular case of $\kappa = 5/3$, this condition is satisfied for $\beta_{\mathrm{pl},0} < 0.91$. Instability is only possible above some minimum magnetization.

In the hydrodynamic limit ($\beta_{\mathrm{pl},0} \to \infty$), the Parker dispersion relation reduces to:

$$\omega^4 - \left(\frac{1}{4\lambda_\rho^2} + k_{xz}^2\right)v_{s,0}^2\omega^2 + (\kappa - 1)k_x^2 g^2 = 0,$$
(5.79)

which is consistent with Eq. (5.35): no unstable solutions for $\kappa > 1$.

Solutions to the Parker dispersion relation for $\kappa = 5/3$ and $k_z = 0$ are presented in Figure 3. This plot confirms that unstable solutions exist only for $\beta_{\mathrm{pl},0} \lesssim 0.9$. The most rapid growth rates with $\omega^2 \simeq -0.034(g/|\lambda_\rho|)$ occur for $\beta_{\mathrm{pl},0} \simeq 0.18$ at the wavenumber $k_x \simeq 0.66/\lambda_\rho$.

The Parker instability is driven solely by the $-k_x^2 g^2$ term, which can be traced to the gravitational perturbation $-g\rho_1$. The density perturbation ρ_1 includes the term $-(k_x/\omega)\rho_0 v_{1,x}$, with the longitudinal velocity perturbation $v_{1,x}$ (Eq. 5.69) contributing an additional $k_x g$ factor (while the $k_x k_z v_{s,0}^2$ term cancels out).

6 MHD shocks

The shock problem Consider a stationary discontinuity along the $z = 0$ plane, the *shock front*, with a normal vector $\vec{n} = [0, 0, 1]$. The standard convention for describing vector components relates them to the normal vector, hence a parallel component is the component parallel to $\vec{n}$, etc. A fluid flows from the uniform *upstream region 1* ($z < 0$) to the uniform *downstream region 2* ($z > 0$) with velocity components $v_{1,z}, v_{2,z} > 0$. Given the upstream fluid parameters, the objective is to determine the possible downstream fluid parameters.

Hydrodynamic shock Consider the relativistic stationary continuity equation (Eq. 3.29): $\vec{\nabla} \cdot (\Gamma \rho \vec{v}) = 0$, hence $\partial_z(\Gamma \rho v_z) = 0$. Across the continuity this means $\Gamma_2 \rho_2 v_{2,z} = \Gamma_1 \rho_1 v_{1,z}$, or one can write that in the form $[\Gamma \rho v_z] = 0$. Similarly, the conservation of energy and momentum $\partial_\mu T_{\mathrm{fl}}^{\mu\nu} = 0$ (Eq. 3.30) can be written as $[T_{\mathrm{fl}}^{\mu z}] = 0$. In the hydrodynamic case one can choose a reference frame where $v_{1,x} = v_{1,y} = 0$ and $v_{2,x} = v_{2,y} = 0$, leaving two non-trivial jump equations (energy and momentum, respectively):

$$0 = [T_{\mathrm{fl}}^{0z}] = [\Gamma^2 w \beta_z], \tag{6.1}$$

$$0 = [T_{\mathrm{fl}}^{zz}] = [\Gamma^2 w (\beta_z)^2 + P], \tag{6.2}$$

where $\vec{\beta} = \vec{v}/c$. Adopting an adiabatic equation of state for the downstream fluid, with relativistic enthalpy density $w_2 = \rho_2 c^2 + [\kappa_2/(\kappa_2 - 1)]P_2$, pressure $P_2 = \Theta_2 \rho_2 c^2$, relativistic temperature $\Theta_2 = k_\mathrm{B} T_2/mc^2$, and adiabatic index $4/3 < \kappa_2(\Theta_2) < 5/3$, the problem reduces to 3 equations for three variables v_2, ρ_2, Θ_2.

Non-relativistic hydrodynamic shock. Consider the limit of non-relativistic velocities $v_1, v_2 \ll c$ and non-relativistic temperatures $\Theta_1, \Theta_2 \ll 1$ (hence $\kappa_1, \kappa_2 = 5/3$). The shock jump equations can be reduced to the *Rankine-Hugoniot conditions* (conservation of mass, momentum and energy, respectively):

$$\rho_2 v_2 = \rho_1 v_1, \tag{6.3}$$

$$\rho_2 v_2^2 + P_2 = \rho_1 v_1^2 + P_1, \tag{6.4}$$

$$\left(\frac{\rho_2 v_2^2}{2} + \frac{5}{2} P_2 \right) v_2 = \left(\frac{\rho_1 v_1^2}{2} + \frac{5}{2} P_1 \right) v_1. \tag{6.5}$$

Let us introduce the *shock velocity jump*, equivalent to the compression ratio: $r = v_1/v_2 \equiv \rho_2/\rho_1$. Eliminating v_2 and P_2, the Rankine-Hugoniot conditions can be reduced to a single linear equation for r:

$$(r - 4)\rho_1 v_1^2 + 5r P_1 = 0. \tag{6.6}$$

The solution can be represented in terms of the *Mach number* $M_1 = v_1/v_{\mathrm{s},1}$, where $v_{s,1} = \sqrt{5P_1/3\rho_1}$ is the upstream speed of sound: $r = 4M_1^2/(M_1^2 + 3)$. One can also find the pressure jump $P_2/P_1 = (4r - 1)/(4 - r)$.

It can also be shown that for $r > 1$ the specific entropy $s = \delta S/\delta M$ satisfies $s_2 > s_1$, and also that $M_1 > 1$ and $M_2 < 1$. *The solution is physical when a supersonic upstream flow converts into a subsonic downstream flow.*

Magnetic field jump. The change of magnetic field components across the shock front is calculated from stationary source-free Maxwell's equations in ideal MHD.

From the Gauss's law for magnetism $\vec{\nabla} \cdot \vec{B} = 0$, hence $\partial_z B_z = 0$ or $[B_z] = 0$. *Magnetic field parallel to the shock normal is conserved.*

From the Maxwell-Faraday equation $\vec{\nabla} \times \vec{E} = 0$ we have conditions for two perpendicular components $\partial_z E_x = \partial_z E_y = 0$, hence $[B_x v_z - B_z v_x] = [B_y v_z - B_z v_y] = 0$. *Magnetic field perpendicular to the shock normal is compressed.*

The Gauss's law for electricity would predict a surface density of electric density $\Sigma_\mathrm{e} = [E_z]/4\pi$, however, $E_z \neq 0$ requires a perpendicular velocity component. The Ampère-Maxwell equation predicts a surface density of electric current, e.g. $\mathcal{J}_y = (c/4\pi)[B_x]$, it requires the presence of perpendicular magnetic field.

Magnetized shocks. In the presence of uniform magnetic fields $\vec{B}_1, \vec{B}_2$, shocks can be classified as:

- *parallel shocks*: $\vec{B}_1, \vec{B}_2 \parallel \vec{n}$. Parallel magnetic field cancels out from the shock jump equations, which reduce to the hydrodynamic form.

- *perpendicular shocks*: $\vec{B}_1, \vec{B}_2 \perp \vec{n}$. Perpendicular magnetic field contributes to the shock jump equations, as will be shown below.

- *oblique shocks*: $B_z \neq 0$ and $B_{1,\perp} \neq 0$, which implies that $B_{2,\perp} \neq 0$, but also that $v_{2,\perp} \neq 0$ even for $v_{1,\perp} = 0$ (perpendicular acceleration).

Magnetic energy-momentum tensor Consider an oblique upstream magnetic field $\vec{B}_1 = (B_{1,x}, 0, B_z)$ and parallel upstream velocity $\vec{\beta}_1 = \vec{v}_1/c = (0, 0, \beta_{1,z})$. The corresponding upstream energy-momentum tensor in ideal MHD (Eqs. 2.32 - 2.33) has three non-zero components:

$$T_{\mathrm{EM},1}^{0z} \;=\; \beta_{1,z} \frac{B_{1,x}^2}{4\pi}\,, \tag{6.7}$$

$$T_{\mathrm{EM},1}^{xz} \;=\; -\frac{B_{1,x} B_z}{4\pi}\,, \tag{6.8}$$

$$T_{\mathrm{EM},1}^{zz} \;=\; \frac{B_{1,x}^2}{8\pi} + \frac{\beta_{1,z}^2 B_{1,x}^2}{8\pi} - \frac{B_z^2}{8\pi}\,. \tag{6.9}$$

The first equation represents the flux density of electromagnetic energy. The second equation represents the flux density of perpendicular electromagnetic momentum (*perpendicular Poynting flux*), which is non-zero only for oblique shocks and generates perpendicular downstream velocity $\beta_{2,x}$. The third equation represents the *parallel Poynting flux* (perpendicular field contributes magnetic pressure with positive sign, parallel field contributes magnetic tension with negative sign); however, note that the B_z^2 and $\beta_{1,z}^2 B_{1,x}^2$ terms cancel out across the shock, hence only the $B_{1,x}^2$ term features in the shock jump conditions.

Non-relativistic perpendicular shock. In the presence of perpendicular magnetic field $B_{1,x}, B_{2,x} \neq 0$, the shock jump equations are generalized to:

$$\rho_2 v_2 \;=\; \rho_1 v_1\,, \tag{6.10}$$

$$\rho_2 v_2^2 + P_2 + \frac{B_{2,x}^2}{8\pi} \;=\; \rho_1 v_1^2 + P_1 + \frac{B_{1,x}^2}{8\pi}\,, \tag{6.11}$$

$$\left(\frac{\rho_2 v_2^2}{2} + \frac{5}{2} P_2 + \frac{B_{2,x}^2}{4\pi} \right) v_2 \;=\; \left(\frac{\rho_1 v_1^2}{2} + \frac{5}{2} P_1 + \frac{B_{1,x}^2}{4\pi} \right) v_1\,, \tag{6.12}$$

$$B_{2,x} v_2 \;=\; B_{1,x} v_1\,. \tag{6.13}$$

Using the shock velocity jump $r = v_1/v_2$, the downstream magnetic field can be eliminated as $B_{2,x} = r B_{1,x}$, and the above equations reduce to a quadratic equation for r:

$$(r-4)\rho_1 v_1^2 + 5r P_1 + r(r+5) \frac{B_{1,x}^2}{8\pi} = 0\,. \tag{6.14}$$

In addition to the standard Mach number M_1, we introduce the Alfvén Mach number $M_{\mathrm{A},1} = v_1/v_{\mathrm{A},1}$, where $v_{\mathrm{A},1} = B_{1,x}/\sqrt{4\pi\rho_1}$ is the upstrem Alfvén speed:

$$r - 4 + \frac{3r}{M_1^2} + \frac{r(r+5)}{2 M_{\mathrm{A},1}^2} = 0\,. \tag{6.15}$$

This equation has only one physical solution:

$$r \;=\; \frac{M_{\mathrm{A},1}^2}{2} \left[\sqrt{q^2 + \frac{32}{M_{\mathrm{A},1}^2}} - q \right]\,, \tag{6.16}$$

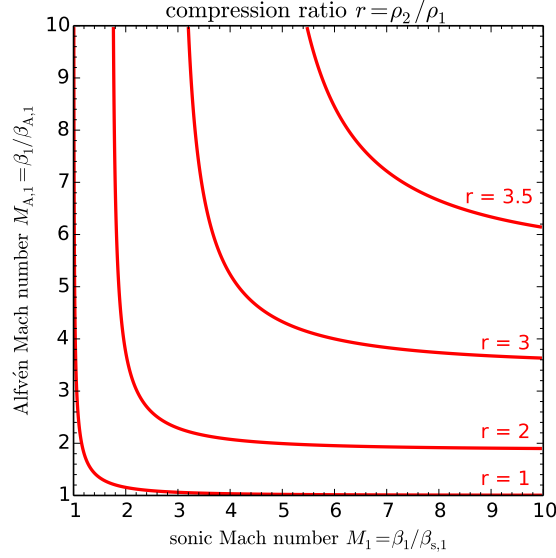$$q \;=\; 2 + \frac{6}{M_1^2} + \frac{5}{M_{\mathrm{A},1}^2}\,, \tag{6.17}$$

Figure 4: Non-relativistic shock compression ratio as function of the sonic and Alfvén Mach numbers.

which is illustrated in Figure 4. Requiring that $r > 1$ leads to $v_1^2 > v_{A,1}^2 + v_{s,1}^2 \equiv v_{FM,1}^2$, i.e., *super-fast-magnetosonic upstream flow*.

Relativistic perpendicular shock. In the case of relativistic fluid with perpendicular magnetic field, the shock jump equations take the following form:

$$\Gamma_2 \rho_2 \beta_2 = \Gamma_1 \rho_1 \beta_1 \,, \tag{6.18}$$

$$\Gamma_2^2 w_2 \beta_2^2 + P_2 + \frac{B_{2,x}^2}{8\pi} = \Gamma_1^2 w_1 \beta_1^2 + P_1 + \frac{B_{1,x}^2}{8\pi} \,, \tag{6.19}$$

$$\Gamma_2^2 w_2 \beta_2 + \frac{B_{2,x}^2}{4\pi} \beta_2 = \Gamma_1^2 w_1 \beta_1 + \frac{B_{1,x}^2}{4\pi} \beta_1 \,, \tag{6.20}$$

$$B_{2,x} \beta_2 = B_{1,x} \beta_1 \,. \tag{6.21}$$

It is a bit difficult to solve them analytically in the general case, because they correspond to a 4th order polynomial. Numerical solutions in the limit of cold upstream fluid ($\Theta_1 = 0$, hence $P_1 = 0$ and $w_1 = \rho_1 c^2$) are presented in Figure 5. The main effect of magnetic fields is that the shock becomes weaker, reducing the four-velocity jump u_1/u_2 (and the velocity jump β_1/β_2), the compression ratio ρ_2/ρ_1, and the downstream temperature Θ_2.

Ultra-relativistic perpendicular shock. Consider the limit of $\Gamma_1 \gg 1$, hence $\beta_1 \simeq 1$. The shock velocity jump is $r = \beta_1/\beta_2 \simeq 1/\beta_2$. As usual, we can eliminate $B_{2,x} = r B_{1,x}$. Ancitipating a relativistic downstream temperature $\Theta_2 \gg 1$, we adopt $\kappa_2 \simeq 4/3$ and $w_2 \simeq 4P_2$.

The momentum equation (Eq. 6.19) becomes:

$$\frac{r^2 + 3}{r^2 - 1} P_2 \simeq \left[1 - (r^2 - 1) \frac{\sigma_1}{2} \right] \Gamma_1^2 w_1 \,, \tag{6.22}$$

where we introduced the upstream magnetization $\sigma_1 = B_{1,x}^2/(4\pi\Gamma_1^2 w_1)$. The energy equation (Eq. 6.20) takes a similar form:

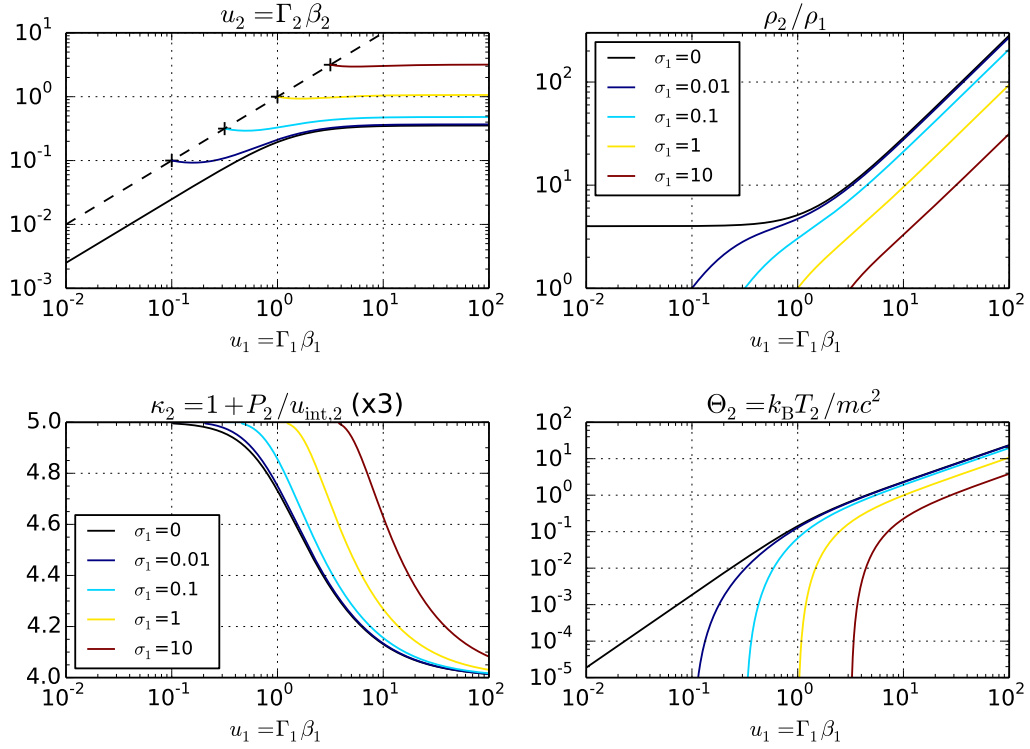$$\frac{4r}{r^2 - 1} P_2 \simeq \left[1 - (r - 1)\sigma_1 \right] \Gamma_1^2 w_1 \,. \tag{6.23}$$

31

Figure 5: Numerical solutions to the cold ($\Theta_1 = 0$) magnetized perpendicular shock jump equations (Eqs. 6.18 - 6.21). The solutions are presented as functions of upstream four-velocity $u_1 = \Gamma_1\beta_1$ for several values of the upstream magnetization σ_1. The upper left panel shows the downstream four-velocity $u_2 = \Gamma_2\beta_2$; the upper right panel shows the compression ratio n_2/n_1; the lower left panel shows the downstream adiabatic index κ_2 (multiplied by factor 3); and the lower right panel shows the downstream dimensionless temperature $\Theta_2 = k_B T_2/mc^2$. For $\sigma_1 > 0$, the marginal solutions with $u_2 = u_1$, $n_2/n_1 = 1$, etc., are indicated.

Combining the above equations allows to eliminate the downstream pressure:

$$\frac{P_2}{(r^2-1)\Gamma_1^2 w_1} \simeq \frac{2-(r^2-1)\sigma_1}{2(r^2+3)} \simeq \frac{1-(r-1)\sigma_1}{4r} \,.$$ (6.24)

The last two sides relate the upstream magnetization and the velocity jump:

$$\sigma_1 \simeq -\frac{(r-3)}{(r-1)(r+3)} \,.$$ (6.25)

This is a quadratic equation for r, the solution to which is:

$$r \simeq \frac{1+2\sigma_1}{2\sigma_1}\left[2\sqrt{1-\frac{3}{4(1+2\sigma_1)^2}} - 1\right] \,.$$ (6.26)

One can further distinguish two special limits:

- *Hydrodynamic limit* ($\sigma_1 = 0$): the result is $r \simeq 3$, hence the downstream region is characterized by velocity $\beta_2 \simeq 1/3$, density $\rho_2 \simeq \sqrt{8}\,\Gamma_1\rho_1$, pressure $P_2 \simeq (2/3)\Gamma_1^2 w_1$, and temperature $\Theta_2 \simeq (1/3\sqrt{2})(\Gamma_1 w_1/\rho_1 c^2)$.

- *Relativistic magnetization* ($\Gamma_1 > \sigma_1 \gg 1$): the result is $r \simeq 1 + 1/(2\sigma_1)$, hence in the downstream: velocity $\beta_2 \simeq 1 - 1/(2\sigma_1)$, density $\rho_2 \simeq \Gamma_1\rho_1/\sqrt{\sigma_1}$, pressure $P_2 \simeq \Gamma_1^2 w_1/(8\sigma_1)$, and temperature $\Theta_2 = P_2/\rho_2 c^2 = (1/8\sqrt{\sigma_1})(\Gamma_1 w_1/\rho_1 c^2)$.

7   Magnetic reconnection

Magnetic reconnection is a dissipation mechanism, in which the energy of ordered magnetic fields is converted to other forms of energy: kinetic, internal and non-thermal. The idea of magnetic reconnection has been first proposed by Giovanelli (1946) to explain energization of particles during the solar flares.

A specific scenario for reconnection at the origin of solar flares has been described by Parker (1957). It considers two sunspots of opposite magnetic polarities, the footpoints of separate coronal loops. These sunspots may be forced by subphotospheric convective motions to approach each other. The opposite vertical magnetic field lines from the two sunspots will be dragged to a close proximity. In a highly symmetric situation, a magnetic null (point/line/surface) may be present. If the field lines are able to reconnect, the magnetic connections of both sunspots will change, including some direct connections between them that were not present initially. See the Phenomenology notes for alternative scenarios informed by modern numerical simulations.

Current layer.   Consider locally reversed magnetic fields separated by an interface of thickness δ. Specifically, let $B_x \simeq B_0$ for $y > \delta/2$ and $B_x \simeq -B_0$ for $y < \delta/2$[6]. This implies a magnetic field gradient across the interface $\partial_y B_x \sim B_0/\delta$, which is actually the z component of magnetic curl that by the Ampère equation implies the presence of electric current density $j_z = (c/4\pi)(\vec{\nabla} \times \vec{B})_z \sim cB_0/(4\pi\delta)$. The thinner the interface, the stronger current density must be. A thin interface separating reversed magnetic fields is thus known as the *current layer*. A reversing magnetic field also implies a gap in the magnetic pressure $P_{yy} = B_x^2/8\pi$. This gap can be filled by the gas pressure.

By matching the magnetic field gradient with profiles of current density and pressure, one can achieve an equilibrium across the current layer. The most popular solution for a current layer structure is the *Harris equilibrium* (Harris, 1962). It adopts the magnetic field profile $B_x = B_0 \tanh(y/\delta)$ and a population of hot drifting particles of density $n = n_{\rm d}/\cosh^2(y/\delta)$. The value of $n_{\rm d}$, together with the z-directed uniform drift velocity $v_{\rm d}$ and uniform temperature $T_{\rm d}$, can be adjusted to normalize the current density and pressure profiles to obtain the exact equilibrium. One can also include a second population of background particles with uniform density n_0, which can be adjusted to obtain the desired background magnetization $\sigma_0 = B_0^2/(4\pi n_0 mc^2)$.

---

[6]This is an anti-parallel magnetic reversal, it can be modified by adding a uniform B_z component - the guide field.

Reconnection inflows and outflows. A current layer of thickness δ along y can be expected to have a finite length $L \gg \delta$ along x. The background magnetic field lines extend largely along x. Once two such lines are reconnected (in the *magnetic diffusion region*), magnetic tension will act to shorten the resulting overstretched lines as much as possible, creating a *magnetic slingshot* that will drive *outflows* in the $\pm x$ directions. These outflows can be treated as large-amplitude perturbations propagating along the background magnetic field lines, their characteristic speed is the Alfvén speed for the background plasma $v_{\text{out}} \sim v_{\text{A},0} = c\sqrt{\sigma_0/(1+\sigma_0)}$. These outflows can be relativistic in cases of relativistic background magnetizations $\sigma_0 \gg 1$.

Outflows from a reconnection region must be balanced by inflows from the $\pm y$ directions in order for the reconnection to be sustained (steady-state). The characteristic speed of reconnection inflows v_{in} is known as the *reconnection rate*. It is a fundamental parameter to characterize the efficiency of magnetic reconnection, because it determines the strength of electric field induced in the reconnection layer $E \sim (v_{\text{in}}/c)B_0$. This electric field strength is the motional (ideal MHD) field in the background regions. In stationary situation $\partial_t B_x = -c(\vec{\nabla} \times \vec{E})_x \simeq -c\partial_y E_z \simeq 0$, hence E_z should be uniform along y. It can thus extend uniformly into the reconnection layer despite ideal MHD breaking down there. This electric field is directly responsible for non-thermal acceleration of particles. Reconnection rate can be related to the outflow speed via the geometry (aspect ratio) of the reconnection layer: $v_{\text{in}} \sim (\delta/L)v_{\text{out}} \sim (\delta/L)v_{\text{A},0}$.

Diffusive reconnection rate. Reversed magnetic fields can in principle reconnect due to magnetic diffusion. Recall that in resistive MHD the electric field can be expressed as:

$$\vec{E} \simeq \vec{B} \times \vec{\beta} + \frac{\vec{j}}{\sigma} \simeq \frac{1}{c}\left[\vec{B} \times \vec{v} + \eta(\vec{\nabla} \times \vec{B})\right] \tag{7.1}$$

Since E_z should be uniform along y, we can set $E_z \simeq 0$ (although that precludes non-thermal particle acceleration):

$$cE_z \simeq \left[\vec{B} \times \vec{v} + \eta(\vec{\nabla} \times \vec{B})\right]_z = B_x v_y - \eta\partial_y B_x \simeq 0, \tag{7.2}$$

This provides the *diffusive reconnection rate* $v_{\text{in}} \sim \eta/\delta$. For fixed η, the reconnection rate is maximized for the thinnest possible layers. A lower limit on δ can be set by microphysical plasma parameters such as the skin depth $d = \sqrt{mc^2/(4\pi e^2 n_0)}$ or the thermal gyroradius $\rho_0 = kT_0/eB_0$.

Lundquist number. Combining the current layer L, the background Alfvén speed $v_{\text{A},0}$, and the magnetic diffusivity η, one can define a magnetic Reynolds number $R_{\text{m}} = v_{\text{A},0}L/\eta$ also known as the *Lundquist number*. Using R_{m} and the diffusive reconnection rate $v_{\text{in}} = \eta/\delta$, one can estimate the layer thickness $\delta \sim \sqrt{\eta L/v_{\text{A},0}} = L/\sqrt{R_{\text{m}}}$, and express the reconnection rate as $v_{\text{in}} \sim \sqrt{\eta v_{\text{A},0}/L} = v_{\text{A},0}/\sqrt{R_{\text{m}}}$.

Based on these parameters, one can also define three characteristic time scales: (1) dynamical (Alfvén) $t_{\text{A}} = L/v_{\text{A}}$, (2) reconnection $t_{\text{rec}} = L/v_{\text{in}} \sim \sqrt{R_{\text{m}}}t_{\text{A}}$, and (3) diffusive $t_{\eta} = L^2/\eta = R_{\text{m}}t_{\text{A}}$.

Sweet-Parker model. The diffusive reconnection rate is the basis of the first model of magnetic reconnection – the *Sweet-Parker model*, co-developed by Sweet (1958) and Parker (1957). They assumed that reconnection layer is uniform along macroscopic lengths L (the global system size). They also adopted standard magnetic diffusivity η based on the Spitzer resistivity (see Section 2). With this, they could estimate the Lundquist number R_{m} and determine other key parameters.

As an example, consider solar flares with length scale $L \sim 10^4$ km $= 10^9$ cm, Alfvén speed $v_{\text{A}} \sim 10^{-3} c = 3 \times 10^7$ cm s^{-1}, and magnetic diffusivity $\eta \sim 10^4$ cm^2 s^{-1}. This yields $R_{\text{m}} \sim 3 \times 10^{12}$. This implies a diffusive reconnection rate $v_{\text{in}} \sim 2$ cm/s, and a current layer thickness $\delta \sim 600$ cm. The three characteristic time scales are: dynamical $t_{\text{A}} \sim 30$ s, reconnection $t_{\text{rec}} \sim 6 \times 10^7$ s $\simeq 2$ yr, diffusive $t_{\eta} \sim 10^{14}$ s $\simeq 3$ Myr. Therefore, an extremely high value of R_{m} implies extremely slow reconnection rate and extremely long reconnection time scale.

Petschek model. In order to increase the reconnection rate, one should try to decrease the Lundquist number, and this can be achieved by decreasing the effective length L of the magnetic diffusion region. Petschek (1964) proposed to introduce a scale separation with a highly localized magnetic diffusion region of length $L^* \ll L$. A small diffusion region would be connected with the large-scale system by stationary shock waves along oblique lines called separatrices. This model was designed to produce sufficient reconnection rates $v_{\mathrm{in}} \sim 0.1c$ to explain the energetics and time scales of solar flares, but for decades it was incomplete. It did not explain the localization mechanism for the magnetic diffusion region, and did not even allow to calculate the reconnection rate from physical principles. It appears that these objectives have been achieved most recently in the work of Liu et al. (2022). These authors analyzed the structure of two nested diffusion regions in a collisionless electron-ion plasma (an electron diffusion region, EDR, inside a much larger ion diffusion region, IDR; outside IDR ideal MHD applies with all particles magnetized; inside IDR but outside EDR Hall MHD applies with demagnetized/kinetic ions; inside EDR both ions and electrons are demagnetized/kinetic), using particle-in-cell simulations to verify analytical calculations. They showed that localization of each diffusion region can be explained by a pressure gap, that the geometric aspect ratio of each diffusion region $S = \delta/L \simeq 0.5$ is determined by the particle mass ratio, and that reconnection rate of $v_{\mathrm{in}} \simeq 0.15c$ is determined by S.

Minijets. The idea that magnetic reconnection drives outflows with speed of the order of the Alfvén speed for the background plasma $v_{\mathrm{out}} \sim v_{\mathrm{A},0}$ has interesting consequences in case of relativistic magnetizations $\sigma_0 \gg 1$, for which the Alfvén Lorentz factor is $\Gamma_{\mathrm{A},0} \simeq \sqrt{\sigma_0}$ (see Section 4). Relativistic reconnection can thus be expected to drive localized relativistic outflows called *minijets*. This idea has been applied by Giannios et al. (2009) as an explanation of rapid (time scale of a few minutes) gamma-ray flares occasionally observed in blazars (see the Phenomenology notes), using the fact that a minijet located within a larger relativistic jet of Lorentz factor Γ_{j} would have an effective Lorentz factor of $\sim \Gamma_{\mathrm{j}}\Gamma_{\mathrm{A},0}$. Radiative output of minijets has been calculated in the work of Nalewajko et al. (2011), which was based on the relativistic version of the Petschek model formulated by Lyubarsky (2005). In particular, this model of minijets emission allowed to explain a rapid TeV flare of blazar PKS 2155-304 together with simultaneous constraints on the X-ray emission.

Plasmoids. Extremely elongated current layers postulated by the Sweet-Parker model are not stable, they are subject a few unstable models, of which the most important is the *tearing mode* (Furth et al., 1963). Tearing of a long current layer means that it spontaneously breaks up into a chain of closed magnetic loops described as *plasmoids* (in 2D) or *magnetic flux ropes* (in 3D). In current layers characterized by uniform scalar magnetic diffusivity η, tearing into plasmoids becomes important for Lundquist numbers $R_{\mathrm{m}} > 10^4$ (Loureiro et al., 2007). This has immediate consequences for the Sweet-Parker model: it can only be valid for $R_{\mathrm{m}} < 10^4$, which implies a lower limit on the reconnection rate $v_{\mathrm{in}} > 10^{-2}v_{\mathrm{A},0}$. Plasmoids evolve along the reconnection layers by growth, bulk acceleration and mergers (which involves secondary reconnection), they can also act as particle traps (not perfect in 3D) and can even faciliate particle acceleration. Plasmoid chains are complex and dynamical structures with interesting radiative signatures, they offer an alternative to the minijets in explaining rapid gamma-ray flares of blazars (e.g., Petropoulou et al., 2016).

7.1 Kinetic simulations of relativistic reconnection

Particle-in-cell algorithm. Astrophysical plasmas are often characterized by such low particle densities that Coulomb collisions can be neglected the fluid (e.g. MHD) description of plasma is inadequate. When the kinetic effects become important, it is also an opportunity to investigate the mechanisms of non-thermal particle acceleration. An elegant numerical tool for investigating such plasmas is the particle-in-cell (PIC) algorithm.

In the PIC method, the plasma is treated as a collection of individual macroparticles, each characterized by position and momentum. The electric and magnetic fields are independently discretized on a special staggered (which means using full and half nodes; staggering is also used in time using the leapfrog algorithm) lattice (called *Yee lattice*) that allows for easy calculation of differential operators (div,

curl) with second-order accuracy (the Gauss's law for magnetism, $\vec{\nabla} \cdot \vec{B} = 0$, can be satisfied with numerical accuracy). Particle momenta are advanced in time according to the interpolated local Lorentz force. The fields are advanced in time according to the Maxwell-Faraday equation (for $\partial_t \vec{B}$) and the Ampère-Maxwell equation (for the displacement current $\partial_t \vec{E}$, using current density $\vec{j}$ deposited on the lattice by local macroparticles). The PIC algorithm is generally more expensive than fluid algorithms, as it requires multiple macroparticles per cell in order to reduce the Poisson noise that is inevitable imposed on the fields. I have been using a version of the PIC code `Zeltron` developed by Benoît Cerutti[7] (Cerutti et al., 2013).

Particle acceleration in relativistic reconnection. Kinetic simulations of magnetized plasmas allow to investigate acceleration of individual particles or to follow the evolution of particle energy distribution. In regions where magnetic fields are strong and regular, the plasma behaves like a fluid (despite being collisionless), and the electric fields are motional (satisfying the ideal MHD relation $\vec{E} = \vec{B} \times \vec{\beta}$), hence no particle acceleration takes place. In regions where reversed magnetic fields undergo reconnection, the electric fields have significant non-ideal component, and the particles depart from fluid description, undergoing acceleration. Efficient particle acceleration in magnetic diffusion regions (magnetic X-points) in relativistically magnetized plasma has been first demonstrated using PIC simulations by Zenitani & Hoshino (2001). The particle energy distributions produced in the magnetic X-points were found to be power laws $N(\gamma) \propto \gamma^{-p}$ with index $p \simeq 1$. Such distributions are considered to be very hard, with most of the integrated energy contained in the highest-energy particles. Such distributions cannot extend indefinitely, and it has been shown using an iterative calculation that they terminate with an exponential cutoff $\exp(-\gamma/\gamma_{\rm c})$ (Larrabee et al., 2003). This result has been confirmed by large-scale PIC simulations for a broad range of background magnetizations σ, it was found that with increasing value of σ, the distribution becomes harder with $p \to 1$ in the limit of $\sigma \gg 1$ (Sironi & Spitkovsky, 2014; Guo et al., 2014; Werner et al., 2016). In that limit, it was also found that $\gamma_{\rm c} \propto \sigma$, i.e., that the maximum particle energy is limited by background magnetization. Even larger PIC simulations of Petropoulou & Sironi (2018) showed that in the presence of very large plasmoids the power-law index softens to $p \simeq 2$, which is now thought to be an artifact of 2D simulations (energetic particles cannot escape from plasmoids due to artificial symmetry). The latest 3D simulations converge at $p \simeq 1.5$ (and demonstrate that energetic particles can escape the flux ropes that have finite length) (Zhang et al., 2021).

The next question is what kind of electric field is responsible for particle acceleration. While early studies emphasized the role of non-ideal electric fields at magnetic X-points, with increasing size of numerical simulations the non-ideal fields become more and more localized. Besides the magnetic X-points, possible sites of particle acceleration are reconnection outflows (minijets), plasmoids and plasmoid mergers (Nalewajko et al., 2015). It has been argued that most particles are accelerated by motional electric fields, in which they spend most of their time, in a Fermi-type process (Guo et al., 2019). One of the key questions is, whether a particle needs to pass through a region of non-ideal electric field with $E > B$ to become highly energetic, the latest results of Sironi (2022) suggest that this is indeed the case.

The relative contribution of minijets and plasmoids to particle acceleration and radiative signatures has been clarified in the work of Ortuño-Macías & Nalewajko (2020). First, it was shown that minijets and plasmoids co-exist in the same reconnection layers. Second, both minijets and plasmoids accelerate particles under different conditions. Minijets are characterized by weaker magnetic fields, and allow the particles to achieve higher energies, as compared with the plasmoids. The key difference is that plasmoids are much denser, containing more energetic particles that produce stronger signals of synchrotron radiation. Hence, plasmoids are expected to dominate the overall radiation output, moreover, plasmoid mergers (even in the tail-on configuration) are able to produce rapid flares of energetic radiation.

Another important result that was obtained from PIC simulations of relativistic reconnection is the *kinetic beaming* effect, which is energy-dependent particle anisotropy, with the highest-energy particles forming tightly focused beams (Cerutti et al., 2012). Kinetic beaming is a contributing factor to shorten the characteristic time scale of radiation signatures produced from the sites of relativistic reconnection. The appearance of rapid flares may result either from finite duration of energetic particle beams or from gyration of the beams sweeping the line of sight (Yuan et al., 2016).

---

[7] http://benoit.cerutti.free.fr/Zeltron/

8 Relativistic motion

This section will discuss aspects of special relativity related to relativistic motions in jets, which are essential to understand how the effects of viewing angle make blazars a distinct class of AGN (see the Phenomenology notes).

Apparently superluminal motion. Motions with apparent speeds exceeding the speed of light $v_{\mathrm{app}} > c$ are routinely observed in astrophysical jets. It does not mean that jets are really superluminal, it means that their true speeds are very close to c, but always a bit subluminal. One can consider a source moving with true speed $v = \beta c$ with $\beta < 1$, with the velocity vector $\vec{v}$ making a viewing angle θ_{obs} with the *line of sight*. The source emits two photons (#1,#2) towards the observer at time interval Δt_{em}. Let us introduce a Cartesian coordinate system (r, x), where r measures the distance to the source along the line of sight, and x measures its position in the *plane of the sky* (the plane perpendicular to the line of sight), such that $\vec{v}$ is confined to the (r, x) plane. One can write $\vec{v} = -v \cos\theta_{\mathrm{obs}} \hat{r} + v \sin\theta_{\mathrm{obs}} \hat{x}$, using the unit vectors $\hat{r}, \hat{x}$. Over the time interval Δt_{em}, the path of photon #2 will be shifted from the path of photon #1 by $\Delta x = v \Delta t_{\mathrm{em}} \sin\theta_{\mathrm{obs}}$. Photon #1 is closer to the observer than photon #2 by $\Delta r = -(c - \mathrm{v}\cos\theta_{\mathrm{obs}})\Delta t_{\mathrm{em}}$, it will thus be registered earlier by $\Delta t_{\mathrm{obs}} = -\Delta r/c = (1 - \beta\cos\theta_{\mathrm{obs}})\Delta t_{\mathrm{em}}$. Then, the *apparent speed* of the source is:

$$\beta_{\mathrm{app}} = \frac{\Delta x}{c\Delta t_{\mathrm{obs}}} = \frac{\beta\sin\theta_{\mathrm{obs}}}{1 - \beta\cos\theta_{\mathrm{obs}}} \,. \tag{8.1}$$

It can be shown that apparent speed is maximized at the value of $v_{\mathrm{app}} = \Gamma v$ for the viewing angle satisfying $\sin\theta_{\mathrm{obs}} = 1/\Gamma$ and $\cos\theta_{\mathrm{obs}} = \beta$. This means that observation of an apparently superluminal motion with $\beta_{\mathrm{app}} > 1$ sets a lower limit on the true Lorentz factor of the source $\Gamma > \beta_{\mathrm{app}}$. Superluminal motion not due to Lorentz transformation, it is a light-travel effect.

Relativistic Doppler effect. For two photons emitted by a relativistically fast (but subluminal) source, emission interval can be calculated in the co-moving reference frame denoted with $\mathcal{O}'$ (to distinguish it from the observer reference frame $\mathcal{O}$). The Lorentz transformation from $\mathcal{O}'$ to $\mathcal{O}$ gives $\Delta t_{\mathrm{em}} = \Gamma(\Delta t'_{\mathrm{em}} + \vec{\beta}\cdot\Delta\vec{r}')$. However, since $\Delta\vec{r}' = 0$ (the source is at rest in its co-moving frame), this yields $\Delta t'_{\mathrm{em}} = \Delta t_{\mathrm{em}}/\Gamma$. Note that the relation between co-moving emission interval ($\Delta t'_{\mathrm{em}}$) and the interval observed in $\mathcal{O}$ (Δt_{obs}) implies the frequency transformation or the *Doppler effect*:

$$\frac{\nu_{\mathrm{obs}}}{\nu'_{\mathrm{em}}} = \frac{\Delta t'_{\mathrm{em}}}{\Delta t_{\mathrm{obs}}} = \frac{1}{\Gamma(1 - \beta\cos\theta_{\mathrm{obs}})} \equiv \mathcal{D} \,, \tag{8.2}$$

where $\mathcal{D}$ is the *relativistic Doppler factor*. For the characteristic viewing angle that maximizes β_{app} ($\cos\theta_{\mathrm{obs}} = \beta$) one has $\mathcal{D} = 1/[\Gamma(1 - \beta^2)] = \Gamma$. Moreover, for $\theta_{\mathrm{obs}} \leq \arcsin(1/\Gamma)$ (known as the Doppler cone) one has $\mathcal{D} \geq \Gamma$, with the maximum value $\mathcal{D} = (1 + \beta)\Gamma < 2\Gamma$ for $\theta_{\mathrm{obs}} = 0$. Outside the Doppler cone, for $\theta_{\mathrm{obs}} > \arcsin(1/\Gamma)$, one has $\mathcal{D} < \Gamma$. For $\theta_{\mathrm{obs}} = \pi/2$ one has $\mathcal{D} = 1/\Gamma$, and for $\theta_{\mathrm{obs}} = \pi$ one has $\mathcal{D} = 1/[(1 + \beta)\Gamma] > 1/(2\Gamma)$.

In case that both β_{app} and $\mathcal{D}$ are independently determined (which has been achieved for a substantial sample of blazars; see Hovatta et al. 2009), Eqs. (8.1) and (8.2) can be reversed, yielding explicit expressions for the Lorentz factor and viewing angle:

$$\Gamma = \frac{\mathcal{D}^2 + \beta_{\mathrm{app}}^2 + 1}{2\mathcal{D}} \,, \tag{8.3}$$

$$\tan\theta_{\mathrm{obs}} = \frac{2\beta_{\mathrm{app}}}{\mathcal{D}^2 + \beta_{\mathrm{app}}^2 - 1} \,. \tag{8.4}$$

Relativistic luminosity boost. Another important effect of relativistic motion is the *relativistic aberration*. This can be expressed as the transformation of the solid angle from the co-moving frame of the emitter to the observer frame $\Delta\Omega_{\mathrm{obs}} = \Delta\Omega'_{\mathrm{em}}/\mathcal{D}^2$. The viewing angles within the Doppler cone in the observer frame ($\sin\theta_{\mathrm{obs}} < 1/\Gamma$) receive all signals emitted in the co-moving frame at $\theta'_{\mathrm{obs}} < \pi/2$. Relativistic aberration, in combination with the Doppler effect, implies a very strong amplification of the radiation intensity I_ν. Invoking

a fundamental invariant $I_\nu/\nu^3 = \text{const}$, the intensity transformation is $I_{\nu,\text{obs}} = \mathcal{D}^3 I'_{\nu,\text{em}}$, and likewise is the transformation of apparent luminosity spectrum $L_\nu = 4\pi d_{\text{L}}^2 I_\nu$, where d_{L} is the luminosity distance. The bolometric luminosity $L = \int L_\nu \, \mathrm{d}\nu \propto \nu^4$ transforms like $L_{\text{obs}} = \mathcal{D}^4 L'_{\text{em}}$. This means that for a typical blazar with $\mathcal{D} \simeq \Gamma \sim 10$ the apparent luminosity of radiation produced in the jet is boosted by factor 10^4. This makes blazars a very special class of AGN.

9   Formation of relativistic jets

Relativistic jets are thought to be rooted in a rotating magnetosphere including *poloidal magnetic fields*. The essential axisymmetric stationary force-free model based on Keplerian accretion disk in Newtonian gravity has been formulated by Blandford (1976) (see also Lovelace 1976). Rotation of the poloidal fields induces perpendicular electric fields in the poloidal plane. A magnetosphere populated by dilute ionized plasma will redistribute electric charges by electric currents in order to satisfy the *force-free* condition $\vec{f}_{\text{L}} = \rho\vec{E} + (\vec{j} \times \vec{B})/c = 0$. As the particles are constrained to move along the magnetic field lines, one expects poloidal electric currents to generate *toroidal magnetic fields* (allowing the particles to rotate subluminally beyond the *light surface*). The toroidal magnetic fields with the perpendicular electric fields produce a *poloidal Poynting flux* that depending on the geometry of poloidal magnetic fields may be directed outwards (away from the accretion disk plane). This poloidal Poynting flux drives the electromagnetic outflow that eventually becomes a collimated relativistic jet.

Blandford & Payne (1982) showed that even cold outflows can be driven from accretion disks centrifugally along the poloidal magnetic field lines making an inclination angle with the accretion disk plane less than $60°$ (see Problem 7; in the Kerr metric this critical inclination angle approaches $90°$ at the innermost stable circular orbit - ISCO - in the limit of maximum black hole spin $a \to 1$, Cao 1997).

The model of rotating force-free magnetosphere has been extended to General Relativity in the famous work of Blandford & Znajek (1977) (BZ). Using the Kerr metric, they considered two examples of poloidal magnetic field geometries (split monopole - radial field lines, and paraboloidal) with a net magnetic flux Φ_{BH} threading the black hole horizon. In the limit of slow BH spin ($a \lesssim 0.3$), they showed that the electromagnetic power that can be extracted from the BH scales like $P_{\text{BZ}} \propto (a\Phi_{\text{BH}}/M_{\text{BH}})^2$ (this has been generalized to higher spin values by means of numerical simulations and high-order perturbative methods). The BZ mechanism can be viewed as an electromagnetic version of the *Penrose process* (Lasota et al., 2014), in which energy can be extracted from a spinning black hole by dropping particles of negative energy that can be created in the *ergosphere* region (Penrose & Floyd, 1971). The plausibility of the BZ mechanism has been questioned even very recently (King & Pringle, 2021), however, see Komissarov (2022). It is therefore very helpful that the BZ mechanism has been demonstrated from first principles by means of general relativistic kinetic numerical simulations (Parfrey et al., 2019).

In the MHD limit, formation of relativistic jets at spinning black holes has been investigated extensively by numerical simulations. Typically this involves a geometrically thick accretion flow of weakly magnetized gas carrying vertical magnetic fields. The jets stand out as bipolar regions of very low gas density and strong poloidal magnetic fields, with the vertically extended gas providing a pressure support to collimate the jets (e.g., Barkov & Komissarov, 2008). With advances in numerical resolution, it has recently been demonstrated that even geometrically thin accretion disks can produce collimated jets (e.g., Liska et al., 2019), as expected from observations of radio-loud quasars. Since the BZ jet power scales with the magnetic flux Φ_{BH} crossing the BH horizon, it has been numerically demonstrated that pressing a sufficiently large Φ_{BH} allows to achieve jet power exceeding the rest-mass energy accretion rate $P_{\text{j}} > \dot{M}_{\text{acc}}c^2$ (Tchekhovskoy et al., 2011). At large Φ_{BH} values, the magnetic field pushes the accretion flow away from the BH, forming a *magnetically arrested disk* (MAD) (Narayan et al., 2003). There is, however, an upper limit on the value of Φ_{BH}, above that limit magnetic reconnection in the equatorial plane of the Kerr metric disconnects excess magnetic flux from the BH, ejecting asymmetric magnetic bubbles along the jet boundary (Ripperda et al., 2022).

9.1 Acceleration of jets

Acceleration of jets to relativistic bulk velocities can be considered as a separate physical process. In the simplest terms, the process involves conversion of relativistic magnetization $\sigma \gg 1$ to a high Lorentz factor $\Gamma \gg 1$. This process cannot be investigated in the force-free approximation (in which $\sigma \to \infty$), but can be investigated in the ideal MHD regime. Acceleration along poloidal streamlines cannot involve poloidal magnetic fields, which contribute tension force that acts to pull plasma back onto the black hole. However, the pressure of toroidal magnetic fields (produced from the poloidal fields by shear due to differential rotation) can do the job (Davis & Tchekhovskoy, 2020).

Acceleration of jets can be studied using stationary conservation laws. Conservation of energy along the velocity vector $\vec{\beta}$ can be written as $T^{0i} = \Gamma^2 (1 + \sigma') w' \beta^i = \text{const}$, where the prime indicates the co-moving frame, and $\sigma' = B'^2 / (4\pi w')$ is the co-moving magnetization. Together with the conservation of mass (continuity equation) $\Gamma \rho' \beta^i = \text{const}$, this makes the Bernoulli's equation

$$\frac{T^{0i}}{\Gamma \rho' \beta^i} = \Gamma (1 + \sigma') \frac{w'}{\rho'} \equiv \mu \frac{w'}{\rho'} = \text{const}, \tag{9.1}$$

where we introduced the Michel parameter $\mu \equiv \Gamma(1 + \sigma')$. This relation shows that $\sigma' \gg 1$ can indeed be converted into $\Gamma \gg 1$. However, how exactly this happens is governed by the conservation of momentum, which involves a complex relativistic MHD stress tensor $T^{ij} = \text{const}$. This is the hard part of the problem of acceleration of relativistic jets, to which unfortunately there are no analytic solutions. It can be solved using complex semi-analytical models (e.g., Li et al., 1992) or full numerical simulations. Relativistic MHD simulations demonstrated that efficient acceleration (conversion of magnetic to kinetic energy) may occur even in uncollimated outflows initiated with radial magnetic fields (split monopole) (Tchekhovskoy et al., 2009). Such conversion is largely complete ($\sigma' \sim 1$, beyond which the conversion becomes much slower) by radial distance $r \sim 10^5 R_{\rm g}$, and it results with a broadly collimated jet with opening angle $\theta > 1/\Gamma$, typical for gamma-ray burst afterglows. On the other hand, when collimation by external pressure is imposed on the outflow with paraboloidal magnetic fields (e.g., by using closed outer boundaries), the conversion is faster ($r \sim 10^3 R_{\rm g}$), resulting in a tightly collimated jet with opening angle $\theta < 1/\Gamma$, typical for blazars and radio galaxies (Komissarov et al., 2007).

The region of the jet where it undergoes active acceleration can be described as the *acceleration-collimation zone*. This zone ends where $\sigma' \sim 1$, and the magnetic fields are roughly in equipartition with the plasma (which means comparable energy densities $u'_{\rm B} \sim u'_{\rm e}$). It is presumed that at this point the jets may become turbulent and dissipative, accelerating particles that produce non-thermal emission that dominates the spectral energy distribution of blazars, this region can be described as the *blazar zone*. The location of the blazar zone can be constrained from the characteristics of blazar emission to distances $\sim 10^3 - 10^5 R_{\rm g}$, which typically corresponds to $\sim 0.03 - 3 \text{ pc}$ (Nalewajko et al., 2014). The dissipation mechanism is difficult to determine, since both shock waves and magnetic reconnection may produce similar radiative signatures (Sironi et al., 2015).

9.2 Instabilities in magnetized jets

The presence of toroidal magnetic fields may destabilize jets, in analogy to the laboratory experiments on magnetically confined plasmas (tokamaks) (Kruskal & Schwarzschild, 1954). Although the jets are presumed to be initially dominated by poloidal magnetic fields, as they expand in lateral radius R, the toroidal field strength scales like $B_\phi \propto R^{-1}$, decaying more slowly than the poloidal field strength ($B_{\rm p} \propto R^{-2}$), hence the jets are expected to eventually become dominated by toroidal fields and hence unstable. It has been argued that such instabilities are inevitable in relativistic jets, enhancing the dissipation of their magnetic energy (Giannios & Spruit, 2006).

Toroidal magnetic fields may be balanced in unstable radial equilibrium by poloidal fields or by the gas pressure. The corresponding instability modes are known as current-driven or pressure-driven, respectively. In the case of current-driven instability, the fastest growing mode is the kink ($m = 1$) that deforms jets along a helical pattern. The development of instabilities in magnetized jets has been investigated by various numerical simulations (e.g., Mizuno et al., 2009, in relativistic MHD). Recently, such instabilities have also been investigated by means of kinetic (particle-in-cell) numerical simulations, both in the case of

gas pressure balanced equilibrium (Alves et al., 2018), and in the case of poloidal field pressure balanced equilibrium (Davelaar et al., 2020). Both of these studies demonstrated that such instabilities result in efficient particle acceleration. My student José Ortuño-Macías performed a follow-up study (Ortuño-Macías et al., 2022) using a generalized equilibrium configuration bridging the gas pressure balanced and poloidal field pressure balanced cases. We confirmed the results of these previous works that particles can be accelerated rapidly until they reach the confinement energy limit $\gamma_{\lim} = eB_0R_0/mc^2$ (where R_0 is the jet radius at which the toroidal field peaks at B_0 strength), and demonstrated connection with rapid dissipation of toroidal field flux.

10 Accretion

Accretion is the inwards transfer of matter onto a central object, which can be a protoplanet, star or compact object, including a black hole. Accretion requires an outwards transfer of angular momentum, i.e., a viscosity. Molecular (Spitzer) viscosity is highly insufficient, which has been recognized already by Lynden-Bell (1969) and Shakura & Sunyaev (1973), who both suggested a fundamental role of magnetized turbulence. However, a specific mechanism of magnetically mediated viscosity has not been recognized until the work of Balbus & Hawley (1991), who re-discovered (after Velikhov (1959) and Chandrasekhar (1960) in the context of Couette flow experiments) the *magnetorotational instability* (MRI) (see Section 10.1 for details).

Observational evidence shows that some accretion flows are accompanied by the production of relativistic jets. We have seen that a key ingredient for the emergence of jets is the poloidal magnetic field. The origin of poloidal fields in accretion flows is an interesting problems. Two alternatives have been considered: (1) that poloidal fields can be transported inwards (advection), (2) that poloidal fields can be generated locally (dynamo).

In the local picture of resistive MHD, fields can be dragged inwards if they are sufficiently well frozen into the gas to resist diffusion outwards. The condition for efficient field dragging can be expressed in terms of a dimensionless parameter $\mathcal{D} = (R/H)(\eta/\nu) \lesssim 1$, where H is the disk half-thickness at radius R, η is the magnetic diffusivity, ν is the kinematic viscosity (note that $\eta/\nu \equiv P_{\rm m}^{-1}$ is the inverse magnetic Prandtl number) (Lubow et al., 1994). Incidentally or not, this parameter also determines the field line inclination angle $\tan\theta \simeq 1.5/\mathcal{D}$, and the condition for efficient field transport coincides closely with the condition for magnetocentrifugal extraction of angular momentum in the Blandford & Payne (1982) mechanism. An alternative picture has been proposed, in which the poloidal magnetic flux can be transported through the corona, connecting the black hole horizon with outer disk regions by elongated loops (Beckwith et al., 2009).

Can poloidal field be generated locally? Note that toroidal field can be readily created from the poloidal field by means of velocity shear due to differential rotation (the Ω effect) that is inevitable property of accretion flows. Successful dynamo theories suggest that the most likely mechanism for generation of poloidal field from the toroidal field is the α effect that utilizes a turbulent electromotive force. Such $\alpha\Omega$ dynamo has been recently demonstrated in global numerical simulations of accretion flows initiated with purely toroidal magnetic fields (Liska et al., 2020). The most spectacular aspect of this demonstration is that a powerful jet is launched from the dynamo-generated black hole flux, sustained on the time scale of at least $\sim 10^5 R_{\rm g}/c$.

Accumulation of significant magnetic flux on the central object can modify the accretion flow (and power relativistic jets, as discussed in Section 9). An influential model for such modification is known as the *magnetically arrested disk* (MAD) (Narayan et al., 2003), somewhat similar to a much earlier model of Bisnovatyi-Kogan & Ruzmaikin (1974). The MAD model postulates that an accretion disk can be 'arrested' at a finite magnetospheric radius, below which extends a regular magnetosphere dominated by poloidal magnetic field. That model was motivated by the results of non-relativistic resistive MHD 3D numerical simulations of Igumenshchev et al. (2003) of limited resolution, injecting magnetic flux through the boundaries. Subsequent GRMHD simulations of thick accretion flows onto black holes suggest a slightly different picture, in which the accretion flow is not 'arrested', but rather 'choked', hence called the *magnetically choked accretion flows* (MCAF) (McKinney et al., 2012). The key difference is that in an MCAF almost all of the ordered poloidal magnetic flux of the magnetosphere forming the base of the relativistic jets is connected to the BH horizon, while in a MAD part of this flux crosses the equatorial plane. Simulations also show that strongly magnetized accretion flows are highly non-axisymmetric, and the interface between gas-dominated accretion flow and the magnetosphere develops spiral substructures that significantly complicate the picture

(e.g., Ripperda et al., 2022).

Toroidal magnetic fields are increasingly recognized to be an important ingredient of geometrically thin accretion disks, in particular they offer a potential solution to the problem of various instabilities (thermal, viscous, fragmentation) that menace the standard accretion disk models (Begelman & Pringle, 2007). Some of these predictions have been confirmed by numerical investigations using global 3D radiative GRMHD simulations (e.g., Sądowski, 2016). Toroidal fields also have an interesting effect on the MRI: relatively weak fields suppress it, but sufficiently strong fields promote the growth of new modes (Das et al., 2018).

10.1   Magnetorotational instability (MRI).

An accretion disk threaded by weak vertical magnetic field develops unstable axisymmetric modes including perturbation of radial velocity. A domain of negative (positive) radial velocity propagates inwards (outwards) and has its specific angular momentum reduced (increased) even below (above) the Keplerian value at the new radius. This situation means a positive feedback for radial displacement and a redistribution of angular momentum, hence an effective viscosity.

Derivation of the MRI dispersion relation.   Consider two background components of magnetic field: vertical $B_{0,z}(r)$ and toroidal $B_{0,\phi}(r,z)$. The background current density is thus

$$\vec{j}_0 \;\; = \;\; \frac{c}{4\pi}\left[-\frac{\partial B_{0,\phi}}{\partial z}, -\frac{\partial B_{0,z}}{\partial r}, \frac{B_{0,\phi}}{r} + \frac{\partial B_{0,\phi}}{\partial r}\right], \tag{10.1}$$

and the background Lorentz force density is

$$\begin{aligned}
\vec{f}_{\text{B},0} \;\; &= \;\; \frac{\vec{j}_0 \times \vec{B}_0}{c} = \frac{1}{c}\left[j_{0,\phi}B_{0,z} - j_{0,z}B_{0,\phi}, -j_{0,r}B_{0,z}, j_{0,r}B_{0,\phi}\right] = \\
&\quad \frac{1}{8\pi}\left[-\frac{\partial(B_0^2)}{\partial r} - \frac{2B_{0,\phi}^2}{r}, 2B_{0,z}\frac{\partial B_{0,\phi}}{\partial z}, -\frac{\partial(B_{0,\phi}^2)}{\partial z}\right].
\end{aligned} \tag{10.2}$$

The background equilibrium is:

$$-r\Omega_0^2 \;\; = \;\; -\frac{1}{\rho_0}\frac{\partial P_0}{\partial r} + g_r - \frac{1}{8\pi\rho_0}\left(\frac{\partial(B_0^2)}{\partial r} + \frac{2B_{0,\phi}^2}{r}\right), \tag{10.3}$$

$$0 \;\; = \;\; g_\phi + \frac{B_{0,z}}{4\pi\rho_0}\frac{\partial B_{0,\phi}}{\partial z}, \tag{10.4}$$

$$0 \;\; = \;\; -\frac{1}{\rho_0}\frac{\partial P_0}{\partial z} + g_z - \frac{1}{8\pi\rho_0}\frac{\partial(B_{0,\phi}^2)}{\partial z}, \tag{10.5}$$

where $\Omega_0 = v_{0,\phi}/r$ is the *orbital frequency*. For simplicity, we will assume that $\partial_z B_{0,\phi} = 0$, i.e., that toroidal field is not vertically stratified, and that $\partial_r B_{0,z} = 0$. This defines the gravitational acceleration vector:

$$g_r \;\; = \;\; \frac{1}{\rho_0}\frac{\partial P_0}{\partial r} - r\Omega_0^2 + \frac{1}{8\pi\rho_0}\left(\frac{d(B_{0,\phi}^2)}{dr} + \frac{2B_{0,\phi}^2}{r}\right), \tag{10.6}$$

$$g_z \;\; = \;\; \frac{1}{\rho_0}\frac{\partial P_0}{\partial z}. \tag{10.7}$$

The linearized current and Lorentz force densities:

$$\vec{j}_0 \;\; = \;\; \frac{c}{4\pi}\left[0, 0, \frac{B_{0,\phi}}{r} + \frac{dB_{0,\phi}}{dr}\right], \tag{10.8}$$

$$\vec{j}_1 \;\; = \;\; \frac{c}{4\pi}\left[-\frac{\partial B_{1,\phi}}{\partial z}, \frac{\partial B_{1,r}}{\partial z} - \frac{\partial B_{1,z}}{\partial r}, \frac{B_{1,\phi}}{r} + \frac{\partial B_{1,\phi}}{\partial r}\right], \tag{10.9}$$

$$\begin{aligned}
\vec{f}_{\text{B},1} \;\; &= \;\; \frac{\vec{j}_1 \times \vec{B}_0}{c} + \frac{\vec{j}_0 \times \vec{B}_1}{c} \\
&= \;\; \frac{1}{c}\left[j_{1,\phi}B_{0,z} - j_{1,z}B_{0,\phi} - j_{0,z}B_{1,\phi}, -j_{1,r}B_{0,z} + j_{0,z}B_{1,r}, j_{1,r}B_{0,\phi}\right].
\end{aligned} \tag{10.10}$$

The linearized Euler equations:

$$\frac{\partial v_{1,r}}{\partial t} - 2\Omega_0 v_{1,\phi} = -\frac{1}{\rho_0}\frac{\partial P_1}{\partial r} + \frac{\partial P_0}{\partial r}\frac{\rho_1}{\rho_0^2} + \frac{B_{0,z}}{4\pi\rho_0}\left(\frac{\partial B_{1,r}}{\partial z} - \frac{\partial B_{1,z}}{\partial r}\right)$$

$$-\frac{B_{0,\phi}}{4\pi\rho_0}\left(\frac{2B_{1,\phi}}{r} + \frac{\partial B_{1,\phi}}{\partial r}\right) - \frac{B'_{0,\phi}B_{1,\phi}}{4\pi\rho_0}\,, \tag{10.11}$$

$$\frac{\partial v_{1,\phi}}{\partial t} + (2\Omega_0 + r\Omega'_0)v_{1,r} = \frac{B_{0,z}}{4\pi\rho_0}\frac{\partial B_{1,\phi}}{\partial z} + \left(\frac{B_{0,\phi}}{r} + B'_{0,\phi}\right)\frac{B_{1,r}}{4\pi\rho_0}\,, \tag{10.12}$$

$$\frac{\partial v_{1,z}}{\partial t} = -\frac{1}{\rho_0}\frac{\partial P_1}{\partial z} + \frac{\partial P_0}{\partial z}\frac{\rho_1}{\rho_0^2} - \frac{B_{0,\phi}}{4\pi\rho_0}\frac{\partial B_{1,\phi}}{\partial z}\,. \tag{10.13}$$

The linearized induction equation under incompressibility:

$$\frac{\partial \vec{B}_1}{\partial t} = \left(\vec{B}_0\cdot\vec{\nabla}\right)\vec{v}_1 + \left(\vec{B}_1\cdot\vec{\nabla}\right)\vec{v}_0 - \left(\vec{v}_1\cdot\vec{\nabla}\right)\vec{B}_0 - \left(\vec{v}_0\cdot\vec{\nabla}\right)\vec{B}_1\,, \tag{10.14}$$

$$B_{1,r} = \frac{k_z}{\omega}B_{0,z}v_{1,r}\,, \tag{10.15}$$

$$i\omega B_{1,\phi} = \left(\frac{B_{0,\phi}}{r} - B'_{0,\phi}\right)v_{1,r} + ik_z B_{0,z}v_{1,\phi} + r\Omega'_0 B_{1,r}$$

$$= \left(\frac{B_{0,\phi}}{r} - B'_{0,\phi}\right)v_{1,r} + ik_z B_{0,z}v_{1,\phi} + \frac{k_z}{\omega}r\Omega'_0 B_{0,z}v_{1,r}\,, \tag{10.16}$$

$$B_{1,z} = \frac{k_z}{\omega}B_{0,z}v_{1,z}\,. \tag{10.17}$$

The short-wavelength approximation. $|k_r|, |k_z| \gg 1/r$

$$B_{1,\phi} \simeq \frac{k_z}{\omega}B_{0,z}\left(-\frac{i}{\omega}r\Omega'_0 v_{1,r} + v_{1,\phi}\right)\,. \tag{10.18}$$

The perturbed magnetic field becomes independent of $B_{0,\phi}$.

$$\vec{j}_1 \simeq \frac{ic}{4\pi}\left[-k_z B_{1,\phi}, k_z B_{1,r} - k_r B_{1,z}, k_r B_{1,\phi}\right]\,, \tag{10.19}$$

$$f_{\mathrm{B},1,\mathrm{r}} \simeq ik_z\frac{B_{0,z}B_{1,r}}{4\pi} - ik_r\frac{B_{0,\phi}B_{1,\phi}}{4\pi} - ik_r\frac{B_{0,z}B_{1,z}}{4\pi}\,, \tag{10.20}$$

$$f_{\mathrm{B},1,\phi} \simeq ik_z\frac{B_{0,z}B_{1,\phi}}{4\pi}\,, \tag{10.21}$$

$$f_{\mathrm{B},1,\mathrm{z}} \simeq -ik_z\frac{B_{0,\phi}B_{1,\phi}}{4\pi}\,. \tag{10.22}$$

The Euler equations:

$$i\omega v_{1,r} - 2\Omega_0 v_{1,\phi} = -\frac{ik_r}{\rho_0}\left(P_1 + \frac{B_{0,\phi}B_{1,\phi}}{4\pi}\right) + \frac{\partial P_0}{\partial r}\frac{\rho_1}{\rho_0^2}$$

$$+i\frac{B_{0,z}}{4\pi\rho_0}(k_z B_{1,r} - k_r B_{1,z})\,, \tag{10.23}$$

$$i\omega v_{1,\phi} + (2\Omega_0 + r\Omega'_0)v_{1,r} = ik_z\frac{B_{0,z}B_{1,\phi}}{4\pi\rho_0}\,, \tag{10.24}$$

$$i\omega v_{1,z} = -ik_z\left(\frac{P_1}{\rho_0} + \frac{B_{0,\phi}B_{1,\phi}}{4\pi}\right) + \frac{\partial P_0}{\partial z}\frac{\rho_1}{\rho_0^2}\,. \tag{10.25}$$

Combining the r-momentum equation multiplied by k_z with the z-momentum equation multiplied by $-k_r$, we eliminate the P_1 terms:

$$ik_z\omega v_{1,r} - 2k_z\Omega_0 v_{1,\phi} - ik_r\omega v_{1,z} = \left(k_z\frac{\partial P_0}{\partial r} - k_r\frac{\partial P_0}{\partial z}\right)\frac{\rho_1}{\rho_0^2} + ik_z\frac{B_{0,z}}{4\pi\rho_0}(k_z B_{1,r} - k_r B_{1,z}) \tag{10.26}$$

42

We have thus eliminated the dependence on $B_{0,\phi}$.

Substituting $B_{1,r}$ and $B_{1,z}$, introducing the vertical Alfven velocity $v_{A,0,z}^2 = B_{0,z}^2/4\pi\rho_0$, rearranging and multiplying by $-i\omega/k_z$:

$$ik_z\omega\left(v_{1,r} - \frac{k_r}{k_z}v_{1,z}\right) - 2k_z\Omega_0 v_{1,\phi} = \left(k_z\frac{\partial P_0}{\partial r} - k_r\frac{\partial P_0}{\partial z}\right)\frac{\rho_1}{\rho_0^2}$$
$$+ \frac{ik_z}{\omega}k_z^2 v_{A,0,z}^2\left(v_{1,r} - \frac{k_r}{k_z}v_{1,z}\right), \qquad (10.27)$$

$$(\omega^2 - k_z^2 v_{A,0,z}^2)\left(v_{1,r} - \frac{k_r}{k_z}v_{1,z}\right) + (2\Omega_0)i\omega v_{1,\phi} = -i\omega\left(\frac{\partial P_0}{\partial r} - \frac{k_r}{k_z}\frac{\partial P_0}{\partial z}\right)\frac{\rho_1}{\rho_0^2}. \qquad (10.28)$$

Eliminating $v_{1,\phi}$, using the ϕ-momentum equation with substituted $B_{1,\phi}$, and introducing $\tilde{\omega}^2 = \omega^2 - k_z^2 v_{A,0,z}^2$ and the (squared) *epicyclic frequency* $\Omega_{ec,0}^2 \equiv 2\Omega_0(2\Omega_0 + r\Omega_0')$:

$$i\omega v_{1,\phi} = -\left(2\Omega_0\frac{\omega^2}{\tilde{\omega}^2} + r\Omega_0'\right)v_{1,r}, \qquad (10.29)$$

$$\tilde{\omega}^2\left(v_{1,r} - \frac{k_r}{k_z}v_{1,z}\right) - 4\Omega_0^2\frac{\omega^2}{\tilde{\omega}^2}v_{1,r} - 2r\Omega_0\Omega_0'v_{1,r} = -i\omega\left(\frac{\partial P_0}{\partial r} - \frac{k_r}{k_z}\frac{\partial P_0}{\partial z}\right)\frac{\rho_1}{\rho_0^2}, \qquad (10.30)$$

$$\tilde{\omega}^2\left(v_{1,r} - \frac{k_r}{k_z}v_{1,z}\right) - \Omega_{ec,0}^2 v_{1,r} - 4\Omega_0^2\frac{k_z^2 v_{A,0,z}^2}{\tilde{\omega}^2}v_{1,r} = -i\omega\left(\frac{\partial P_0}{\partial r} - \frac{k_r}{k_z}\frac{\partial P_0}{\partial z}\right)\frac{\rho_1}{\rho_0^2}. \qquad (10.31)$$

Eliminating ρ_1 and $v_{1,z}$:

$$v_{1,z} = -\frac{k_r}{k_z}v_{1,r}, \qquad (10.32)$$

$$\rho_1 = \frac{i}{\omega}\left(\frac{\partial\rho_0}{\partial r} - \frac{k_r}{k_z}\frac{\partial\rho_0}{\partial z}\right)v_{1,r}, \qquad (10.33)$$

$$\frac{k^2}{k_z^2}\tilde{\omega}^2 - \Omega_{ec,0}^2 - 4\Omega_0^2\frac{k_z^2 v_{A,0,z}^2}{\tilde{\omega}^2} = \frac{1}{\rho_0^2}\left(\frac{\partial P_0}{\partial r} - \frac{k_r}{k_z}\frac{\partial P_0}{\partial z}\right)\left(\frac{\partial\rho_0}{\partial r} - \frac{k_r}{k_z}\frac{\partial\rho_0}{\partial z}\right), \qquad (10.34)$$

where $k^2 = k_r^2 + k_z^2$. Finally, rearranging and multiplying by (k_z^2/k^2), we obtain the dispersion relation:

$$\tilde{\omega}^4 - \left[\Omega_{ec,0}^2 + \frac{1}{\rho_0^2}\left(\frac{\partial P_0}{\partial r} - \frac{k_r}{k_z}\frac{\partial P_0}{\partial z}\right)\left(\frac{\partial\rho_0}{\partial r} - \frac{k_r}{k_z}\frac{\partial\rho_0}{\partial z}\right)\right]\frac{k_z^2}{k^2}\tilde{\omega}^2 - 4\Omega_0^2 v_{A,0,z}^2\frac{k_z^4}{k^2} = 0 \qquad (10.35)$$

In case of no vertical stratification ($\partial_z\rho_0 = 0$ and $\partial_z P_0 = 0$) and $k_r = 0$, the dispersion relation simplifies to:

$$\tilde{\omega}^4 - \left(\Omega_{ec,0}^2 + \frac{P_0'\rho_0'}{\rho_0^2}\right)\tilde{\omega}^2 - 4\Omega_0^2 k_z^2 v_{A,0,z}^2 = 0. \qquad (10.36)$$

Let us denote $\Omega_{BV,0}^2 \equiv P_0'\rho_0'/\rho_0^2$, the Brunt-Väisälä frequency. The solution is given by $\Delta = (\Omega_{ec,0}^2 + \Omega_{BV,0}^2)^2 + (16\Omega_0^2)k_z^2 v_{A,0,z}^2$, $\omega^2 = (\Omega_{ec,0}^2 + \Omega_{BV,0}^2 - \sqrt{\Delta})/2 + k_z^2 v_{A,0,z}^2$. Denoting $\Omega_{ec,0}^2 + \Omega_{BV,0}^2 \equiv \xi\Omega_0^2$ and $x^2 = k_z^2 v_{A,0,z}^2/\Omega_0^2$, this becomes $\omega^2/\Omega_0^2 = (\xi - \sqrt{\xi^2 + 16x^2})/2 + x^2$.

The simplest case of MRI. Consider the limit of no vertical stratification ($\partial_z X_0 = 0$ for any background parameter X_0), cold gas ($P_0 = 0$, hence $\Omega_{BV,0}^2 = 0$) and $k_r = 0$. The MRI dispersion relation (Eq. 10.36) simplifies to:

$$\tilde{\omega}^4 - \Omega_{ec,0}^2\tilde{\omega}^2 - 4\Omega_0^2 k_z^2 v_{A,0,z}^2 = 0. \qquad (10.37)$$
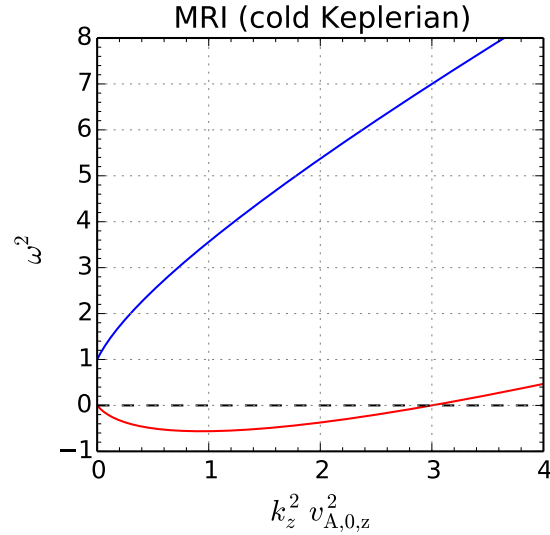
43

Figure 6: Solutions to the MRI dispersion relation (Eq. 10.37) for a cold unstratified Keplerian accretion disk.

In the hydrodynamic limit of $B_{0,z} = 0$, we have $v_{\mathrm{A},0,z} = 0$ and $\tilde{\omega} = \omega$, and the dispersion relation reduces to $(\omega^2 - \Omega_{\mathrm{ec},0}^2)\omega^2 = 0$. A hydrodynamic disk is stable if $\Omega_{\mathrm{ec},0}^2 > 0$. A Keplerian disk has $\Omega_0 \propto r^{-3/2}$, hence $\Omega_{\mathrm{ec},0}^2 = \Omega_0^2$, it is thus stable.

In the case of Keplerian disk with weak vertical magnetic field ($B_{0,z} \neq 0$), solutions to Eq. (10.37) are shown in Figure 6. The red line shows a branch of solutions that are unstable ($\omega^2 < 0$) for $0 < k_z^2 v_{\mathrm{A},0,z}^2 < 3$. The fastest growth rate with $\omega^2 = -(9/16)\Omega_0^2$ occurs for $k_z^2 v_{\mathrm{A},0,z}^2 = 15/16$.

11 Dynamo

In the context of magnetic fields, *dynamo* is a mechanism of amplification of non-zero magnetic fields using the kinetic energy of plasma motions. Such process can operate in the MHD regime. A mechanism of generation of magnetic fields from zero strength is termed the *battery*, it requires departing from the MHD.

In this lecture (see the Phenomenology notes), dynamo has been mentioned in very different contexts:

- planets (including the Earth), supporting their magnetospheres against diffusion and polarity reversals;

- low-mass stars (including the Sun), explaining their activity cycles with polarity reversals;

- spiral galaxies (including the Milky Way), explaining their globally ordered fields.

It is probably not a coincidence that we evolved on the planet orbiting the star within the galaxy that all operate dynamos.

Dynamos have also been proposed to operate in the accretion disks, for which it is a hypothesis for the origin of poloidal fields that launch relativistic jets; and also in proto-neutron stars during a supernova, for which it is a hypothesis for the origin of the extremely strong fields of the magnetars (Duncan & Thompson, 1992).

Stretch-twist-fold-merge (STFM).   An influential heuristic model of a dynamo cycle has been proposed by Zeldovich (Zeldovich, 1983). The cycle begins from a single closed loop of magnetic flux (Figure 7).
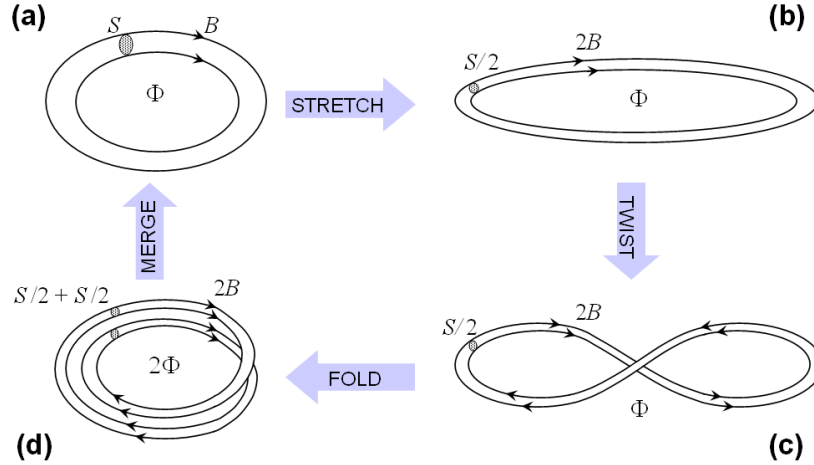
Figure 7: The stretch-twist-fold-merge (STFM) dynamo cycle proposed by Zeldovich (1983). Credit: MPIfR.

First, plasma motions should *stretch* the loop to double length, doubling also the field strength but preserving the magnetic flux. Second, plasma motions should *twist* the loop to a figure 8 shape (with two smaller loops), preserving the length, field strength and magnetic flux. Third, plasma motions should *fold* the two smaller loops into one, effectively doubling its magnetic flux. Finally, a local reconnection of magnetic field lines would *merge* the two smaller loops into one that would have double the field strength and magnetic flux compared to the initial loop. The STFM cycle was proposed as an elementary ingredient of a turbulent dynamo in the kinematic regime which is dominated by the kinetic energy of plasma (backreaction of magnetic field on the plasma is not important) and magnetic diffusivity η is small (diffusion is required locally for the merge step, but the growth rate of magnetic energy should be independent of η – the *fast dynamo*; Childress & Gilbert 1995).

Local change of magnetic energy density.   The rate of change of magnetic field in ideal MHD is expressed by the induction equation $\partial_t \partial \vec{B} = \vec{\nabla} \times \left(\vec{v} \times \vec{B} \right)$. The induction equation is sufficient to describe problems where a given velocity field affects the magnetic field, but the magnetic field does not affect the velocity field, such limit is known as the *kinematic dynamo*. Expanding the curl of vector cross product yields the following form:

$$\frac{\partial \vec{B}}{\partial t} = \left(\vec{B} \cdot \vec{\nabla} \right) \vec{v} - \left(\vec{v} \cdot \vec{\nabla} \right) \vec{B} - \vec{B} \left(\vec{\nabla} \cdot \vec{v} \right) . \tag{11.1}$$

The three RHS terms have the following meaning: (1) velocity *shear* along $\vec{B}$; (2) *transport* (advection) of $\vec{B}$ along $\vec{v}$; (3) *compression* of $\vec{B}$ due to velocity convergence. The change of $\vec{B}$ corresponds to a change of the magnetic energy density $u_{\mathrm{B}} = B^2/(8\pi) \equiv (\vec{B} \cdot \vec{B})/(8\pi)$, the evolution which can be expressed as:

$$\frac{\partial u_{\mathrm{B}}}{\partial t} = \frac{\vec{B}}{4\pi} \cdot \frac{\partial \vec{B}}{\partial t} = \frac{1}{4\pi} \left[\vec{B} \cdot \left(\vec{B} \cdot \vec{\nabla} \right) \vec{v} - \left(\vec{v} \cdot \vec{\nabla} \right) \frac{B^2}{2} - B^2 \left(\vec{\nabla} \cdot \vec{v} \right) \right] . \tag{11.2}$$

The three terms in the square bracket represent the contributions from shear, transport and compression, respectively.

Example: sheared velocity field with uniform magnetic field.   Consider a sheared velocity field $\vec{v} = v_x(y)\hat{e}_x$. The only non-zero velocity gradient is $\partial_y v_x$, assume that it has a positive constant and uniform value. The shear term of the induction equation is $(\vec{B} \cdot \vec{\nabla})\vec{v} = B_y(\partial_y v_x)\hat{e}_x$ and the corresponding magnetic energy growth term is $B_x B_y \partial_y v_x/(4\pi)$. The presence of constant uniform $B_y > 0$ will induce the growth of $B_x(t) = B_y(\partial_y v_x)t > 0$. The velocity field has no divergence, hence the compression term is zero. The transport term is also zero, since the magnetic field is uniform at all times.

45

Example: uniform velocity field with non-uniform magnetic field. Consider a uniform velocity field $\vec{v} = v_x \hat{e}_x$. The transport term of the magnetic energy density evolution equation is $-v_x(\partial_x B^2)/(8\pi)$. The shear and compression terms are zero due to uniform velocity. Magnetic energy density increases by transport in the regions where magnetic energy gradient is opposite to the velocity vector.

Example: converging velocity field with initially uniform magnetic field. Consider a converging velocity field $\vec{v} = v_x(x)\hat{e}_x$ with uniform negative divergence $\partial_x v_x < 0$, assume also that $\vec{B} = [B_x, B_y, 0]$. The compression term of the magnetic energy density evolution equation is $-B^2(\partial_x v_x)/(4\pi) > 0$, hence the magnetic energy density grows everywhere. The shear term $B_x^2(\partial_x v_x)/(4\pi) < 0$ is actually negative, and it cancels out partially with the compression term. The transport term $-v_x(\partial_x B^2)/(8\pi)$ is zero initially and henceforth, since the B-field remains uniform. The net magnetic energy growth rate is the sum of compression and shear terms $-B_y^2(\partial_x v_x)/(4\pi) > 0$. Converging velocity field amplifies only the perpendicular magnetic field component.

Amplification of axisymmetric fields. Motivated by the evidence for dynamos in axisymmetric bodies such as the Earth or the Sun, consider a magnetic field structure with axial symmetry in cylindrical coordinates (r, ϕ, z) (slightly simpler than spherical coordinates). Such magnetic fields can be decomposed into *toroidal and poloidal* components $\vec{B} = B_\phi \hat{\phi} + \vec{B}_{\mathrm{p}}$, where $\hat{\phi}$ is the unit vector along the ϕ coordinate. The poloidal component $\vec{B}_{\mathrm{p}} \equiv B_r \hat{r} + B_z \hat{z}$ can be represented by the toroidal component of a magnetic vector potential $\vec{B}_{\mathrm{p}} = \vec{\nabla} \times (A_\phi \hat{\phi})$. If both B_ϕ and A_ϕ are independent of ϕ, the Gauss's law for magnetism $\vec{\nabla} \cdot \vec{B} = 0$ is satisfied automatically.

Consider how a given azimuthal velocity $\vec{v} = v_\phi \hat{\phi}$ affects the toroidal magnetic field B_ϕ. Assume that $v_\phi = r\,\Omega(z)$, where $\Omega(z)$ is the angular velocity that allows for an axially differential rotation $\mathrm{d}\Omega/\mathrm{d}z \neq 0$. The azimuthal induction equation includes the shear and transport terms (not that $\vec{\nabla} \cdot \vec{v} = 0$, hence there is no compression term):

$$\partial_t B_\phi = \left[(\vec{B} \cdot \vec{\nabla})\vec{v}\right]_\phi - \left[(\vec{v} \cdot \vec{\nabla})\vec{B}\right]_\phi . \tag{11.3}$$

Both RHS terms are material derivatives that in any curved coordinates need to be carefully calculated:

$$\partial_t B_\phi = \left[(\vec{B}_{\mathrm{p}} \cdot \vec{\nabla})v_\phi\,\hat{\phi}\right]_\phi - \frac{B_r v_\phi}{r} = r\left[(\vec{B}_{\mathrm{p}} \cdot \vec{\nabla})\frac{v_\phi}{r}\hat{\phi}\right]_\phi = rB_z\frac{\mathrm{d}\Omega}{\mathrm{d}z} . \tag{11.4}$$

The RHS is a source term for the growth of B_ϕ. This source term includes a combination of differential rotation with poloidal magnetic field. This represents the Ω *effect* for generation of toroidal magnetic field. For example, differential rotation is evident in the Sun, not only on the surface, but also across the convective zone (see the Phenomenology notes), hence the Ω effect is an important element of the solar dynamo.

Next, consider the axial component of the induction equation:

$$\partial_t B_z = \left[(\vec{B} \cdot \vec{\nabla})\vec{v}\right]_z - \left[(\vec{v} \cdot \vec{\nabla})\vec{B}\right]_z . \tag{11.5}$$

It turns out that for $v_z = 0$ and $\partial_\phi B_z = 0$ both RHS terms vanish, hence the vertical magnetic field cannot be induced under the adopted assumptions. This means that the expected loop $B_z \to B_\phi \to B_z$ cannot be closed. This is the simplest case of the *Cowling's antidynamo theorem* (Cowling, 1933) that historically had been a serious obstacle to developing dynamo theories.

Mean-field electrodynamics. A solution to the problem of generating poloidal fields from the toroidal fields has been proposed by Parker (1955). This solution involved vertical motions of convective cells that in a rotating body are twisted by the Coriolis force into 'cyclones'. Such small-scale motions break the axial symmetry of the velocity field. Both the velocity field and the magnetic field can be decomposed into globally symmetric *mean fields* $\vec{v}_0, \vec{B}_0$ and small-scale (possibly turbulent) fluctuations $\vec{v}_1, \vec{B}_1$, so that $\vec{v} = \vec{v}_0 + \vec{v}_1$ and $\vec{B} = \vec{B}_0 + \vec{B}_1$. Such decomposition is not linearization, i.e., the amplitudes of $\vec{v}_1$ and $\vec{B}_1$ do

not need to be small, but these fluctuations should vanish upon averaging over a sufficiently large volume, leaving $\langle \vec{v} \rangle \simeq \vec{v}_0$ and $\langle \vec{B} \rangle \simeq \vec{B}_0$. Applying such averaging to the induction equation:

$$\partial_t \langle \vec{B}_0 \rangle = \vec{\nabla} \times \left\langle (\vec{v}_0 + \vec{v}_1) \times (\vec{B}_0 + \vec{B}_1) \right\rangle . \tag{11.6}$$

Assuming that $\langle \vec{v}_0 \times \vec{B}_1 \rangle + \langle \vec{v}_1 \times \vec{B}_0 \rangle = 0$, one obtains:

$$\partial_t \langle \vec{B}_0 \rangle = \vec{\nabla} \times \left(\langle \vec{v}_0 \rangle \times \langle \vec{B}_0 \rangle + \langle \vec{v}_1 \times \vec{B}_1 \rangle \right) . \tag{11.7}$$

The second RHS term $\vec{\mathcal{E}} \equiv \langle \vec{v}_1 \times \vec{B}_1 \rangle$ is called the *mean turbulent electromotive force*. The simplest form of this force is $\mathcal{E}_i = \alpha_{ij} \langle B_0 \rangle_j$, where α_{ij} is a symmetric tensor. With this, the mean-field induction equation becomes:

$$\partial_t \langle \vec{B}_0 \rangle = \vec{\nabla} \times \left(\langle \vec{v}_0 \rangle \times \langle \vec{B}_0 \rangle + \alpha \langle \vec{B}_0 \rangle \right) . \tag{11.8}$$

The second RHS term now represents the α *effect* from correlated small-scale fluctuations. Let us apply the mean-field induction equation to the problem of dynamo in axisymmetric mean fields. Its axial and toroidal components become:

$$\partial_t \langle B_z \rangle = \frac{1}{r} \partial_r \left(r\alpha \langle B_\phi \rangle \right) , \tag{11.9}$$

$$\partial_t \langle B_\phi \rangle = r \langle B_z \rangle \frac{\mathrm{d}\Omega}{\mathrm{d}z} - \partial_r \left(\alpha \langle B_z \rangle \right) . \tag{11.10}$$

Three regimes of the axisymmetric mean-field dynamo are usually distinguished:

- $\alpha\Omega$ *dynamo* (e.g., stars), when the $r \langle B_z \rangle (\mathrm{d}\Omega/\mathrm{d}z)$ term dominates the toroidal component;

- α^2 *dynamo* (e.g., planets), when the $\partial_r \left(\alpha \langle B_z \rangle \right)$ term dominates;

- $\alpha^2\Omega$ *dynamo* (e.g., galaxies), when these terms are comparable.

Biermann battery. We have remarked that the problem of battery, obtaining $\partial_t \vec{B} \neq 0$ when $\vec{B} = 0$, requires a departure from the MHD regime (even resistive). A more general plasma regime is the *two-fluid plasma*, where both electron and ions can be treated as fluids, but not strictly coupled. The dynamics of the electrons fluid can be characterized by a balance of Lorentz force and pressure gradient $\vec{f}_e = -\vec{\nabla}P_e - en_e\vec{E} = 0$. Using the ideal gas law $P_e = n_e k_{\mathrm{B}} T_e$, one can use that force balance to express the electric field $\vec{E} = -(k_{\mathrm{B}}/en_e)\vec{\nabla}(n_e T_e)$. Substitute this to the Maxwell-Faraday equation:

$$\partial_t \vec{B} = -c\vec{\nabla} \times \vec{E} = \frac{ck_{\mathrm{B}}}{e} \vec{\nabla} \times \left[\frac{\vec{\nabla}(n_e T_e)}{n_e} \right] = \frac{ck_{\mathrm{B}}}{e} \left(\frac{\vec{\nabla} n_e}{n_e} \right) \times \left(\vec{\nabla} T_e \right) . \tag{11.11}$$

Magnetic field can thus be generated when the electron density gradient is misaligned with the electron temperature gradient. Biermann battery is being considered as a potential mechanism for generating seed magnetic fields in the young Universe, before the onset of dynamos in the first stars and protogalaxies (for review see Durrer & Neronov, 2013).

A   Problems

Problem 1 (magnetic mirror).   Consider the case of $\vec{\nabla}B \parallel \vec{B}$. What may happen to a charged particle? Two suggestions: (1) solve particle motion along $\vec{B}$ by linearizing about uniform gyration, (2) prove that $\mu = v_\perp^2/B$ is invariant, what is the implication?

Solution to Problem 1. Consider a non-uniform magnetic field $B_x = B_0 + B_1(x/L)$ with $|B_1| \ll B_0$. In order to satisfy the Gauss law, we assume that $\partial_y B_y = \partial_z B_z = -(1/2)\partial_x B_x = -B_1/2L$, hence $B_y = -B_1 y/2L$ and $B_z = -B_1 z/2L$. Let $\Omega_{L,0} = qB_0/(\gamma mc^2)$ and $\Omega_{L,1} = (B_1/B_0)\Omega_{L,0}$. The equations of motion are the following:

$$\ddot{x} = \frac{\Omega_{L,0}}{B_0}(B_z \dot{y} - B_y \dot{z}) = \frac{\Omega_{L,1}}{2L}(-z\dot{y} + y\dot{z}) \tag{A.1}$$

$$\ddot{y} = \frac{\Omega_{L,0}}{B_0}(B_x \dot{z} - B_z \dot{x}) = \Omega_{L,0}\dot{z} + \frac{\Omega_{L,1}}{2L}(z\dot{x} + 2x\dot{z}) \tag{A.2}$$

$$\ddot{z} = \frac{\Omega_{L,0}}{B_0}(B_y \dot{x} - B_x \dot{y}) = -\Omega_{L,0}\dot{y} - \frac{\Omega_{L,1}}{2L}(y\dot{x} + 2x\dot{y}) \tag{A.3}$$

Let us linearize the particle trajectory $\vec{r} = \vec{r}_0 + \vec{r}_1$, such that $\vec{r}_0$ is a solution in the $B_1 = 0$ limit: $x_0 = v_{0,x}t$, $y_0 = R_{L,0}\sin(\Omega_{L,0}t)$, $z_0 = R_{L,0}\cos(\Omega_{L,0}t)$. The linearized equations are:

$$\ddot{x}_1 \simeq \frac{\Omega_{L,1}}{2L}(-z_0\dot{y}_0 + y_0\dot{z}_0) = -\Omega_{L,0}\Omega_{L,1}\frac{R_{L,0}^2}{2L}, \tag{A.4}$$

$$\ddot{y}_1 \simeq \Omega_{L,0}\dot{z}_1 + \frac{\Omega_{L,1}}{2L}(z_0\dot{x}_0 + 2x_0\dot{z}_0)$$

$$= \Omega_{L,0}\dot{z}_1 + \Omega_{L,1}v_{0,x}\frac{R_{L,0}}{2L}[\cos(\Omega_{L,0}t) - 2(\Omega_{L,0}t)\sin(\Omega_{L,0}t)], \tag{A.5}$$

$$\ddot{z}_1 \simeq -\Omega_{L,0}\dot{y}_1 - \frac{\Omega_{L,1}}{2L}(y_0\dot{x}_0 + 2x_0\dot{y}_0)$$

$$= -\Omega_{L,0}\dot{y}_1 - \Omega_{L,1}v_{0,x}\frac{R_{L,0}}{2L}[\sin(\Omega_{L,0}t) + 2(\Omega_{L,0}t)\cos(\Omega_{L,0}t)]. \tag{A.6}$$

A solution for x_1 is:

$$x_1 = -\frac{\Omega_{L,1}}{\Omega_{L,0}}\frac{R_{L,0}^2}{4L}(\Omega_{L,0}t)^2 \tag{A.7}$$

with a parabolic dependence on time.

For y_1 and z_1 one can find the following solution:

$$\dot{y}_1 = \frac{\Omega_{L,1}}{\Omega_{L,0}}\frac{R_{L,0}}{2L}v_{0,x}\left[-\frac{(\Omega_{L,0}t)^2}{2}\sin(\Omega_{L,0}t) + (\Omega_{L,0}t)\cos(\Omega_{L,0}t)\right] \tag{A.8}$$

$$\dot{z}_1 = \frac{\Omega_{L,1}}{\Omega_{L,0}}\frac{R_{L,0}}{2L}v_{0,x}\left[-(\Omega_{L,0}t)\sin(\Omega_{L,0}t) - \frac{(\Omega_{L,0}t)^2}{2}\cos(\Omega_{L,0}t)\right] \tag{A.9}$$

The linearized parallel equation of motion can also be written as:

$$\dot{v}_\parallel \simeq -\frac{v_\perp^2}{2B_0}\frac{B_1}{L} = -\frac{v_\perp^2}{2B_0}\frac{\partial B_x}{\partial x} \simeq -\frac{v_\perp^2}{2B}\frac{1}{v_\parallel}\frac{dB}{dt} \tag{A.10}$$

Since the particle energy is conserved, we have:

$$0 = \frac{d(v_\perp^2 + v_\parallel^2)}{dt} = \frac{d(v_\perp^2)}{dt} + 2v_\parallel\frac{dv_\parallel}{dt} \simeq \frac{d(v_\perp^2)}{dt} - \frac{v_\perp^2}{B}\frac{dB}{dt} = v_\perp^2\frac{d\ln(v_\perp^2/B)}{dt} \tag{A.11}$$

hence $v_\perp^2/B = \mathrm{const}$. Introducing the pitch angle such that $v_\perp = v\sin\alpha$, we have $\sin^2\alpha/B = \mathrm{const}$ (since $v = \mathrm{const}$, hence $B_{\max} = B/\sin^2\alpha$ is the maximum field strength to which a particle at local B, α can penetrate, and upon reaching such a *mirror point* it would be reflected. The parallel force $F_{L,\parallel} = m\dot{v}_\parallel \simeq -\mu\nabla_\parallel B$ is called the *mirror force*[8], with $\mu = mv_\perp^2/2B$ called the particle *magnetic moment* or the *first adiabatic invariant*.

---

[8]Note that $\nabla_\parallel B \simeq \nabla_\parallel B_\parallel$, with contributions from $B_\perp$ of the second order.

Problem 3 (magnetic braking). Consider a thin ring of radius R centered in cylindrical coordinates (r, ϕ, z) of conducting plasma rotating with angular velocity $\vec{\Omega} = \Omega \hat{z}$ and threaded by an axisymmetric magnetic field $\vec{B} = [B_r(r), B_\phi(r), 0]$. By considering how Ω changes due to the torque exerted by the Lorentz force, derive an expression for the magnetic braking time scale $t_L \equiv \Omega |\mathrm{d}\Omega/\mathrm{d}t|^{-1}$.

Solution to Problem 3. Torque or the moment of force is defined as $\delta\vec{\mathcal{T}} = \vec{r} \times \delta\vec{F} = \mathrm{d}(\delta\vec{L})/\mathrm{d}t$, where $\delta\vec{L} = \vec{\Omega}\,\delta I$ is the angular momentum element for an moment of inertia element $\delta I = r^2\,\delta M$ with rotating with angular velocity $\vec{\Omega} = (\vec{r} \times \vec{v})/r^2$. We introduce a torque density $\vec{\tau} = \delta\vec{\mathcal{T}}/\delta V = \vec{r} \times \vec{f} = \mathrm{d}\vec{l}/\mathrm{d}t$, where $\vec{l} = \delta\vec{L}/\delta V$ is the angular momentum density.

Under axial symmetry, $\vec{\Omega} = \Omega\hat{z} = (v_\phi/r)\hat{z} = (2\pi/P)\hat{z}$, hence its variation is driven by the vertical torque component $\tau_z = \mathrm{d}l_z/\mathrm{d}t = \rho r^2 (\mathrm{d}\Omega/\mathrm{d}t)$. The braking time scale is $t_\Omega = \Omega|\mathrm{d}\Omega/\mathrm{d}t|^{-1} = \rho v_\phi r/|\tau_z|$.

Vertical torque density due to Lorentz force is $\tau_{L,z} = -r f_{L,\phi}$.

The Lorentz force density in ideal MHD:

$$\vec{f}_L \;=\; \frac{1}{4\pi}\left(\vec{B}\cdot\vec{\nabla}\right)\vec{B} - \frac{1}{8\pi}\vec{\nabla}\left(B^2\right). \tag{A.12}$$

For the toroidal component $f_{L,\phi}$, axisymmetry ensures that the second term (magnetic pressure gradient) vanishes, leaving only the first term (magnetic tension).

For $B_z = 0$ one finds:

$$f_{L,\phi} \;=\; \frac{B_r}{4\pi r}\frac{\partial(rB_\phi)}{\partial r}, \tag{A.13}$$

i.e., the toroidal Lorentz force is the tension of the radial field line. The vertical torque density becomes:

$$\tau_{L,z} \;=\; -\frac{B_r}{4\pi}\frac{\partial(rB_\phi)}{\partial r} = -\left[\frac{\partial(rB_\phi)/\partial r}{B_r}\right]\frac{B_r^2}{4\pi}, \tag{A.14}$$

where $B_r^2/(4\pi)$ can be identified as the enthalpy density of radial magnetic field, and the square bracket is a dimensionless measure of field line curvature.

The braking time scale becomes:

$$t_\Omega \;=\; \frac{\rho v_\phi r}{|\tau_z|} = \left|\frac{B_r}{\partial(rB_\phi)/\partial r}\right|\frac{v_\phi r}{B_r^2/4\pi\rho} = \left|\frac{B_r}{\partial(rB_\phi)/\partial r}\right|\left(\frac{v_\phi}{v_{A,r}}\right)^2\frac{P}{2\pi}, \tag{A.15}$$

where $v_{A,r} = |B_r|/\sqrt{4\pi\rho}$ is the Alfvén velocity corresponding to the radial magnetic field. The braking time scale is thus shown in relation to the orbital period P, which is a natural time scale in this problem.

Problem 4 (magnetic helicity). Magnetic helicity is defined for a system of volume V as the integral $\mathcal{H} = \int_V \left(\vec{A}\cdot\vec{B}\right)\mathrm{d}V$, where $\vec{A}$ is the magnetic vector potential. Calculate $\mathrm{d}\mathcal{H}/\mathrm{d}t$ in the regime of resistive MHD in terms of $\vec{B}$. Assume that potentials $\vec{A}, \phi$ vanish at the system boundaries.

Solution to Problem 4. We begin by calculating the time derivative of $\vec{A}\cdot\vec{B}$. The time derivative of $\vec{B}$ is obtained from the Maxwell-Faraday equation:

$$\frac{\partial\vec{B}}{c\,\partial t} = -\vec{\nabla}\times\vec{E}. \tag{A.16}$$

The time derivative of $\vec{A}$ is involved in the expression for electric field in terms of potentials:

$$\frac{\partial\vec{A}}{c\,\partial t} = -\vec{E} - \vec{\nabla}\phi, \tag{A.17}$$

where ϕ is the electric scalar potential. We can now calculate that:

$$\frac{\partial}{c\,\partial t}\left(\vec{A}\cdot\vec{B}\right) = \frac{\partial \vec{A}}{c\,\partial t}\cdot\vec{B} + \vec{A}\cdot\frac{\partial \vec{B}}{c\,\partial t} = -\vec{E}\cdot\vec{B} - \vec{B}\cdot\vec{\nabla}\phi - \vec{A}\cdot\left(\vec{\nabla}\times\vec{E}\right) . \tag{A.18}$$

The last two RHS terms can be identified as part of a divergence

$$\vec{\nabla}\cdot\left(\vec{A}\times\vec{E} - \phi\vec{B}\right) = \vec{E}\cdot\vec{B} - \vec{B}\cdot\vec{\nabla}\phi - \vec{A}\cdot\left(\vec{\nabla}\times\vec{E}\right) . \tag{A.19}$$

Note that the difference between these two RHSs is the sign of $\vec{E}\cdot\vec{B}$ term. Combining them, one can obtain the following:

$$\frac{\partial}{c\,\partial t}\left(\vec{A}\cdot\vec{B}\right) = -2\vec{E}\cdot\vec{B} + \vec{\nabla}\cdot\left(\vec{A}\times\vec{E} - \phi\vec{B}\right) . \tag{A.20}$$

We can now calculate the derivative of $\mathcal{H}$:

$$\frac{\mathrm{d}\mathcal{H}}{\mathrm{d}t} = \int_V \frac{\partial}{\partial t}\left(\vec{A}\cdot\vec{B}\right)\mathrm{d}V = c\int_V\left[-2\vec{E}\cdot\vec{B} + \vec{\nabla}\cdot\left(\vec{A}\times\vec{E} - \phi\vec{B}\right)\right]\mathrm{d}V . \tag{A.21}$$

Using the divergence theorem:

$$\frac{\mathrm{d}\mathcal{H}}{\mathrm{d}t} = -2c\int_V\left(\vec{E}\cdot\vec{B}\right)\mathrm{d}V + c\oint_{\partial V}\left[\hat{n}\cdot\left(\vec{A}\times\vec{E} - \phi\vec{B}\right)\right]\mathrm{d}S . \tag{A.22}$$

The surface integral vanishes, since it was specified that the potentials $\vec{A}, \phi$ vanish at the boundary.

We now invoke the electric field in resistive MHD $\vec{E} = \vec{B}\times\vec{\beta} + (\eta/c)(\vec{\nabla}\times\vec{B})$ to obtain the final solution:

$$\frac{\mathrm{d}\mathcal{H}}{\mathrm{d}t} = -2\eta\int_V\left[\left(\vec{\nabla}\times\vec{B}\right)\cdot\vec{B}\right]\mathrm{d}V . \tag{A.23}$$

In addition, one can use the quantity called *current helicity* $\mathcal{C} = \int_V(\vec{j}\cdot\vec{B})\,\mathrm{d}V$ to write the result as $\mathrm{d}\mathcal{H}/\mathrm{d}t = -(8\pi\eta/c)\mathcal{C}$.

Problem 6 (superluminal shock). Consider a relativistic shock in reference frame $\mathcal{O}$ with normal upstream velocity $\vec{v}_1 = [0, 0, v_1]$ in coordinates (x, y, z), and oblique upstream magnetic field $\vec{B}_1 = B_1[\sin\theta_1, 0, \cos\theta_1]$. Ideal MHD is satisfied both upstream and downstream.

Consider another reference frame $\mathcal{O}'$ moving in $\mathcal{O}$ with boost velocity $\vec{v}_\mathrm{b} = [v_\mathrm{b}, 0, 0]$. Using the Lorentz transformation, find what are the conditions to have (1) $B'_z = 0$, (2) $\vec{E}'_1 = 0$.

Consider a particle that can only move along the local magnetic field. Such a particle can easily pass from the upstream region to the downstream region. In which case is it possible for this particle to return to the upstream region?

Solution to Problem 6. Let $\vec{\beta}_1 = \vec{v}_1/c$ and $\vec{\beta}_\mathrm{b} = \vec{v}_\mathrm{b}/c$. Let us introduce the boost Lorentz factor $\Gamma_\mathrm{b} = (1-\beta_\mathrm{b}^2)^{-1/2}$. The upstream electric field in $\mathcal{O}$ is $\vec{E}_1 = \vec{B}_1\times\vec{\beta}_1 = -B_1\beta_1\sin\theta_1\hat{y}$. Hence, the cross products of the boost velocity with the upstream fields are $\vec{\beta}_\mathrm{b}\times\vec{E}_1 = -\beta_\mathrm{b}\beta_1 B_1\sin\theta_1\hat{z}$ and $\vec{\beta}_\mathrm{b}\times\vec{B}_1 = -\beta_\mathrm{b}B_1\cos\theta_1\hat{y}$.

Performing the Lorentz transformation of shock-normal magnetic field:

$$B'_{1,z} = \Gamma_\mathrm{b}\left[B_{1,z} - \left(\vec{\beta}_\mathrm{b}\times\vec{E}_1\right)_z\right] = \Gamma_\mathrm{b}B_1\left(\cos\theta_1 + \beta_\mathrm{b}\beta_1\sin\theta_1\right) . \tag{A.24}$$

Setting $B'_{1,z} = 0$ implies that $\beta_\mathrm{b} = -1/(\beta_1\tan\theta_1) \equiv -1/\beta_\mathrm{B}$, where β_B is the 'virtual' speed of the intersection point of a given magnetic field line with the shock front (not a physical entity).

Performing the Lorentz transformation of the electric field component:

$$E'_{1,y} = \Gamma_\mathrm{b}\left[E_{1,y} + \left(\vec{\beta}_\mathrm{b}\times\vec{B}_1\right)_y\right] = -\Gamma_\mathrm{b}B_1\left(\beta_1\sin\theta_1 + \beta_\mathrm{b}\cos\theta_1\right) . \tag{A.25}$$

Setting $E'_{1,y} = 0$ implies that $\beta_{\mathrm{b}} = -\beta_1 \tan\theta_1 \equiv -\beta_{\mathrm{B}}$.

We only admit Lorentz transformations with $|\beta_{\mathrm{b}}| < 1$. Hence, the condition of $E'_{1,y} = 0$ can be obtained only for $|\beta_{\mathrm{B}}| < 1$ (or $|\tan\theta_1| < 1/\beta_1$), which is referred to as the *subluminal shock*. This includes the case of parallel shock with $\theta_1 = 0$. The implication is that $\vec{E}'_1 = 0$ and $\vec{B}'_1 \parallel \vec{\beta}'_1$, hence a particle can cross the shock front both ways.

On the other hand, the condition of $B'_{1,z} = 0$ can be obtained only for $|\beta_{\mathrm{B}}| > 1$ (or $|\tan\theta_1| > 1/\beta_1$), which is referred to as the *superluminal shock*. This includes the case of perpendicual shock with $\theta_1 = \pi/2$. The implication is that $\vec{B}'_1 \perp \vec{n}'$, hence a particle that crossed the shock front downstream with its field line cannot return upstream.

Problem 7 (magnetocentrifuge). Consider an axisymmetric poloidal magnetic field line in cylindrical coordinates (r, ϕ, z): $\vec{B} = B[\cos\theta, 0, \sin\theta]$ crossing the $z = 0$ plane (accretion disk) at $r = r_0$, rotating with Keplerian angular velocity $\Omega^2 = GM/r_0^3$ in the gravitational field of a compact object of mass M located at $(0, 0, 0)$. Calculate the net force acting on a charged particle of mass m tied to this magnetic field line, a combination of gravitational and centrifugal forces projected along $\vec{B}$, as function of z. What is the condition for this net force to point away from the accretion disk?

Solution to Problem 7. Our particle is located at $(r, 0, z)$ that satisfies $r(z) = r_0 + z/\tan\theta$. The gravitational force is $\vec{F}_{\mathrm{g}} = (GMm/R^3)[-r, 0, -z]$, where $R(z) = \sqrt{r^2 + z^2}$. The centrifugal force is $\vec{F}_\Omega = m\Omega^2[r, 0, 0] = (GMm/r_0^3)[r, 0, 0]$. The net force is:

$$\vec{F} = \vec{F}_{\mathrm{g}} + \vec{F}_\Omega = \frac{GMm}{r_0^3}\left[\left(1 - \frac{r_0^3}{R^3}\right)r, 0, -\frac{r_0^3}{R^3}z\right] . \tag{A.26}$$

The net force along $\hat{B} = [\cos\theta, 0, \sin\theta]$ is:

$$\vec{F} \cdot \hat{B} = \frac{GMm}{r_0^3}\left[r\cos\theta - \frac{r_0^3}{R^3}\left(r_0\cos\theta + \frac{z}{\sin\theta}\right)\right] . \tag{A.27}$$

In the limit $z \ll r_0$, $R \simeq r$ and

$$\vec{F} \cdot \hat{B} \simeq \frac{GMm}{r_0^3}\frac{(4\cos^2\theta - 1)}{\sin\theta}z . \tag{A.28}$$

For $\sin\theta > 0$, $\vec{F} \cdot \hat{B} > 0$ for $|\cos\theta| > 1/2$, hence $\theta < 60°$ or $\theta > 120°$.

Problem 8 (black hole field). Estimate (order of magnitude) the magnetic field strength in the immediate vicinity of a black hole of mass (1) $10 M_\odot$, (2) $10^9 M_\odot$ sufficient to drive a Poynting flux (through the $2\pi R_{\mathrm{Sch}}^2$ cross section) equal to the Eddington luminosity.

Solution to Problem 8. The Poynting flux (energy flux density) is $\vec{S} = (c/4\pi)\left(\vec{E} \times \vec{B}\right)$. The electric field strength can be adopted as $E = \beta B \sim B/2$, since motions in the black hole vicinity are trans-relativistic with typical speed $\beta \sim 1/2$. The total Poynting flux through cross section A is thus:

$$\mathcal{S} \sim c\frac{B^2}{8\pi}A \sim \frac{c}{4}B^2 R_{\mathrm{Sch}}^2 . \tag{A.29}$$

The Schwarzshild radius can be expressed as $R_{\mathrm{Sch}} = 2GM/c^2 \simeq 3(M/M_\odot)$ km. The Eddington luminosity is

$$L_{\mathrm{Edd}} = \frac{4\pi GM m_{\mathrm{p}} c}{\sigma_{\mathrm{T}}} = \frac{2\pi R_{\mathrm{Sch}} m_{\mathrm{p}} c^3}{\sigma_{\mathrm{T}}} . \tag{A.30}$$

Equating $\mathcal{S} \sim L_{\mathrm{Edd}}$ leads to $cB^2 R_{\mathrm{Sch}}^2/4 \sim 2\pi R_{\mathrm{Sch}} m_{\mathrm{p}} c^3/\sigma_{\mathrm{T}}$, and hence:

$$B \sim \sqrt{\frac{8\pi m_{\mathrm{p}} c^2}{\sigma_{\mathrm{T}} R_{\mathrm{Sch}}}} \sim \frac{4.4 \times 10^8 \text{ G}}{\sqrt{M/M_\odot}} . \tag{A.31}$$
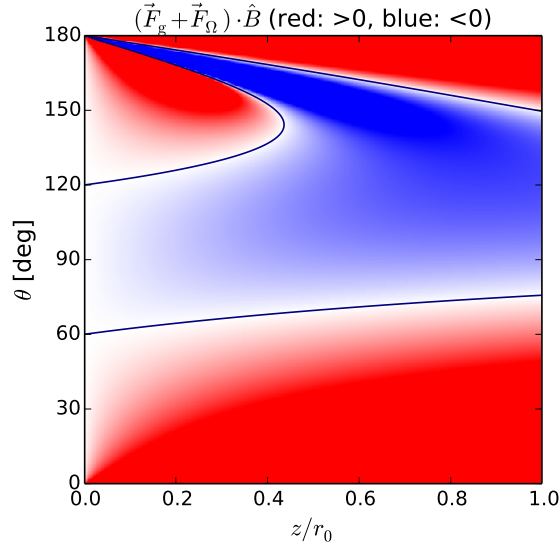
Figure 8: Problem 7 (magnetocentrifuge). The sign of the net gravitational + centrifugal force $\vec{F}_\mathrm{g} + \vec{F}_\Omega$ projected along the magnetic field direction $\hat{B}$ as function of the vertical coordinate z/r_0 and the magnetic field inclination angle θ. Red color means that $(\vec{F}_\mathrm{g} + \vec{F}_\Omega) \cdot \hat{B} > 0$, i.e., that the net force points away from the $z = 0$ plane.

For $M = 10 M_\odot$ one obtains $B \sim 1.4 \times 10^8$ G, and for $M = 10^9 M_\odot$ one obtains $B \sim 1.4 \times 10^4$ G (about one tesla).

This problem can also be approached by using the Blandford-Znajek formula for jet power, which is $P_\mathrm{BZ} \propto kc(a\Phi_\mathrm{BH}/R_\mathrm{Sch})^2$ (missing a constant factor) for moderate black hole spin values $a < 0.5$. This formula includes a geometric parameter k that can be adopted as $1/6\pi$ for the split-monopole geometry of magnetic field lines. Adopting a simplified magnetic flux crossing the black hole $\Phi_\mathrm{BH} \sim AB \sim 2\pi R_\mathrm{Sch}^2 B$, one can show that $P_\mathrm{BZ} \propto (8\pi/3)a^2\mathcal{S}$.

Problem 9 (extragalactic magnetic field). Certain blazars have SEDs extending beyond TeV photon energies. These gamma-ray photons interact with background radiation, producing electron-positron pairs. Consider an electron of energy $E_\mathrm{e} = \gamma m_\mathrm{e} c^2 = 1$ TeV. Such electron is subject to radiative cooling due to inverse Compton (IC) scattering of the Cosmic Microwave Background (CMB). The cooling rate is $\mathrm{d}\gamma/\mathrm{d}t = -(4\sigma_\mathrm{T}/3m_\mathrm{e}c)\gamma^2 u_\mathrm{CMB}$, where $u_\mathrm{CMB} \simeq 0.25$ eV/cm^3 is is the CMB energy density, and σ_T is the Thomson cross section. Calculate the cooling length $D_\mathrm{IC/CMB} = ct_\mathrm{IC/CMB} = c\gamma/|\mathrm{d}\gamma/\mathrm{d}t|$. What is the magnetic field strength B, for which the Larmor radius of our electron is $R_\mathrm{L} = D_\mathrm{IC/CMB}$?

Solution to Problem 9. The electron Lorentz factor is

$$\gamma = \frac{E_\mathrm{e}}{m_\mathrm{e}c^2} = \frac{1\text{ TeV}}{511\text{ keV}} \simeq 2 \times 10^6 \,. \tag{A.32}$$

The cooling length is

$$D_\mathrm{IC/CMB} = \frac{c\gamma}{(4\sigma_\mathrm{T}/3m_\mathrm{e}c)\gamma^2 u_\mathrm{CMB}} = \frac{3m_\mathrm{e}c^2}{4\sigma_\mathrm{T}\gamma u_\mathrm{CMB}} \simeq 0.4\text{ Mpc} \,. \tag{A.33}$$

From the expression for the Larmor radius $R_\mathrm{L} = E_\mathrm{e}/eB = D_\mathrm{IC/CMB}$, the magnetic field strength can be evaluated as

$$B = \frac{E_\mathrm{e}}{eD_\mathrm{IC/CMB}} = \frac{4\sigma_\mathrm{T}}{3e}\gamma^2 u_\mathrm{CMB} \simeq 3 \times 10^{-15}\text{ G} \,. \tag{A.34}$$

References

Alves, E. P., Zrake, J., & Fiuza, F. 2018, PhRvL, 121, 245101. doi:10.1103/PhysRevLett.121.245101

Balbus, S. A. & Hawley, J. F. 1991, ApJ, 376, 214. doi:10.1086/170270

Barkov, M. V. & Komissarov, S. S. 2008, MNRAS, 385, L28. doi:10.1111/j.1745-3933.2008.00427.x

Beckwith, K., Hawley, J. F., & Krolik, J. H. 2009, ApJ, 707, 428. doi:10.1088/0004-637X/707/1/428

Begelman, M. C. & Pringle, J. E. 2007, MNRAS, 375, 1070. doi:10.1111/j.1365-2966.2006.11372.x

Bisnovatyi-Kogan, G. S. & Ruzmaikin, A. A. 1974, Ap&SS, 28, 45. doi:10.1007/BF00642237

Blandford, R. D. 1976, MNRAS, 176, 465. doi:10.1093/mnras/176.3.465

Blandford, R. D. & Znajek, R. L. 1977, MNRAS, 179, 433. doi:10.1093/mnras/179.3.433

Blandford, R. D. & Payne, D. G. 1982, MNRAS, 199, 883. doi:10.1093/mnras/199.4.883

Blandford, R., Yuan, Y., Hoshino, M., et al. 2017, SSRv, 207, 291. doi:10.1007/s11214-017-0376-2

Brandenburg, A. & Subramanian, K. 2005, PhR, 417, 1. doi:10.1016/j.physrep.2005.06.005

Cao, X. 1997, MNRAS, 291, 145. doi:10.1093/mnras/291.1.145

Chandrasekhar, S. 1960, Proceedings of the National Academy of Science, 46, 253. doi:10.1073/pnas.46.2.253

Cerutti, B., Werner, G. R., Uzdensky, D. A., et al. 2012, ApJ, 754, L33. doi:10.1088/2041-8205/754/2/L33

Cerutti, B., Werner, G. R., Uzdensky, D. A., et al. 2013, ApJ, 770, 147. doi:10.1088/0004-637X/770/2/147

Childress, S. & Gilbert, A. D. 1995, The Fast Dynamo, XI, 406 pp.. Springer-Verlag Berlin Heidelberg New York. Also Lecture Notes in Physics, volume 37

Cowling, T. G. 1933, MNRAS, 94, 39. doi:10.1093/mnras/94.1.39

Das, U., Begelman, M. C., & Lesur, G. 2018, MNRAS, 473, 2791. doi:10.1093/mnras/stx2518

Davelaar, J., Philippov, A. A., Bromberg, O., et al. 2020, ApJ, 896, L31. doi:10.3847/2041-8213/ab95a2

Davis, S. W. & Tchekhovskoy, A. 2020, ARA&A, 58, 407. doi:10.1146/annurev-astro-081817-051905

Duncan, R. C. & Thompson, C. 1992, ApJ, 392, L9. doi:10.1086/186413

Durrer, R. & Neronov, A. 2013, A&ARv, 21, 62. doi:10.1007/s00159-013-0062-7

Freidberg, J. P. 1982, Reviews of Modern Physics, 54, 801. doi:10.1103/RevModPhys.54.801

Furth, H. P., Killeen, J., & Rosenbluth, M. N. 1963, Physics of Fluids, 6, 459. doi:10.1063/1.1706761

Giannios, D. & Spruit, H. C. 2006, A&A, 450, 887. doi:10.1051/0004-6361:20054107

Giannios, D., Uzdensky, D. A., & Begelman, M. C. 2009, MNRAS, 395, L29. doi:10.1111/j.1745-3933.2009.00635.x

Giovanelli, R. G. 1946, Nature, 158, 81. doi:10.1038/158081a0

Guo, F., Li, H., Daughton, W., et al. 2014, PhRvL, 113, 155005. doi:10.1103/PhysRevLett.113.155005

Guo, F., Li, X., Daughton, W., et al. 2019, ApJ, 879, L23. doi:10.3847/2041-8213/ab2a15

Harris, E. G. 1962, Il Nuovo Cimento, 23, 115. doi:10.1007/BF02733547

Hovatta, T., Valtaoja, E., Tornikoski, M., et al. 2009, A&A, 494, 527. doi:10.1051/0004-6361:200811150

Igumenshchev, I. V., Narayan, R., & Abramowicz, M. A. 2003, ApJ, 592, 1042. doi:10.1086/375769

Jackson, J. D. 1998, Classical Electrodynamics, 3rd Edition, by John David Jackson, pp. 832. ISBN 0-471-30932-X. Wiley-VCH , July 1998., 832

King, A. R. & Pringle, J. E. 2021, ApJ, 918, L22. doi:10.3847/2041-8213/ac19a1

Komissarov, S. S., Barkov, M. V., Vlahakis, N., et al. 2007, MNRAS, 380, 51. doi:10.1111/j.1365-2966.2007.12050.x

Komissarov, S. S. 2022, MNRAS, 512, 2798. doi:10.1093/mnras/stab2686

Kruskal, M. & Schwarzschild, M. 1954, Proceedings of the Royal Society of London Series A, 223, 348. doi:10.1098/rspa.1954.0120

Larrabee, D. A., Lovelace, R. V. E., & Romanova, M. M. 2003, ApJ, 586, 72. doi:10.1086/367640

Lasota, J.-P., Gourgoulhon, E., Abramowicz, M., et al. 2014, PhRvD, 89, 024041. doi:10.1103/PhysRevD.89.024041

Li, Z.-Y., Chiueh, T., & Begelman, M. C. 1992, ApJ, 394, 459. doi:10.1086/171597

Liska, M., Tchekhovskoy, A., Ingram, A., et al. 2019, MNRAS, 487, 550. doi:10.1093/mnras/stz834

Liska, M., Tchekhovskoy, A., & Quataert, E. 2020, MNRAS, 494, 3656. doi:10.1093/mnras/staa955

Liu, Y.-H., Cassak, P., Li, X., et al. 2022, Communications Physics, 5, 97. doi:10.1038/s42005-022-00854-x

Loureiro, N. F., Schekochihin, A. A., & Cowley, S. C. 2007, Physics of Plasmas, 14, 100703. doi:10.1063/1.2783986

Lovelace, R. V. E. 1976, Nature, 262, 649. doi:10.1038/262649a0

Lubow, S. H., Papaloizou, J. C. B., & Pringle, J. E. 1994, MNRAS, 267, 235. doi:10.1093/mnras/267.2.235

Lynden-Bell, D. 1969, Nature, 223, 690. doi:10.1038/223690a0

Lyubarsky, Y. E. 2005, MNRAS, 358, 113. doi:10.1111/j.1365-2966.2005.08767.x

McKinney, J. C. 2006, MNRAS, 367, 1797. doi:10.1111/j.1365-2966.2006.10087.x

McKinney, J. C., Tchekhovskoy, A., & Blandford, R. D. 2012, MNRAS, 423, 3083. doi:10.1111/j.1365-2966.2012.21074.x

Mizuno, Y., Lyubarsky, Y., Nishikawa, K.-I., et al. 2009, ApJ, 700, 684. doi:10.1088/0004-637X/700/1/684

Nalewajko, K., Giannios, D., Begelman, M. C., et al. 2011, MNRAS, 413, 333. doi:10.1111/j.1365-2966.2010.18140.x

Nalewajko, K., Begelman, M. C., & Sikora, M. 2014, ApJ, 789, 161. doi:10.1088/0004-637X/789/2/161

Nalewajko, K., Uzdensky, D. A., Cerutti, B., et al. 2015, ApJ, 815, 101. doi:10.1088/0004-637X/815/2/101

Narayan, R., Igumenshchev, I. V., & Abramowicz, M. A. 2003, PASJ, 55, L69. doi:10.1093/pasj/55.6.L69

Ortuño-Macías, J. & Nalewajko, K. 2020, MNRAS, 497, 1365. doi:10.1093/mnras/staa1899

Ortuño-Macías, J., Nalewajko, K., Uzdensky, D. A., et al. 2022, arXiv:2205.02259

Parfrey, K., Philippov, A., & Cerutti, B. 2019, PhRvL, 122, 035101. doi:10.1103/PhysRevLett.122.035101

Parker, E. N. 1955, ApJ, 122, 293. doi:10.1086/146087

Parker, E. N. 1957, JGR, 62, 509. doi:10.1029/JZ062i004p00509

Parker, E. N. 1966, ApJ, 145, 811. doi:10.1086/148828

Parker, E. N. 2007, Conversations on Electric and Magnetic Fields in the Cosmos, by Eugene N. Parker. ISBN-10 0-691-12840-5 (HB); ISBN-13 978-0-691-12840-5 (HB). Published by Princeton University Press, Princeton, NJ USA, 2007.

Penrose, R. & Floyd, R. M. 1971, Nature Physical Science, 229, 177. doi:10.1038/physci229177a0

Petropoulou, M., Giannios, D., & Sironi, L. 2016, MNRAS, 462, 3325. doi:10.1093/mnras/stw1832

Petropoulou, M. & Sironi, L. 2018, MNRAS, 481, 5687. doi:10.1093/mnras/sty2702

Petschek, H. E. 1964, NASA Special Publication, 425

Ripperda, B., Liska, M., Chatterjee, K., et al. 2022, ApJ, 924, L32. doi:10.3847/2041-8213/ac46a1

Sądowski, A. 2016, MNRAS, 459, 4397. doi:10.1093/mnras/stw913

Shakura, N. I. & Sunyaev, R. A. 1973, A&A, 24, 337

Sironi, L. & Spitkovsky, A. 2014, ApJ, 783, L21. doi:10.1088/2041-8205/783/1/L21

Sironi, L., Petropoulou, M., & Giannios, D. 2015, MNRAS, 450, 183. doi:10.1093/mnras/stv641

Sironi, L. 2022, PhRvL, 128, 145102. doi:10.1103/PhysRevLett.128.145102

Sweet, P. A. 1958, Electromagnetic Phenomena in Cosmical Physics, 6, 123

Taylor, J. B. 1974, PhRvL, 33, 1139. doi:10.1103/PhysRevLett.33.1139

Tchekhovskoy, A., McKinney, J. C., & Narayan, R. 2009, ApJ, 699, 1789. doi:10.1088/0004-637X/699/2/1789

Tchekhovskoy, A., Narayan, R., & McKinney, J. C. 2011, MNRAS, 418, L79. doi:10.1111/j.1745-3933.2011.01147.x

Thorne, K. S. & Blandford, R. D. 2017, Modern Classical Physics: Optics, Fluids, Plasmas, Elasticity, Relativity, and Statistical Physics, by Kip S. Thorne and Roger D. Blandford. ISBN: 978-0-691-15902-7. Princeton NJ: Princeton University Press, 2017.

Werner, G. R., Uzdensky, D. A., Cerutti, B., et al. 2016, ApJ, 816, L8. doi:10.3847/2041-8205/816/1/L8

Yuan, Y., Nalewajko, K., Zrake, J., et al. 2016, ApJ, 828, 92. doi:10.3847/0004-637X/828/2/92

Zeldovich, Y. B. 1983, The Fluid Mechanics of Astrophysics and Geophysics, New York: Gordon and Breach, 1983

Zenitani, S. & Hoshino, M. 2001, ApJ, 562, L63. doi:10.1086/337972

Zhang, H., Sironi, L., & Giannios, D. 2021, ApJ, 922, 261. doi:10.3847/1538-4357/ac2e08

Zrake, J. & East, W. E. 2016, ApJ, 817, 89. doi:10.3847/0004-637X/817/2/89